An Experimental-Numerical Study of Unsaturated Flow Through a Leach Heap

by

Valda I. Terauds

Submitted in Partial Fulfillment of
the Requirements for the Degree of
Master of Science in Hydrology

New Mexico School of Mining and Technology

Socorro, New Mexico

October 1985

ACKNOWLEDGEMENTS

I would like to express my gratitude for the help and assistance given me by my advisors Dr. Fred Phillips and Dr. Raziuddin Khaleel. They anticipated many potential problems and provided many valuable insights regarding the direction the project should take and approach to be used. This research project was funded by a Bureau of Mines and Mineral Resources research grant.

Appreciation goes to the Sullivan Center for In-Situ Mining for supplying the copper ore used in this study. In terms of construction of the long column apparatus, I would like to thank Floyd Hewitt for welding the oil drums supplied by TERA. Special thanks to Dr. Harold Bentley for supplying the experimental organic tracers and the use of the HPLC at Hydrogeochem, Inc. in Tucson, Arizona. Scott Veggerberg, also of Hydrogeochem Inc., was invaluable in the development of analytic techniques for the experimental tracers. Lynn Brandvold graciously supplied the fluorometer used to analyze the Rhodamine-B.

Finally, my heartfelt thanks and appreciation to all of the graduate students who assisted in various phases of the research: shoveled copper ore; transported the long column and torches; participated in the experiment; and took time and showed interest in disucssions of the various aspects of the project.

ABSTRACT

The hydraulics governing the leach process of copper leach heaps has been poorly understood and severely neglected in the research to date. This two-phase study of the flow processes, involving an experimental laboratory column, and the development of a numerical model attempts to answer some of the questions concerning the flow of leachate through a copper waste heap. Experimental tracers are utilized in the experimental portion of the study in an attempt to identify tracers useful for groundwater flow studies, as well as monitoring efforts for the leach process itself.

An experimental long column was constructed. The scale of the apparatus was representative of a unit volume within a field heap. The column was instrumented with sampling devices designed to provide chemical samples at various times and depths, a drain for effluent monitoring, and piezometers to determine the position of the free surface at the column bottom. A suite of tracers, including conservative and non-conservative chemicals, was added to the column as a single pulse, through a constant flux applicator. Chemical samples were collected and analyzed, representing various solution channels along the vertical axis of the column. Results indicate extensive solution channelization; varying flow velocities among different solution channels; and the degree of ore surface area contacted by the leachate. In addition, new tracers: PFB, m-TFMB, PSA, and NSA, are identified for use in groundwater flow problems.

The transport of tracer through the column was simulated using a numerical model developed from existing finite element codes for one-dimensional unsaturated flow and solute transport. The model UNSAT provides the solution to the matric-potential-based transient flow equation, while the model TRANS solves the advection-dispersion equation utilizing an upstream weighting technique. The model is able to account for varying flow velocities, moisture contents, chemical retardation, and the percent of surface area contacted by the leachate. Results of the tracer tests were compared with those from the numerical model to evaluate the hydraulic processes ongoing in the leach heap.

TABLE OF CONTENTS

LIST OF TABLES

LIST OF FIGURES

INTRODUCTION

The leaching of copper ore is common practice in the mining industry, accounting for up to twenty percent of all copper recovered. The recovery of metals through the leaching process began as the accidental result of rain and snow percolation into the overburden waste piles. Generally, low grade ore, composed mainly of mine waste and overburden, is handled in large heap piles. The ore may or may not be crushed, nevertheless, the character of the leach pile material is fairly coarse. The only constraints in size on these leach piles are topography and haulage costs[1].

The efficiency of the leach process itself is uncertain since not all of the ore is contacted by the leach solution. The coarser sized particles produce less copper than finer particles, due to decreased surface area available for contact with the leachate. In addition, the time required for diffusion of leachate into the unreacted core of coarse particles presents a further limitation on the efficiency of the process.

Previous research, toward understanding and maximizing the efficiency of the leaching process has been conducted by hydrometallurgists, who have concentrated on the chemical aspects of the problem. Generally, the problem of solution flow through a leach heap has received only minimal attention. Prior research has focused on parameters such as

heap hights, bacterial degradation, sulfide oxidation processes, and scale effects. The scaling-up of laboratory results in anticipation of a field leaching operation and new methods of copper extraction are addressed by Kuhn (1976)[2]. The scaling- up process in terms of leachate diffusion rates was studied by Roman (1974). He concentrated his efforts on the process of channelization i.e., the preferential flow of solution along a certain path. Channelization of leachate was proposed to be a result of differing clast sizes within the heap and the degree of compaction undergone by the heap during the leaching process. Roman discovered that heaps of a greater height produced a greater yield of copper (in pounds)[3]. Solution channeling due to greater bulk densities in field sized heaps affected the scale-up process as well. Roman (1977) indicated that particle-size distribution is less important than the channel-separation distribution. "The channel-separation distribution specifies the cummulative percentage of the rock in the dump situated less than a specific distance from a solution channel[4]." This distribution of channels depends on the methods employed in dump construction. Lab results indicate a channel-size separation to particle-size ratio of 30:1 is common in column leaching experiments. For the highest efficiency in leaching, this ratio should be as small as possible.

Laboratory and field-scale models of the leaching process have been conducted by Cathles and Murr (1980) and Murr (1980). These large-scale column studies were conducted at the Sullivan Center for In-Situ Mining Research at NMIMT. Cathles and Murr ran a controlled leach experiment in a 40 ft. x 10 ft. insulated steel tank. Two years of continuous leaching provided data on the leaching of low-grade copper-sulfide ore - a byproduct of open-pit mining. Tracer studies utilizing rhodamine-B dye were conducted to obtain an estimate of leachate-rock contact. The dye was detected by means of u-v light during the systematic unloading of the column. The dye-stained portions of the column reflected the points of contact between leachate and ore. A leaching model was used to simulate the results obtained from the tank experiments. The model, detailed by Cathles and Apps (1975), includes the rate of leaching as controlled by three processes: air convection; bacterial conversion of Fe^{+2} to Fe^{+3}; and the sulfide oxidation of Fe^{+3}. They discovered that the parameters were fairly well constrained, given the amount of leachate- rock contact; and predictions of field dump behaviour may be possible with the use of this model.

Murr (1980) provides a good overall treatment of heap leaching in the field and in-situ. He identified three controlling mechanisms for the leach process: decreasing reaction surface area for individual waste particles, varying diffusion rates through leached rims, and diffusion

limitations by product layers within waste fragments[5]. The most successful analytical models evolved from the concept of a shrinking core or reaction zone concept. Other leaching models dealt with the problems of scaling and optimization of the physical parameters of a leach pile.

Finally, several attempts to characterize the permeability and solution flow in leach dumps were made by Harris (1977) and Roman (1977). They found that leach piles undergo an evolution in matrix characteristics as a result of the leach process. The particles tend to get smaller in size, and with continued leaching, to form particle aggregates that approach the bulk density of consolidated rock. The phenomenon of solution channeling (lixiviant flow paths); in which solution flow paths are separated by numerous particles through which the leachate must diffuse, is also characteristic of changes undergone during leaching of a waste heap. (The channel-separation model (Roman, 1974) was based on clast size distributions and was discussed in the previous paragraphs.)

Although previous researchers have attempted to characterize the chemistry and physical heap parameters affecting the leaching process, the hydrology of leachate flow has not been studied extensively. Jacobson (1971) created a numerical model which dealt with the tendency towards non-linear flow in leach dumps. This model is the most advanced published treatment of solution flow through a

leach dump, yet its level is simple and not sufficiently realistic. One should understand the flow dynamics of the leach heap in order to maximize the leachate-rock contact and thus insure a reasonable efficiency of the leaching process.

Since the particle sizes of a leach dump tend towards the coarse, with cobbles representing greater than 50% of the material, the hydraulic character of the bulk medium must also be determined. The hydraulic properties of coarse materials have been examined by Bouwer and Rice (1984). They dealt with a layered system of stones/gravels and sands in which they attempted to determine which sized particles affected the hydraulic conductivity, water content, and dispersivity of the heterogenious mix. Results indicated that the saturated hydraulic conductivity of a stony soil can be calculated from the void ratios of the stony soil and the saturated condutivity of the sand fraction as determined by a laboratory study. The unsaturated hydraulic conductivity of the heterogeneous mix can be determined from the relations between unsaturated hydraulic condutivity and pressure head of the sand fraction alone. The bulk moisture content can be obtained by weighting the volume fraction of the stony zone with that of the sand fraction. The dispersivity of the heterogeneous system was found to be greater than that in a sand system alone[6].

In view of the research done by previous investigators, it appears that more work is necessary in order to characterize the hydraulic properties of a coarse-textured copper-waste leach heap. Thus the goal of this project is to approach the problem from the hydrologic perspective, utilizing the most current experimental and numerical techniques. Objectives are to investigate the hydraulics of fluid percolation through a laboratory column experiment of a scale approximating a field heap via the use of conservative and non-conservative tracers, to develop a numerical model that simulates flow and transport processes through the leach pile under unsaturated flow conditions comparable to field leaching practices, and to evaluate the numerical code using data collected during the column experiment.

RESEARCH OBJECTIVES

As stated in the title of this report, this is an experimental- numerical study of unsaturated flow through a leach dump. The focus of interest lies with the hydraulic processes governing flow. Thus the objectives of this study are:

1. To investigate the hydraulics of fluid percolation through a leach heap using a suite of tracers during a large scale long column experiment.
2. To adapt existing numerical codes for unsaturated flow and solute transport in order to model the leaching process.
3. To evaluate the numerical code and potential new tracers using data collected from the column experiment.

These objectives were achieved using techniques well known to hydrologists and soil scientists. The hydraulics of fluid percolation through a soil are a function of the hydraulic characteristics of the media. The most influential characteristics (K_{sat}, porosity, the soil moisture characteristic curve), are easily determined in the laboratory using common soil characterization techiques. A suite of conservative and non-conservative tracers was added to the long column in an effort to determine the efficiency of the leach process.

The numerical codes were selected from existing solutions of the unsaturated flow and solute transport equations. They were adapted to account for any specific hydrologic anomalies in leachate flow that occured during the long column experiment. Basic finite element codes were readily available for the unsaturated- flow and solute-transport problems. Modifications were need to account for solution channeling; tracer adsorption; tracer retardation; and varying moisture contents along the length of the column. Finally, the codes were verified using experimental data.

Proposed Techniques of Investigation

The problem of designing and implementing a long column experiment as a model of a field scale leaching process involves special consideration. First, the choice of appropriate and feasible scale must be addressed. For the experiment to reflect the physical nature of the ongoing hydraulic processes, the size of the sample volume is crucial. In studies of scale and leaching efficiency, Murr (1980) discovered that small columns, (0.69 m. high by 0.10 m. in diameter), are more susceptible to short circuiting of leachate via wall channelization than are larger columns. In effect, the preferential flow path for leachate for a small column is the space between the ore and column wall. If short circuiting occurs, the contact between ore and leachate will be minimal, and thus the efficiency of the copper recovery negligible. A column that is large enough to avoid wall channelization is therefore required.

Since solution channels are expected to form as a result of the leaching process, sampling devices need to be positioned in a fairly dense network to intercept fluid for tracer analysis. These solution channels are generally unpredictable in location, and shifting channels have been documented under long continuous flushing cycles. Decisions regarding the type of samplers must be made in anticipation of probable moisture content profiles during the leaching

process.

Application rates and the length of the flushing cycles should approximate conditions encountered in the field. Since copper leaching from waste piles is often the result of rain and snow percolation, a constant flux infiltration apparatus was employed. The length of the flush cycles depends on the hydraulic characteristics of the copper ore. These characteristics can be determined using established techniques. The parameters to be measured are porosity, grain size distribution, soil moisture content - suction relationships, and saturated hydraulic conductivity. The van Genuchten model (1978) was used to construct relative conductivity vs. pressure head relationships from the soil moisture - suction data.

Tracers of a conservative and non-conservative nature were used to determine the velocity, pore volume, dispersivity, and percent of material contacted during the leaching process. Two highly documented tracers,the chloride ion and rhodamine-B, were used. Other experimental tracers were also added in an effort to test their applicability to groundwater-flow problems. A comparison of tracer breakthrough curves along potential channels, from different heights along the column, and from effluent breakthrough curves yielded estimates on the degree of leachate - ore contact, and thus the efficiency of the leach process.

Once the experimental study was completed, work proceeded on development of a numerical model of the leach process utilizing established numerical codes. The programs UNSAT and TRANS were chosen as the codes for simulation of fluid flow and solute transport. Modifications were made in these numerical codes to account for the effects of tracer adsorption, tracer retardation, channelization, and dispersion.

Once the code was modified, the model was evaluated using data from the long column experiment. After model verification using the experimental data, the model was then be used to predict the extent of leachate - ore contact to be expected while varying such parameters as heap height; flow velocity; and degree of channelization. Ideally, the model should be applicable to leach heaps on a field scale.

DEVELOPMENT OF NUMERICAL CODES

The two numerical codes used to model flow through the leach heap are: UNSAT, a one-dimensional unsaturated flow model, and TRANS, a one-dimensional solute transport model. Input to UNSAT consists of soil moisture - suction data obtained from hanging columns, and relative hydraulic conductivity-psi data obtained from the van Genuchten model (1978). The input to TRANS requires information on the flow velocity through the system (as calculated by the flow model UNSAT), and the change in moisture content, to caculate transport of tracers through the system.

UNSAT was written and documented by R. Khaleel and J. Yeh (1982) for one-dimensional flow through a porous medium. Since this program utilized experimental data for the soil-characteristic parameters, no changes were needed. The model solves the pressure- head form of the differential equation for one-dimensional, vertical, unsaturated flow in a homogenous and isotropic soil profile.

$$\mathcal{L}(\psi) = \frac{\delta}{\delta z}\left(K(\psi)\,\frac{\delta}{\delta z}(\psi - z)\right) - C^{*}(\psi)\,\frac{\delta \psi}{\delta t} = 0. \qquad (1)$$

where: L = differential operator
ψ = pressure head, in cm.
$K(\psi)$ = hydraulic conductivity in cm/sec.
$C(\psi)$ = specific water capacity
$\Theta(\psi)$ = volumetric water content
z = coordinate location (+ downward)

With a Neumann, or constant-flux boundary condition at the top boundary, and the following initial condition:

$$\text{Initial Condition: } \psi(z,0) = \psi_o(z)$$

$$\text{Boundary Conditions : } \psi(z,t) = \psi_{s_1}(z,t) \text{ on } s_1 \qquad (2)$$

$$K(\psi)\ (\frac{\delta\psi}{\delta z} - 1)n_i + q_{s_2}(z,t) = 0 \quad \text{on } s_2$$

the flow equation is solved for a semi-infinite column. A non-linear equation of this nature demands an iterative solution technique. A tridiagonal system of matrices is generated at each iteration and solved for the pressure head at the new time step for all nodes using a gaussian elimination scheme. The iterative procedure continues until the difference between the pressure heads from two successive iterations falls within a specified tolerance[7]. This program is documented in greater detail in Appendix 1.

TRANS is an upstream weighted finite element solute transport model written by Miniert (1983). Originally, it accounted for a step input of tracer or solute without retardation, decay or any sources or sinks. Since previous research indicates the potential for solution channeling, tracer adsorption, and tracer retardation, modifications will be required to account for these phenomenon in the numerical model. Additionally, a pulse input will be used instead of a step input in the experimental column, thus the boundary condition will also be changed.

The upstream-weighting technique was developed by Huyakorn and Nilkuha (1979) for transport in a porous medium. It is a discrete solution using a two-nodal point, one-dimensional element. The purpose of the upstream-weighting technique is to prevent numerical oscillation. (See Khaleel and Payne (1984) for a comparison of numerical dispersion by different numerical schemes.) Miniert (1983) used this technique when composing his one-dimensional solute transport model for porous media, TRANS.

TRANS approximates the one-dimensional homogeneous, and isotropic transient convective-dispersive equation shown below. Any sinks or sources, retardation of solute, or bacterial decay effects were disregarded.

$$\mathcal{L}(\psi) = \frac{\delta}{\delta z}\left(D\,\frac{\delta C}{\delta z} - vC\right) - \frac{\delta C}{\delta t} = 0 \qquad (3)$$

where: C = concentration
v = velocity
D = dispersion coefficient
t = time
z = space coordinate

The upstream finite-element scheme developed by Huyakorn and Nilkuha (1979) is supposed to decrease the oscillatory nature of the solution which is encountered when using Galerkin techniques of solution. (See Figure 1 for comparison of the different numerical techniques.) Weighted residuals are employed, of which the Galerkin formulation is

Figure 1. A comparison of the effects of numerical dispersion using various analytical techniques.

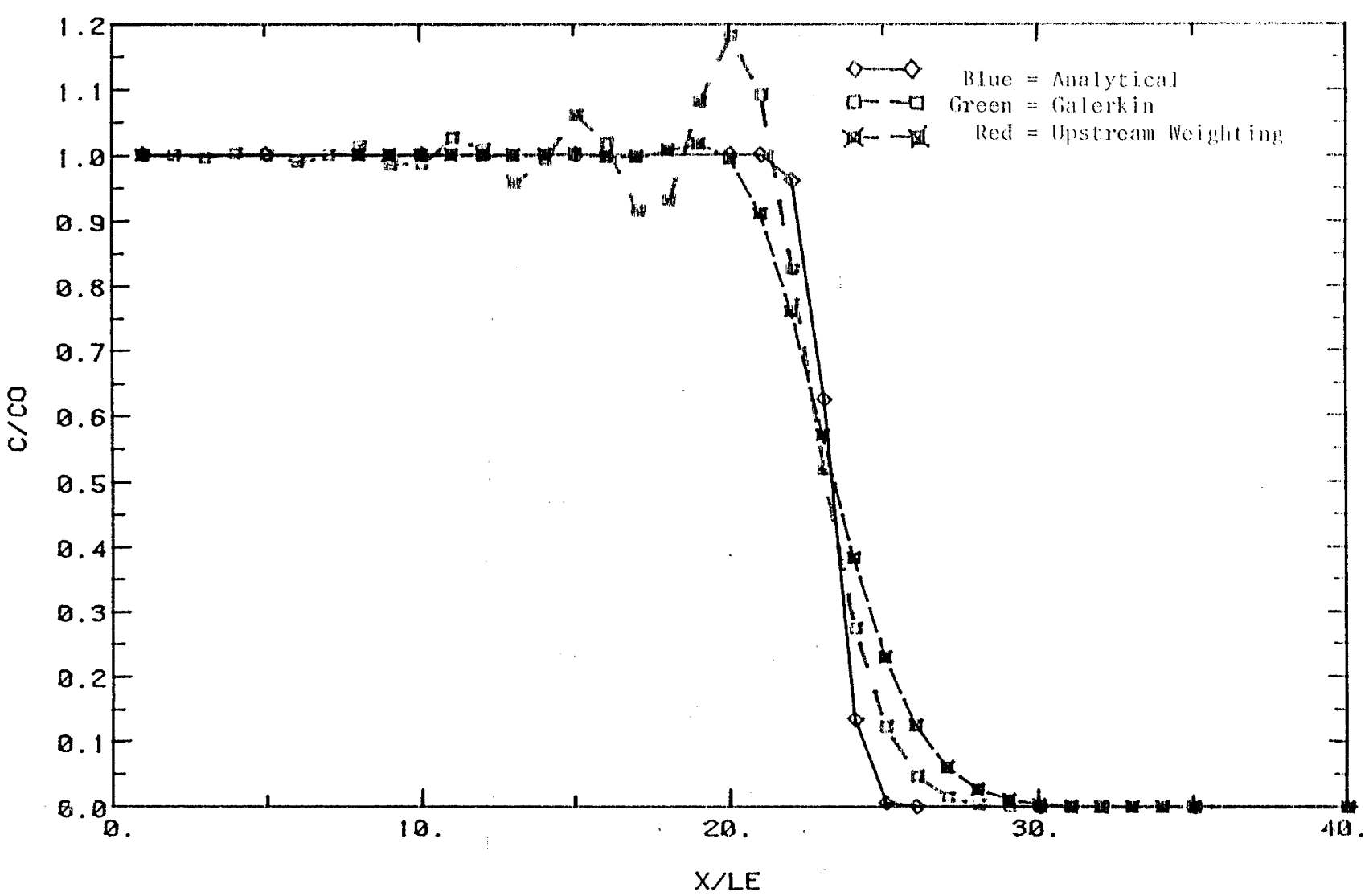

a special case. Asymmetric weighting functions are used on space derivatives, and a linear shape function is used on the time derivatives[8].

$$\int_R \frac{\delta C}{\delta t} N_i \, dR + \int_R \left(v\frac{\delta C}{\delta z} - D\frac{\delta^2 C}{\delta z^2}\right) W_i \, dR = 0, \quad i=1,n \qquad (4)$$

where: N_i = Shape Function; W_i = Assymetric Weight Function

The numerical equation for an interior node is obtained from the global matrix, which can be found in Appendix 1. Oscillations decrease as does overshoot, yet increased smearing of the concentration front occurs as the time-weighting goes from Crank-Nicholson to Full Implicit[9]. The time-weighting factor is resposible for the numerical dispersion causing the smearing, and becomes more pronounced with an increased dispersion coefficient. Figure 1 compares the relative amounts of numerical dispersion; smearing, oscillations, overshoot, and undershoot are all evident in the Galerkin solution. The upstream-weighting technique reduces the degree of oscillation and the amount of overshoot considerably, yet it does promote additional smearing due to the time-weighting factor. In addition, a large dispersion coefficient also tends to enhance the smearing effect for the upstream technique.

Utilizing a step input, the results of smearing, oscillations, and overshoot, for progressive movement of tracer along a vertical column, are shown in Figures 2 to 4.

Figure 2. Effects of numerical dispersion for the upstrem-weighting technique (TRANS) at early time.

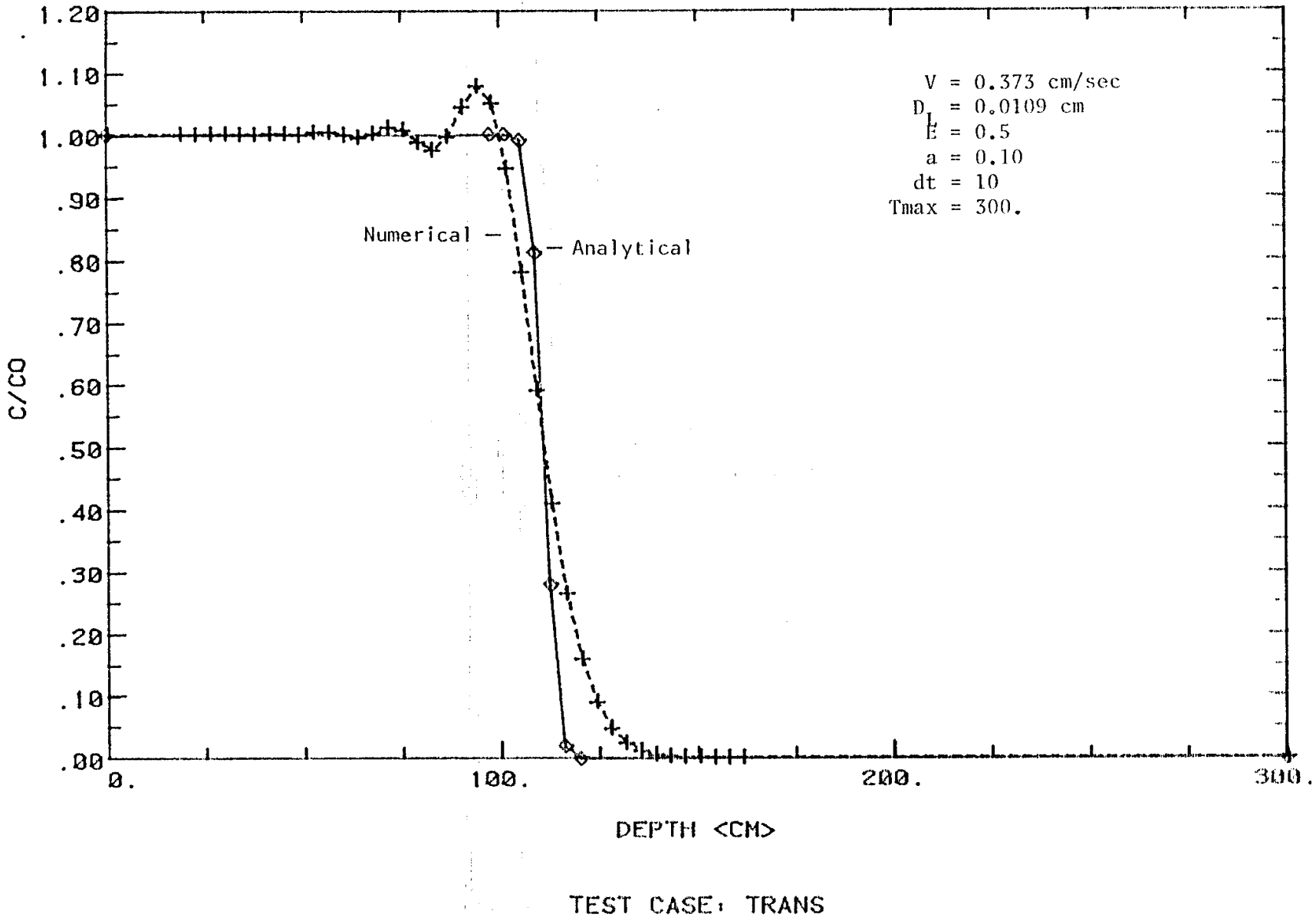

Figure 3. Effects of numerical dispersion for the upstream-weighting technique (TRANS) at t = 8 min.

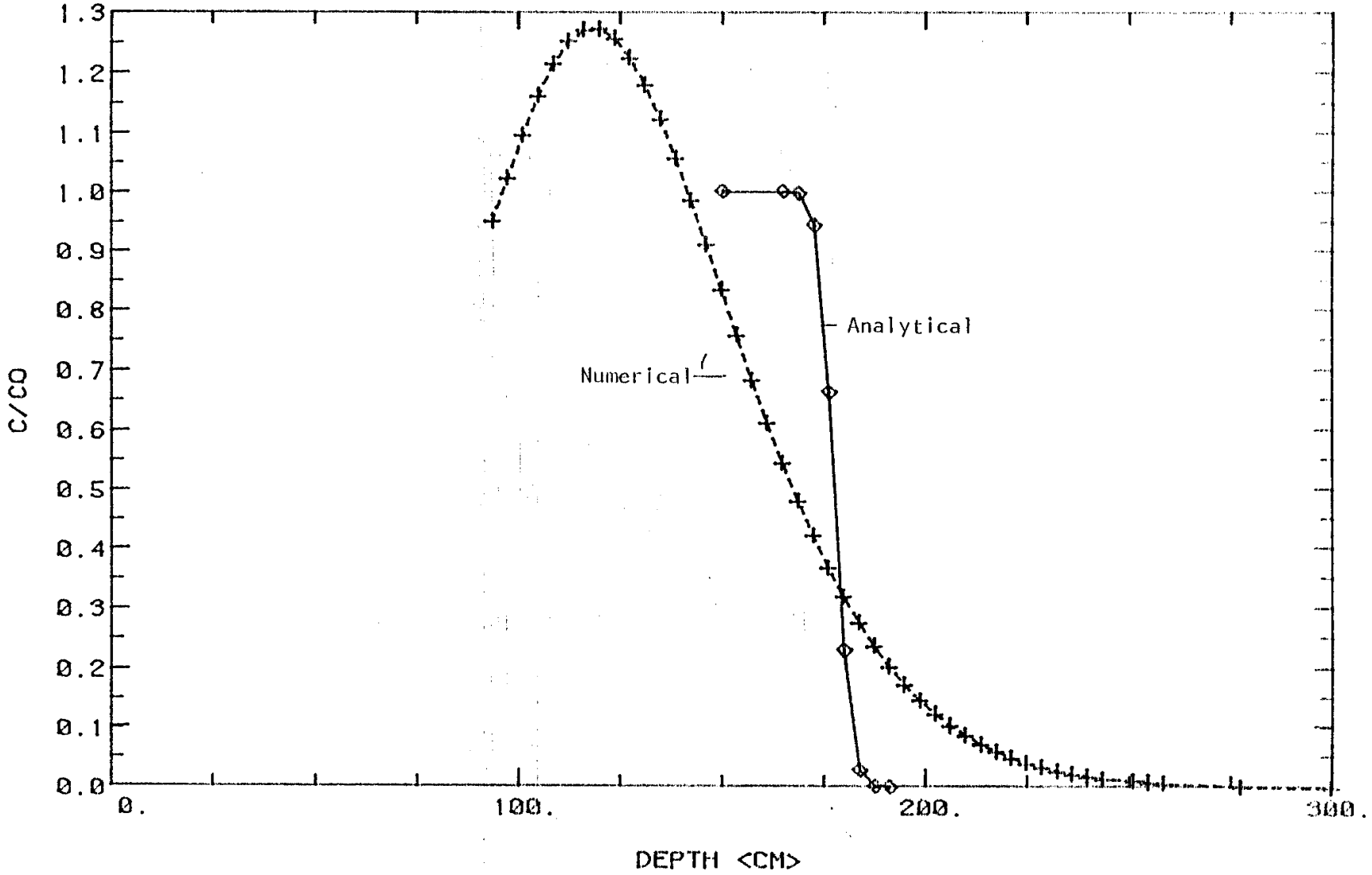

Figure 4. Effects of numerical dispersion for the upstream-weighting technique (TRANS) t = 12 min.

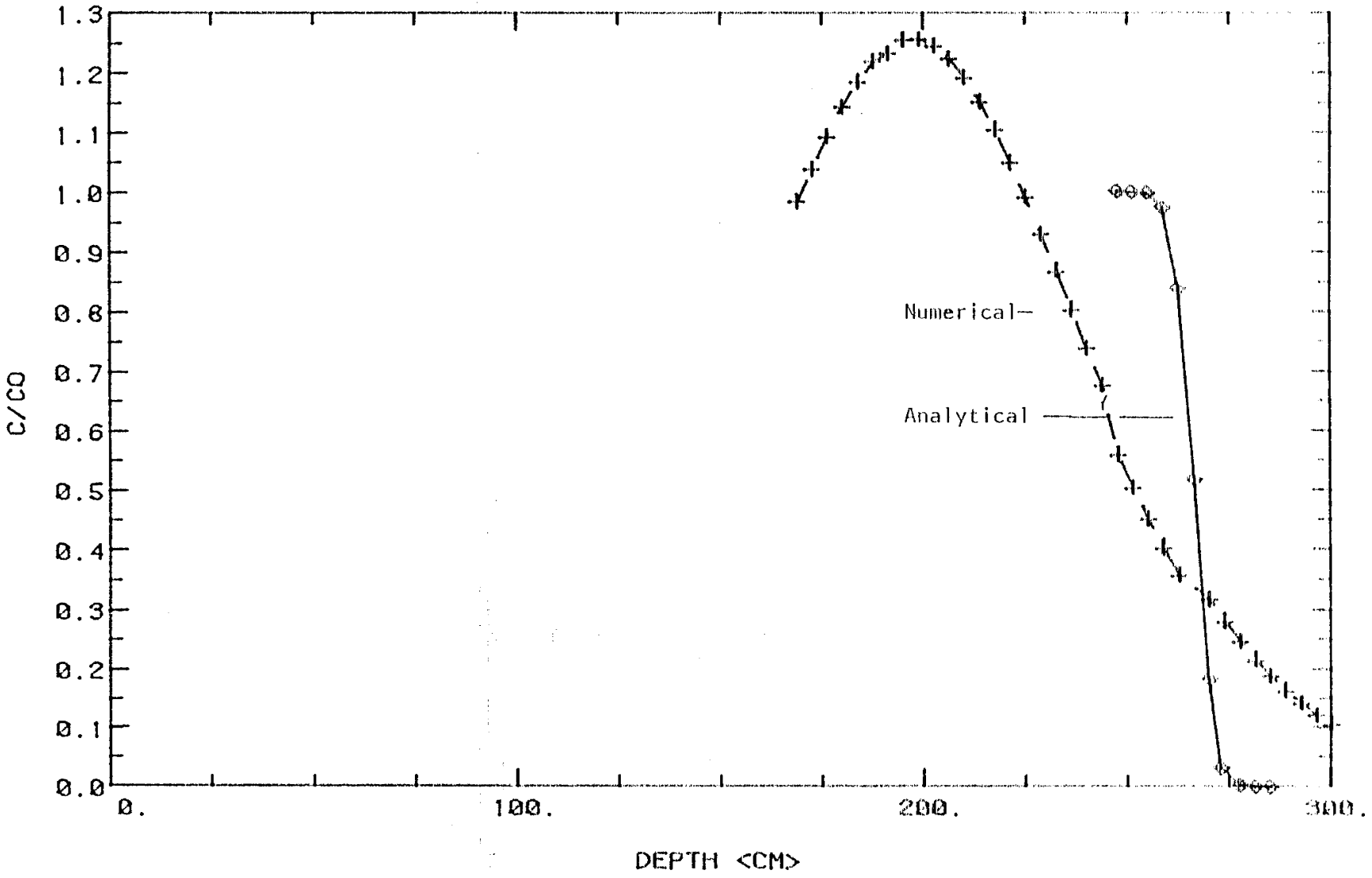

NUMERICAL RESULTS FOR TRACER DISTRIBUTION

This simulation was run for a relatively large dispersion coefficient. The coarse nature of copper ore (cobbles mixed with sands) would seem to indicate behaviour similar to that documented by Bouwer and Rice (1984). They discovered that the dispersivity in a stony soil was eighteen times that of the sand fraction alone. In this case, the dispersion coefficient is 1/30 of the velocity. Note that for the early time (Figure 2) the overshoot is rather minimal. Yet the overshoot increases considerably and the smearing to a lesser degree as the tracer progresses downward through the column (see Figures 3 and 4). Since the numerical code will be modified to account for a pulse input (the type of tracer input to the test column) the overshoot problem should dissipate. Nevertheless, smearing will be the unfortunate result of employing a finite element scheme for solving the convection-dispersion equation.

MODIFICATIONS TO TRANS

The numerical code TRANS incorporates a highly idealized concept of one-dimensional transport through a homogeneous medium. During the leach process, numerous solution channels are established, while other parts of the media remain isolated from contact with leachate. Inasmuch as solution channels may be considered analagous to fractures in a highly permeable system, the equation for solute transport through a fracture was used. Noorishad and Mehran (1982) have developed an upstream-weighted finite element solution for flow through a fracture. The governing equation for solute transport through a fracture is given by:

$$\mathcal{L}(C) = \frac{\delta C}{\delta t} - \frac{\theta D''_{zz}}{R_d} \frac{\delta^2 C}{\delta z^2} + \frac{qz}{R_d} \frac{\delta C}{\delta z} + \lambda C + M = 0 \qquad (5)$$

where: L = differential operator
c = concentration
O = porosity
z = uniaxial coordinate system
M = source/sink term
R_d^f = fracture retardation factor
= $1 + p_b K_d$
q_z = Darcy velocity

D_{zz} = Dispersion coefficient in z direction
λ = First Order Decay rate

Using this general equation for fracture flow, additional sources and sinks were considered negligible for the column

system, as was the first order decay of the tracer. Thus the equation for fracture flow reduces to:

$$\mathcal{L}(C) = \frac{\delta C}{\delta t} - \frac{\theta D_f'}{R_d} \frac{\delta^2 C}{\delta z^2} + \frac{\alpha z}{R_d} \frac{\delta C}{\delta z} = 0 \qquad (6)$$

Further development of shape and weighting functions and matrices for the numerical solution are discussed in Appendix 1.

The original code specified a step input of tracer. It accomplished this by simply setting the RHS (right hand side) matrix equal to one. (See Appendix 1 for details on the programs TRANS and UNSAT.) Since the application of leachate to the experimental column involves the addition of a fixed volume of tracer as a finite pulse, the numerical model will attempt to duplicate this process. In order to change a step input to a pulse input of a finite duration, the RHS matrix was set equal to one for a finite length of time, after which, the RHS matrix was allowed to equal zero. Thus, the input over a long period of time would be representative of a pulse or spike of finite volume.

Retardation of tracers due to adsorption onto the copper ore is intended for the non-conservative tracers. From the differential movement of the conservative vs. the non-conservative tracers, channelization and the degree of

ore contacted by leachate may be observed. In order to calculate the percent of surface area contacted by leachate, the retardation must be expressed in terms of surface area. If solution channels are considered to be analogous to fractures in a system of highly permeable material, then the expression for retardation of a solute may also be analogous. Burkholder (1976) suggested that a more appropriate expression for solute migration through fractured media be expressed on a per-unit-surface-area basis[10]. From Freeze and Cherry (1979), the expression for flow in a fracture is:

$$v/v_c = 1 + A\,K_d \qquad (7)$$

where: vv_c = relative velocity
K_d = distribution coefficient
A = surface area to void-space (vol.) ratio

The equation for the retardation of a solute becomes:

$$v/v_c = 1 + (SA/V_v)K_d \qquad (8)$$

where: v/v_c = relative velocity
V_v = void volume
K_d = distribution coefficient
SA = specific surface area

Therefore, knowing the distribution coefficient from batch tests for a particular tracer, and using the "traditional" equation expressed on a mass, rather than a surface area, basis (equation 8), the surface area of ore contacted may be

back-calculated. The retardation coefficient itself is substituted into the retardation term of the general equation for fracture flow, thus affecting the global and RHS matrices of the numerical code.

As a result of these changes, the modified solute transport model accounts for solution channeling via a changing moisture content along a vertical, adsorption of non- conservative tracers, and the percentage of ore-leachate contact. When coupled with results from the flow model UNSAT, predictions of the hydraulics governing fluid percolation in a leach pile, whether, in the laboratory or the field, should be possible. Results from the column experiment will be used to ascertain the veracity of the model.

The analytical solution used to test the accuracy of the numerical technique is the standard solution for the convection-dispersion equation for a pulse input in a one-dimensional system. This solution is given by:

$$c(z,t) = M/n_e \; G(z,t,z',t') \qquad (9)$$

where: M = mass of solute input
n_e = effective porosity
G = Greene's function

When z' and t' equal zero, equation 9 reduces to:

$$c(z,t) = M/n_e \exp -(z - Vt)^2/4D_L't \qquad (10)$$

This is the equation used as the analytical check for the solute-transport numerical code, TRANS.

CHARACTERIZATION OF ORE PROPERTIES

An ideal source of copper ore, in terms of cost and availability, was located at the Sullivan Center for In-Situ Mining. Waste ore from the large experimental tanks, constructed for the leaching of copper by Murr (1980) and others, was obtained from waste piles near the empty tanks. The only potential problem is the fact that this ore exhibits the rosy tinge characteristic of prior leaching with rhodamine-B tracer. The material represented in the experimental column should exhibit the same hydrologic characteristics as the waste ore which composes leach dumps in the field. For this study prior leaching of the ore is insignificant since only the hydrologic properties are of interest, and not the actual recovery of copper during the leaching process. Several tons of the material were brought to the laboratory for hydraulic characterization and loading into the column.

Prior to actually loading the column, the physical and hydraulic properties of the ore were determined. Properties of interest included particle-size distribution, porosity, available surface area, saturated hydraulic conductivity, the relationship between moisture content and pressure head, and the variation in unsaturated hydraulic conductivity with pressure head. These parameters were determined in the laboratory.

PARTICLE-SIZE DISTRIBUTION -MECHANICAL ANALYSIS

The particle-size distribution of a soil refers to the percentage of different sizes of particles that compose the particular soil. These sizes range from clay and silt to sands, gravels and boulders. Particle-size distribution curves indicate the percentage of soil particles coarser or finer than a given diameter. These curves are useful as indicators of average grain diameter, the type of distribution (distinct particle groups or a continuous array of particle sizes), and the uniformity index (which provides an idea of the relative closeness in size of the particles). Information on particle- size distribution has also been used to estimate hydraulic conductivity (Millington-Quirk, 1961 and others)[11].

The method used for determining the particle-size distribution curve was called mechanical analysis. In this case, only a coarse estimate of the relative amounts of material in each particle class is desired. Also, separation of the finer fraction, clays and silts, is not necessary.

Separation of the soil into its various particle groups was conducted by first weighing a sample of soil; then passing this sample through a series of sieves, graded according to decreasing particle diameter; down to the clay sized particles. The samples were placed on a mechanical

shaker and agitated for approximately 20 minutes. The portions remaining within each sieve were then weighed and the percentage of the total weight was recorded. The data and results of this analysis are presented in Table 1 and Figure 5.

The particle-size distribution curve (Fig. 5) indicates a coarse-textured material, since over fifty percent of the sample falls in the fine to coarse gravel or larger. Forty-eight percent of the sample is in the category of sand and only two percent clay. The average particle size is 6.1 millimeters. The uniformity coefficient is approximately 25, indicating a fairly well sorted soil.

Thus, from the results of the particle-size distribution analysis it is evident that the question of experimental scale will be important, since the majority of the sample is composed of coarse particles. Although the sample is fairly well graded, heterogeneities in packing may also arise during the course of the experiment. Consolidation of the larger grains as a result of leaching may also be a problem.

Table 1.

GRAIN SIZE DISTRIBUTION RESULTS

Total weight of sample and bucket = 3072.81 g.

weight of bucket = 571.35 g.

weight of sample = 2501.46 g.

Sieve Size	Weight of Subsample	Percent Coarser
1/4"	1267.1 g.	50.65
8	470.2 g.	69.45
10	78.9 g.	72.61
16	192.1 g.	80.29
20	113.8 g.	84.80
30	95.9 g.	88.67
40	67.4 g.	91.36
60	75.6 g.	94.39
100	42.3 g.	96.08
140	19.8 g.	96.87
200	13.2 g.	97.39
<200	20.2 g.	98.20

Figure 5. PARTICLE SIZE ANALYSIS

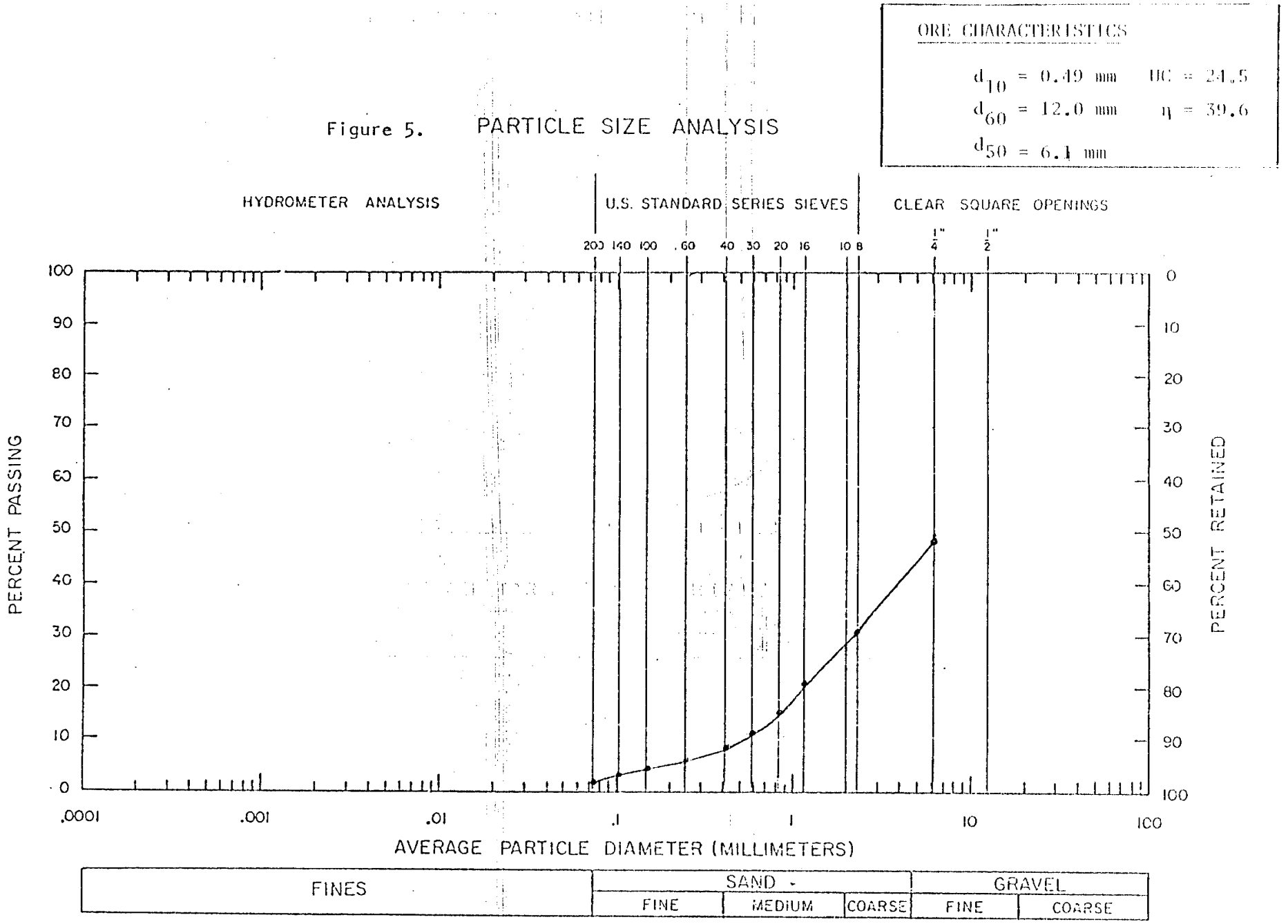

POROSITY

The amount of relative pore volume within a soil is termed porosity, and it is usually measured on a volumetric basis. The porosity is generally defined as the ratio of void volume to total volume and is expressed as a percentage[12]. The porosity may also be determined from the bulk mass and particle mass densities of a given sample.

$$n = V_v/V_t = 1 - p_b/p_s \qquad (11)$$

where: n = porosity
V_v = void volume
V_t = total volume
p_b = bulk mass density
p_s = particle mass density

The procedure for determining these quantities is outlined in Freeze and Cherry (1979, pg. 337).

The results of the porosity determinations can be seen in Table 2. The porosity of the gravel fraction is 56%, while that of the sand fraction is 39.8%. While these values seem to indicate a highly permeable system, the pore-size distribution is the major factor defining the primary avenues for infiltration in an unsaturated soil.

SURFACE AREA DETERMINATION -WATER VAPOR ADSORPTION

The specific surface area of a soil is defined as the total surface area of particles per unit mass or volume. The measurement of this parameter was necessary to determine the total available amount of surface area for adsorption since the column study utilized adsorbing tracers. Fine-grained soils have a much larger surface area than large-grained soils, and thus would be more likely to contact and adsorb greater quantities of tracer.

The method for determining surface area involved the formation of a monomolecular layer over the entire available surface area, generally by a liquid or inert gas. Orchiston (1953) developed a method using water as the adsorbing liquid and a vacuum dessicator for creating a moisture free environment for the soil. His method is as follows:

1. Dry samples over pure concentrated H_2SO_4 within a dessicator.
2. Samples should be placed on aluminum dishes in very thin layers.
3. Place concentrated H_2SO_4 in the evacuated dessicator and maintain temperature constant. (A water bath at 25 degrees C).
4. After four changes of acid on successive days samples should be of constant weight.
5. Add a dish of H_2SO_4/H_2O mixture to measure the relative pressure at equilibrium. (Analyze samples by means of titration).

6. After each equilibrium, add small amounts of acid-water mixture to increase the relative pressure. Equilibrium should be attained in 24 hours.

7. From the weights of the acid-water mixtures at each equilibrium, the relative aqueous vapor pressures can be obtained from plots of water vapor pressure vs. acid concentration data. (International Critical Tables, Vol. 3) [13].

The basis for the liquid or gas vapor adsorption method lies in the work of Brunauer et al. (1938). He proposed an index of surface area which defines the area of the adsorbent completely covered by a monolayer of adsorbate. Water adsorbed increases with increasing relative pressure of the water. Temperature must be kept relatively constant, since the amount of adsorption will decrease if temperature decreases. At relative pressures below 0.05 and above 0.35, values for surface area as determined by the BET theory fall below and above, respectively, experimental results.

An empirical relationship based on the polarity of the water molecule was developed by Bradley (1936), which fits available experimental data for relative pressures up to 0.9. Assuming the first layer of the adsorbed atom is polarized, subsequent layers attract each other through this polarization of charge. As the film thickness increases, however, the strength of polarization as an aid to adsorption, decreases. The specific surface area as determined by the Bradley polarization theory is obtained from the following equation:

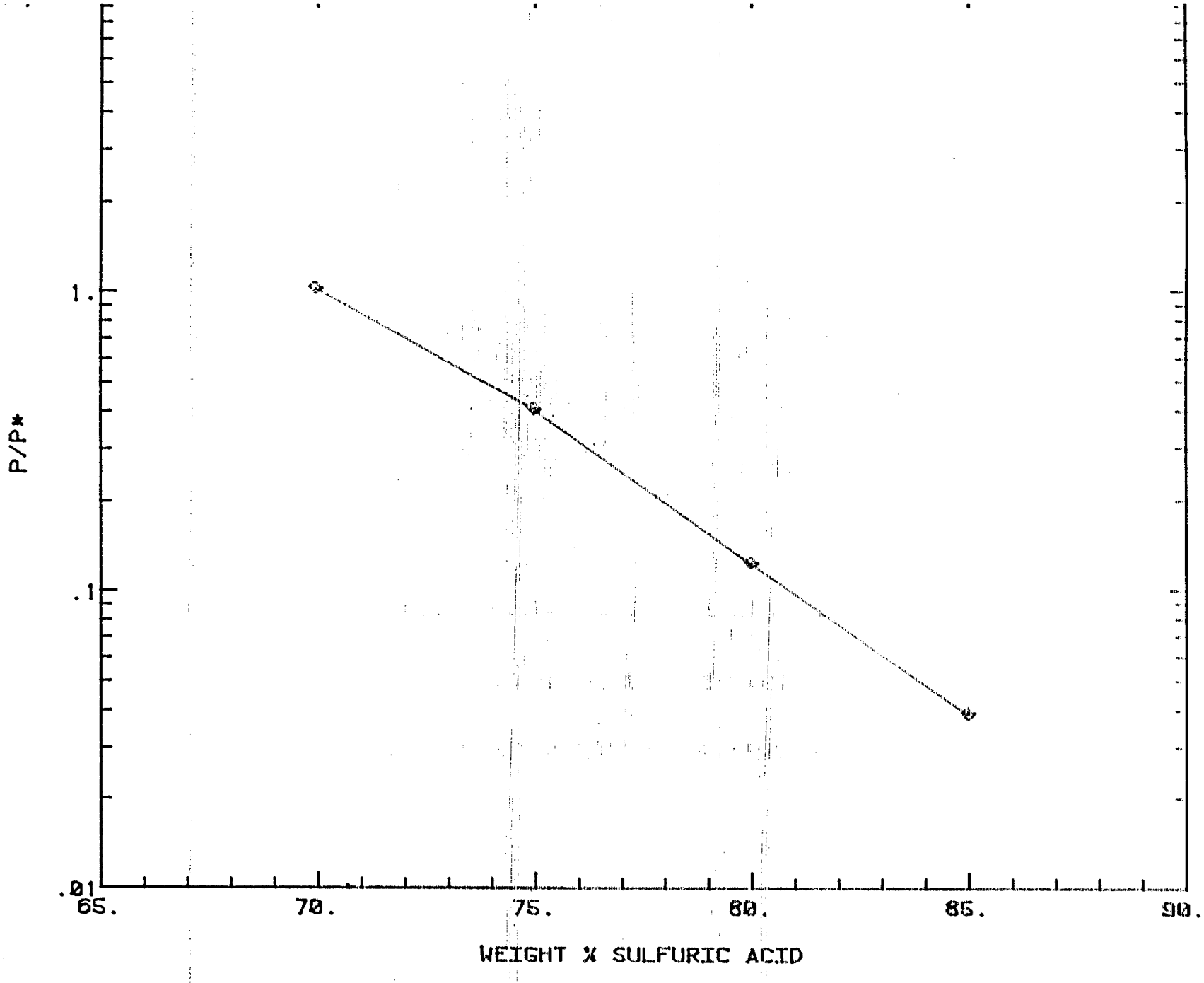

Figure 6. P/P* VS WEIGHT % SULFURIC ACID

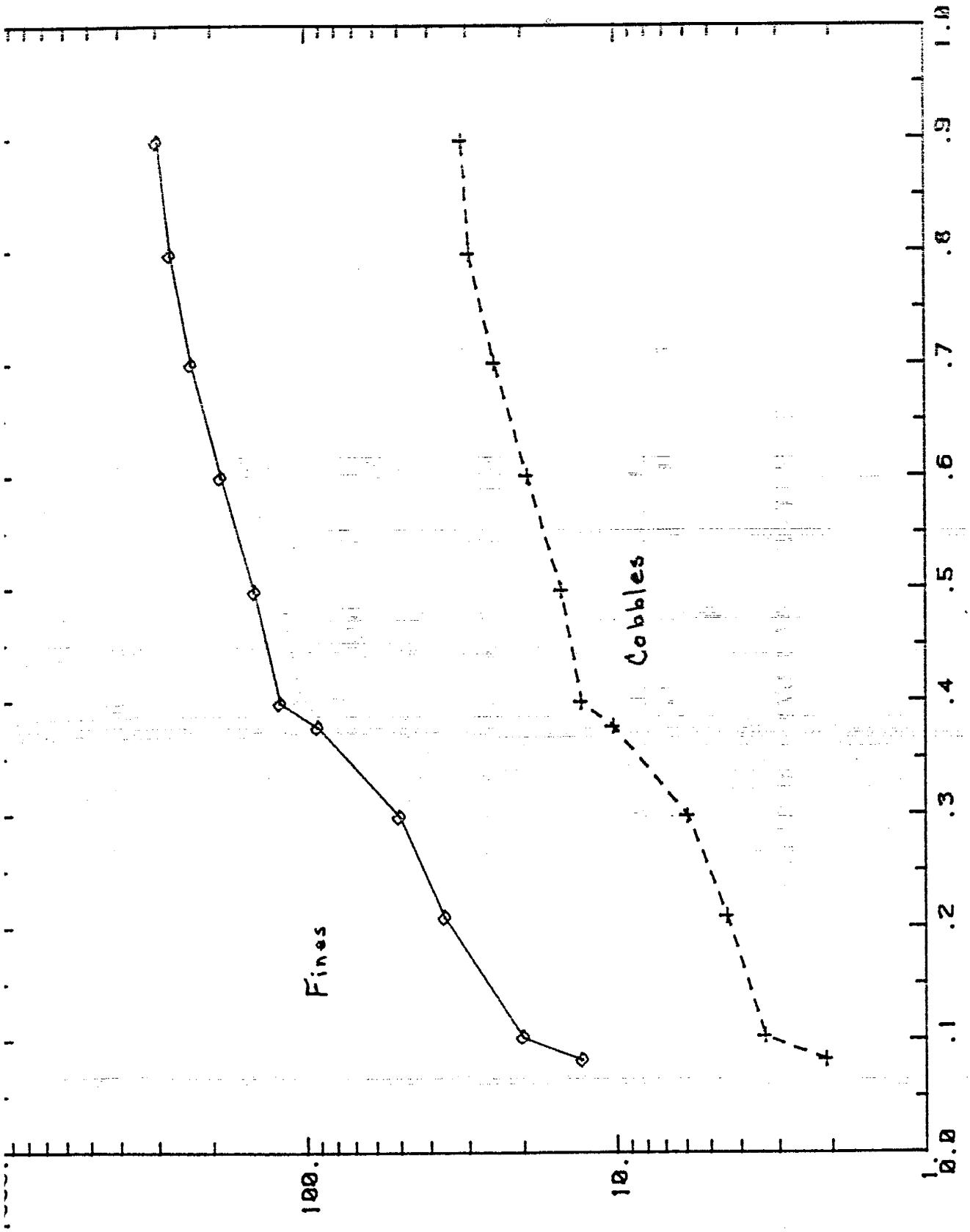

Figure 7. ADSORBED WATER VS. RELATIVE PRESSURE

Table 3. SURFACE AREA DETERMINATIONS - WATER VAPOR ADSORPTION METHOD

Rel. Pressure *P/Po	Fines mg. Ad/100g.	Cobbles mg. Ad/100g.	Sfines m^2/g	Scobbles m^2/g
.0839	13.0	2.1	.0769	.0124
.1043	20.2	3.3	.1057	.0173
.2104	36.1	4.4	.1287	.0157
.2998	50.5	5.9	.1475	.0172
.3792	92.3	10.2	.2339	.0258
.4010	122.2	12.9	.2989	.0312
.4997	147.3	14.8	.3101	.0315
.6013	187.9	19.2	.3418	.0349
.7020	234.8	24.4	.3686	.0383
.7989	273.3	29.3	.3661	.0349
.8991	301.2	31.1	.3253	.0336
.9980	323.9	33.5	.1722	.0179

*P/Po obtained from titrations of H_2SO_4/water mixtures with NaOH to a phenolpthalein endpoint. The results were compared to % H_2SO_4 (by weight) vs. vapor pressure data obtained from the International Critical Tables Vol. III.

$$S = 18.06 \; X \; /(.337 - \log \log Po/P)$$

Where: X = mass of adsorbed water vapor

Po/P = 1 / Relative Pressure

S = Specific surface in m^2/g.

$$S = 18.06\ X/(0.337 - \log \log p^*/p) \qquad (12)$$

where: p^*/p = inverse of relative water vapor pressure
X = mass of adsorbate
S = specific surface

The quantity p/p^* may be obtained from the International Critical Tables, volume 3, pg. 303. This reference contains the vapor pressure vs. acid-concentration values. Figure 6 shows the vapor pressure vs. acid concentration relationship for 65 - 90% H_2SO_4 by weight. Appropriate values for p/p^* were obtained from this figure and substituted in equation 12 along with the mass of water adsorbed. The trend of adsorbed water with relative pressure is shown in Figure 7. As the relative pressure approaches unity, the mg H_2O adsorbed per gram levels off, due largely to a lesser concentration gradient. The values calculated using equation 12 are presented in Table 3. Thus the average values in cm^2/g. obtained from this determination are: $S_{cobbles}$ = 0.03406 cm^2/g; S_{fines} = 0.335 cm^2/g; and S_{clays} (as calculated from Hillel, 1980) = 400 cm^2/g. Accounting for the weight percentage of each fraction in the total samples; the total specific surface area available for adsorption is 8.178 cm^2/g.

It is interesting to note that the small amount of clay material in the soil profile will be responsible for the majority of surface area available for adsorption. However, if strongly sorbing tracers are used, enough tracer should

be adsorbed by contact along the length of the column to show an appreciable decrease in concentration with respect to the conservative tracers. In addition, with progressive leaching of the column, many of the clays will be washed out of the column in suspension, thus leaving an even smaller degree of available surface area for contact.

Saturated Hydraulic Conductivity -Constant Head Permeameter

The hydraulic conductivity of a soil refers to the material's ability to transmit fluid. The coarse texture of the copper ore presents an interesting problem, since the presence of such a large amount of coarse material tends to interfere with soil physicist's methods for characterizing soils. Some work has been done on the hydraulic properties of stony soils: Mehuys et al (1975) determined that the presence of stones did not affect K - Psi curves at low (-) pressures; while for the K - Theta relationship, the bulk conductivity was higher with stones present[14]. Bouwer and Rice (1984) determined the unsaturated and saturated hydraulic conductivity values for the sand fraction of a mixed sample of cobbles and sands. Then using a simple relationship between the void ratios of the sand and cobble fractions, a value for the unsaturated hydraulic conductivity of the bulk medium was obtained. This method, due to its simplicity and reasonable agreement with experimental results, will be employed to approximate the unsat K - Psi curves for the copper ore.

A constant-head permeameter like the one shown in Figure 8a was used to determine the saturated hydraulic conductivity of the sand fraction (everything passing through sieve 8). The following equation was used to calculate the hydraulic conductivities of the samples at the

Figure 8a

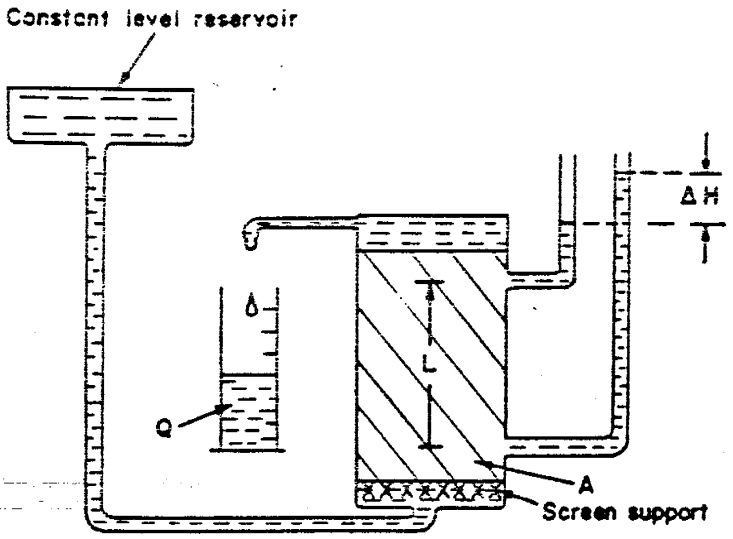

Fig. 8.13. The measurement of saturated hydraulic conductivity with a constant head permeameter; $K = VL/At\,\Delta H$. From: Hillel, Fundamentals of Soil Physics pg. 187.

Figure 8b

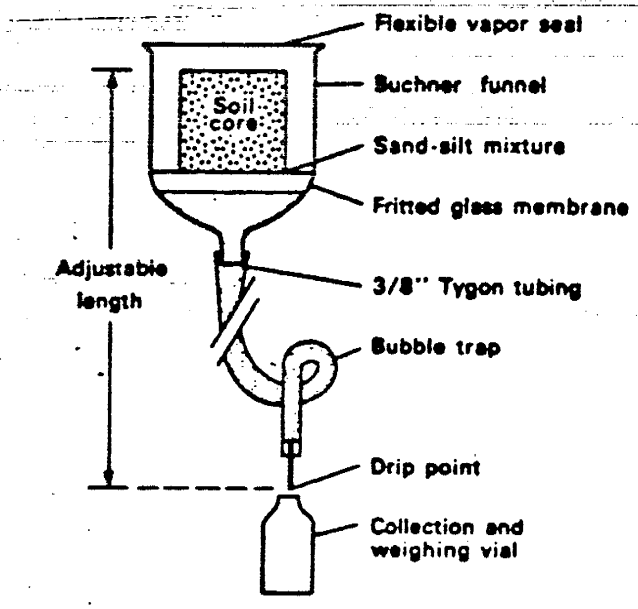

Fig. 1—Schematic of apparatus used for outflow measurements.

From: Jaynes & Tyler. "Comparison of One-Step Outflow ..." SSSAJ 44, pg. 904.

specific water temperature of the permeameter, then the viscosity effects were corrected for to arrive at saturated hydraulic conductivities for temperatures of 20 degrees.

$$K = Q\,L / A(h_s - h_r) \qquad (13)$$

where: K = saturated hydraulic conductivity
Q = volumetric rate of flow
L = length of sampler
A = cross-sectional area of sampler
h_s = height of water in sampler
h_r = height of water in reservoir

The results of the permeameter tests for K_{sat} vs. time are shown in Figure 9. Generally, the hydraulic conductivities stabilized at approximately 72 hours, and the average K_{sat} value obtained for the samples was 0.057 cm/sec. From the relationship developed by Bouwer and Rice:

$$K_b = K_s\,(e_b/e_s) \qquad (14)$$

where: K_b = bulk K of the entire sample
K_s = K_{sat} of the sand fraction
e_b = void ratio of the bulk sample
e_s = void ratio of the sand fraction

the void ratio of the boulder/sand mixture was 0.32; while that for the sand alone was 0.69. The K_{sat} for the sand fraction as determined by the permeameter test results was 0.0566 cm/sec or 48.9 m/day. Substituting these values in Equation 14 provides a K_{sat} value for the bulk medium of 22.68 m/day. The raw experimental data are found in

Figure 9. Hydraulic Conductivity changes with time for saturated samples.

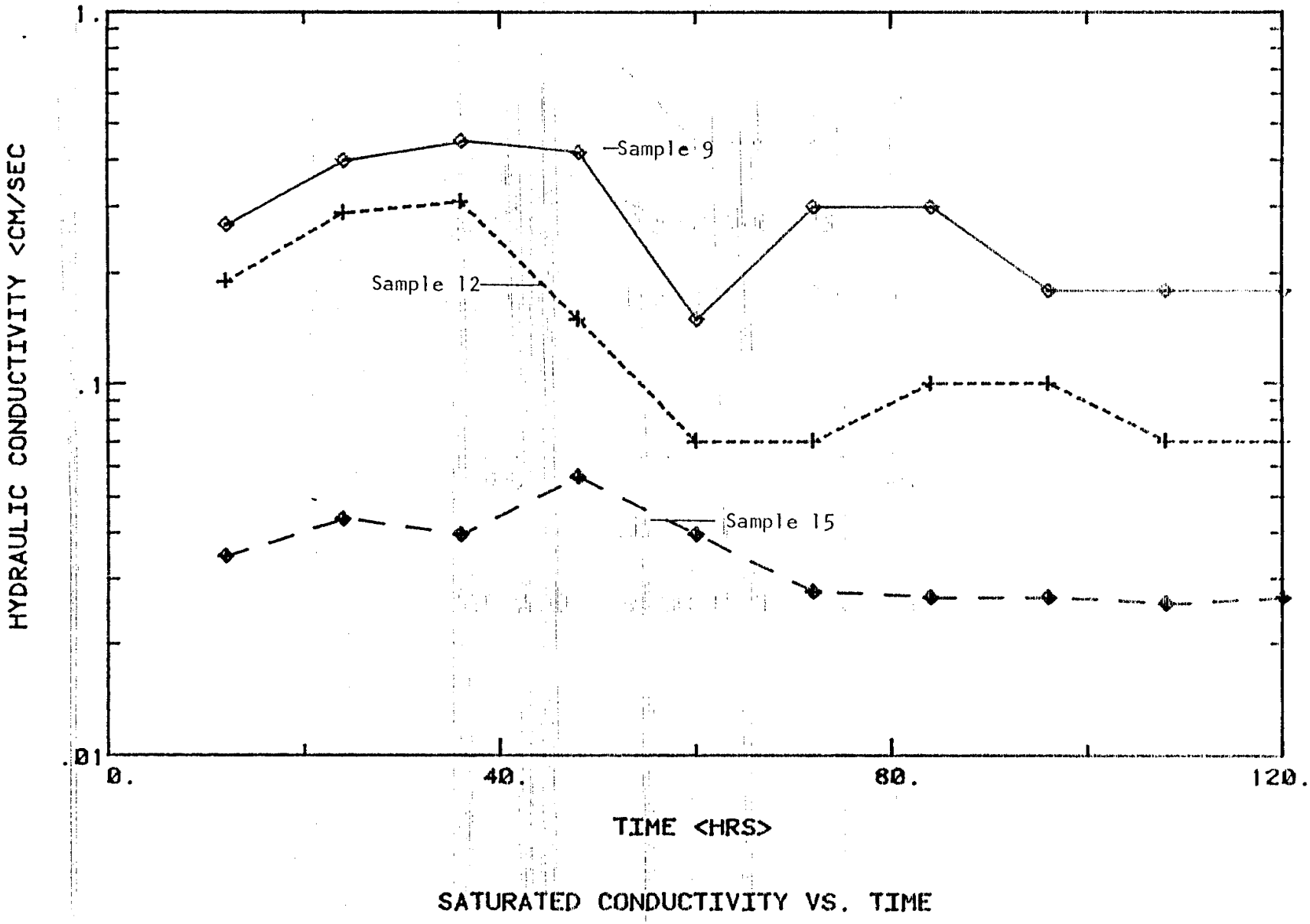

Appendix 2.

Soil Moisture Characteristic Curve -Hanging Column

The procedure for wetting the soil profile during the column experiment involved infiltration from constant flux source. This entailed the wetting of an initially dry sample of copper ore. Thus, the relationship between soil wetness and matric suction (pressure head) is of interest, specifically, the wetting curve.

The hanging-column method for determining the soil-moisture characteristic curve has been described by Bouma et al (1974) and Hillel (1980). The apparatus used is shown in Figure 8b. Samples rest in hydraulic contact with a porous ceramic plate. A graduated burette is adjusted above and below the sample to allow for wetting or drying, as desired. The suction is measured as the position of the equilibrium water meniscus in the burette below the middle of the sample. Water-content changes are reflected in the change of water level, measured in ml, from the gradations of the burette. With a known starting point (saturated or dry), coupled Theta - Psi measurements are obtained. Results of the hanging column analysis for two samples are shown in Figures 10 and 11. Samples were the same ones used in the permeameter estimation of saturated hydraulic conductivity, and correspond to sample numbers 12 and 15. Therefore, saturation was the starting point for the hanging column analysis.

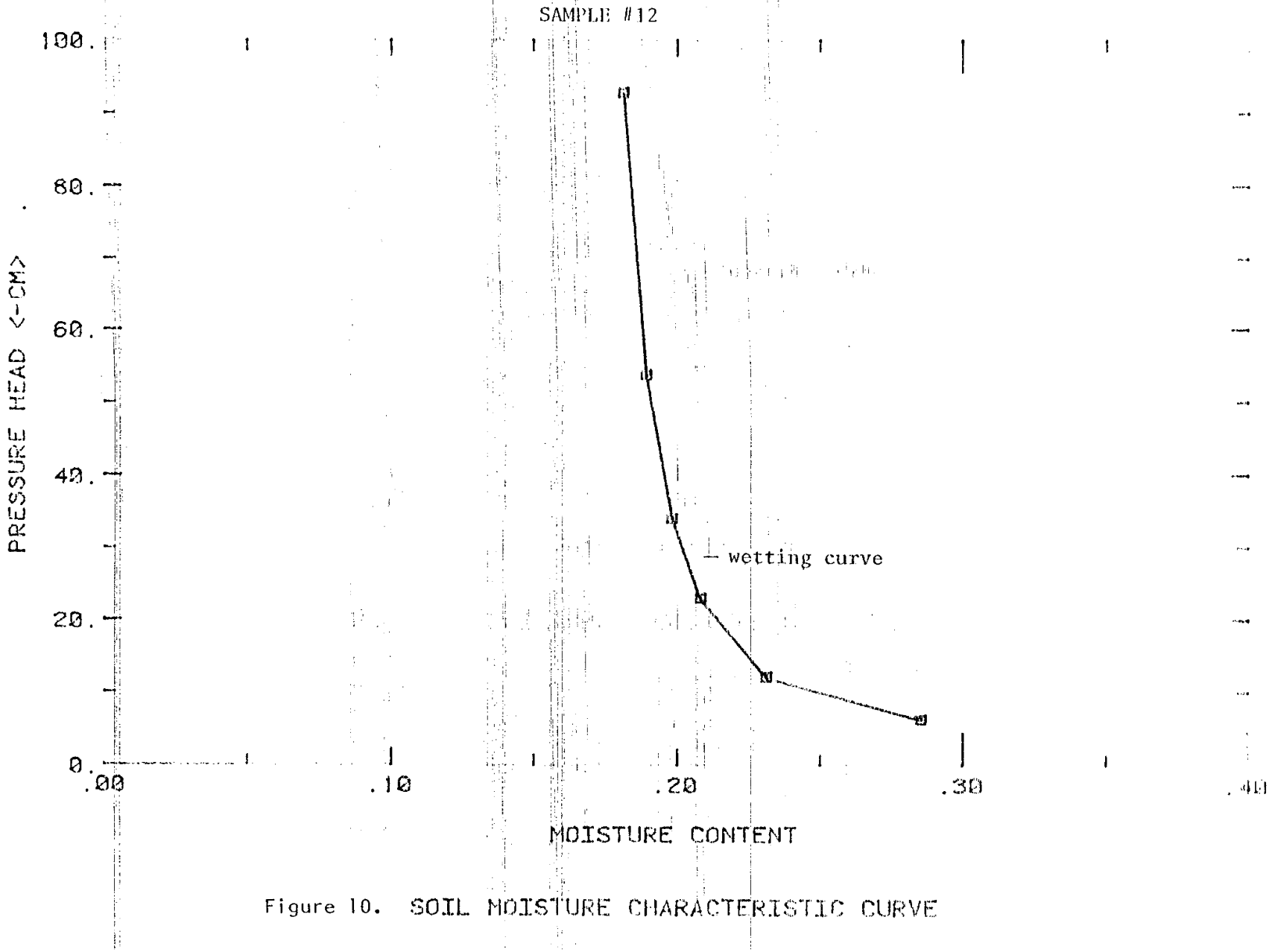

Figure 10. SOIL MOISTURE CHARACTERISTIC CURVE

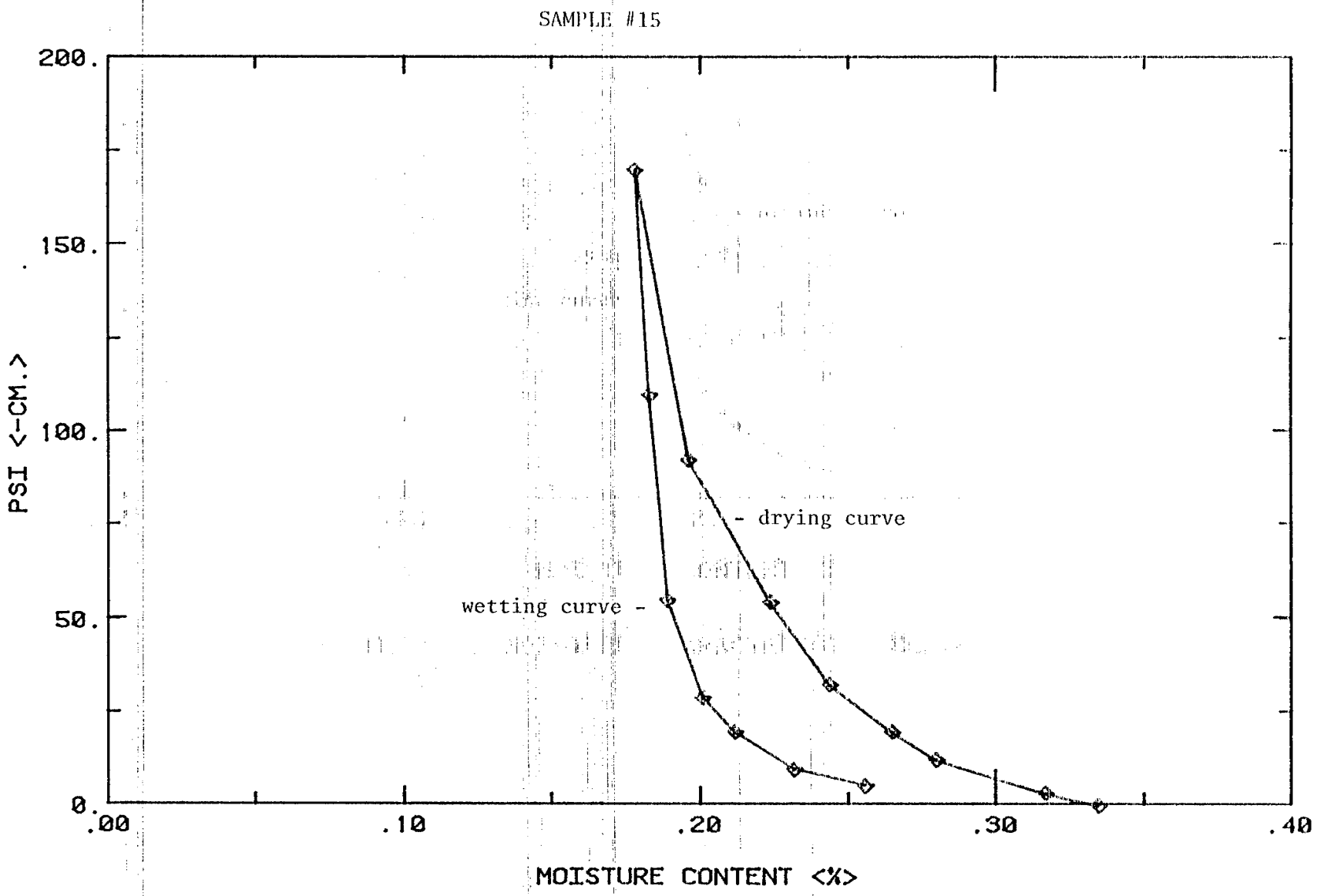

Figure 11. SOIL MOISTURE CHARACTERISTIC CURVE

Sample 12 (Figure 10) shows a slow release of water upon wetting; an indication of very low hydraulic conductivities in the dry regime. But note the high value for the residual-moisture content: $\theta_r = 0.18$. This high residual-moisture content, coupled with a relatively high saturated moisture content, is more characteristic of a clay than a sand.

The drying curve for sample 15 (Figure 11) shows a quick release of water upon a slight increase in suction. However, once psi is greater than -100 cm., the moisture content remains fairly constant at 0.18. Since further increases in suction do not appreciably change the water content of the soil, it must be assumed that the material is rather fine or has a relatively high clay content. The air entry value is essentially negligible, also a characteristic of clay soils. Also note the hysteresis of the wetting and drying curves. It is more difficult to rewet the sample than to dry it, since the low hydraulic conductivities of the dry region must be overcome.

The grain size distribution may have been altered by the prolonged saturation of these samples in the permeameter tests. In leaching experiments, progression towards finer sized particles has been documented by Murr (1980)[15]. As moisture content increases and water diffuses into aggregates of particles, the water penetrates further into the core of the aggregate and may eventually split the

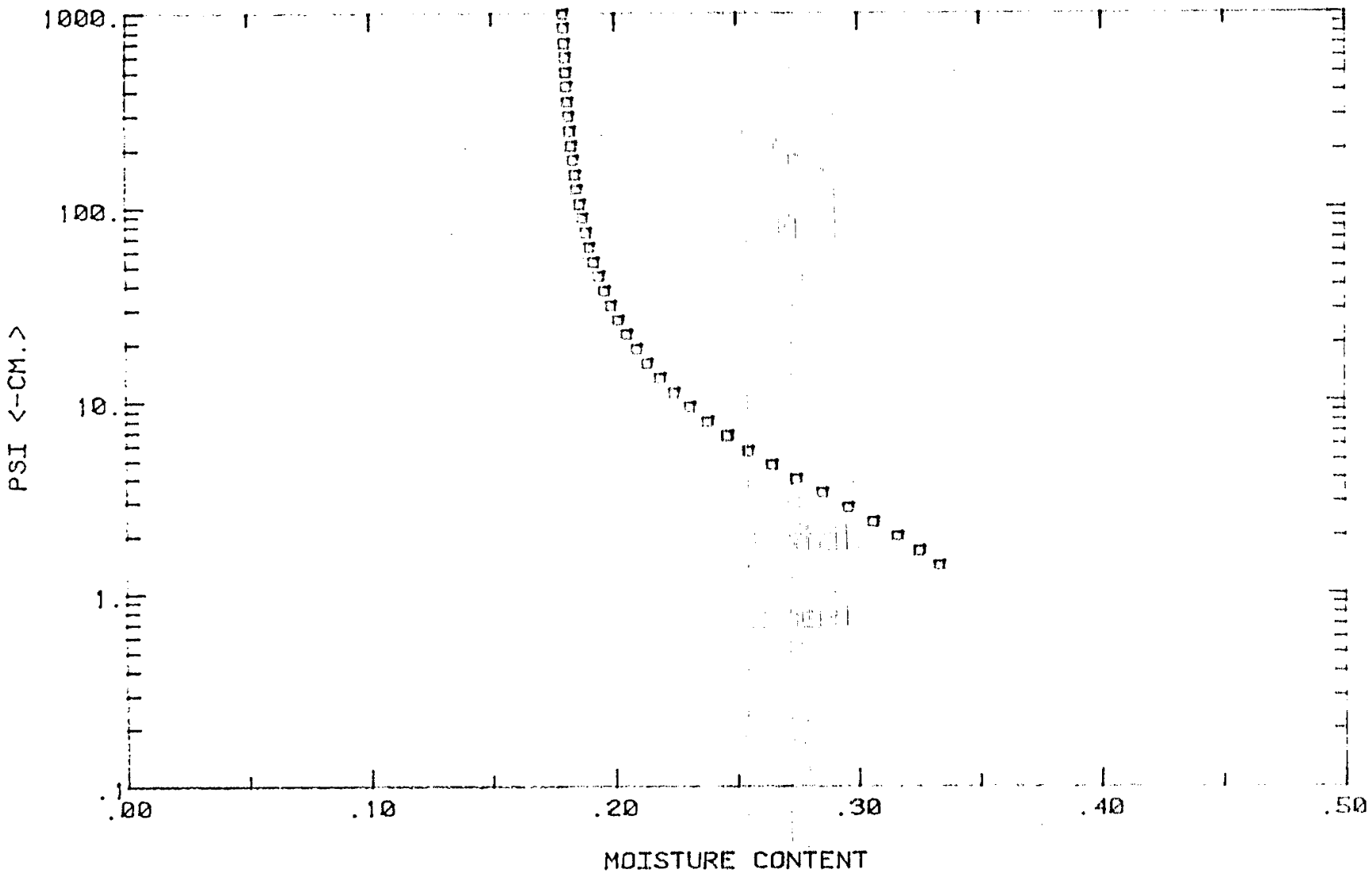

Figure 12. THETA-PSI CURVE - VAN GENUCHTEN MODEL

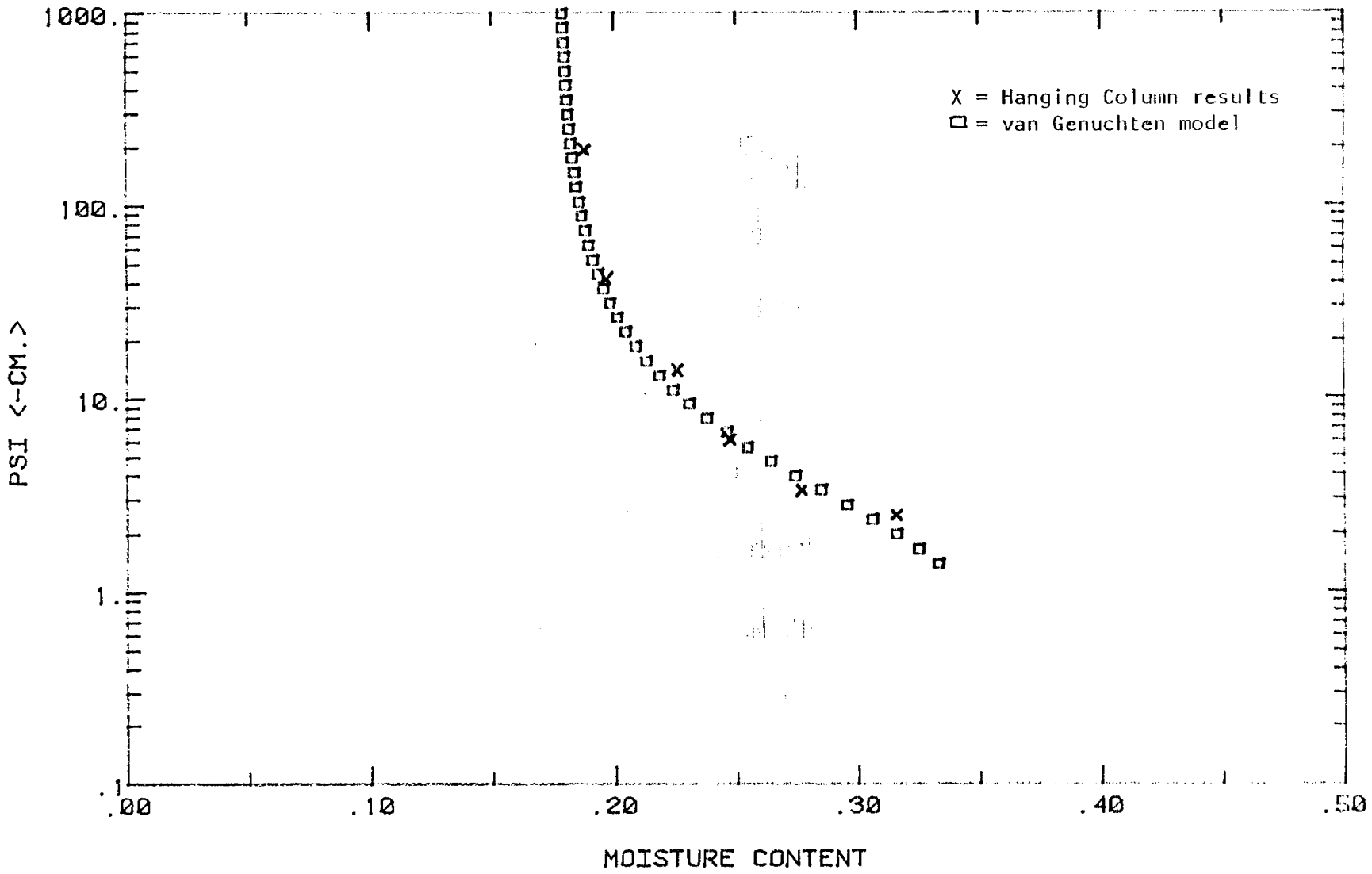

Figure 13. THETA-PSI CURVE - VAN GENUCHTEN MODEL

Relative Conductivity - Psi Relationships

The relative unsaturated hydraulic conductivity is a difficult parameter to measure in the field or in the laboratory, since the range of hydraulic conductivity values may span many orders of magnitude. Thus, many methods for the analytical estimation of relative hydraulic conductivity (K_r) and its relation to pressure head (psi) are available.

Millington-Quirk (1961) developed a method commonly used for estimation of the K_r - Psi relationship. This method, based on grain size distribution, is not very accurate for inhomogeneous media, and may be rather tedious to use[16]. A simple computer model (included in Appendix 4) was written to solve the Millington-Quirk equation:

$$K_i = K_s \left|\frac{\theta_i}{\theta_c}\right|^c \frac{\sum_{j=1}^{m} ((2j+1-2i)\ \psi_j^{-2})}{\sum_{j=1}^{m} ((2j-1)\ \psi_j^{-2})} \qquad (15)$$

Results of the Millington-Quirk analysis are shown in Figure 14.

Brooks and Corey (1964) developed a method as accurate as that of Millington-Quirk, however a discontinuity occurs at the bubbling pressure. This discontinuity may also cause convergence problems in numerical models.

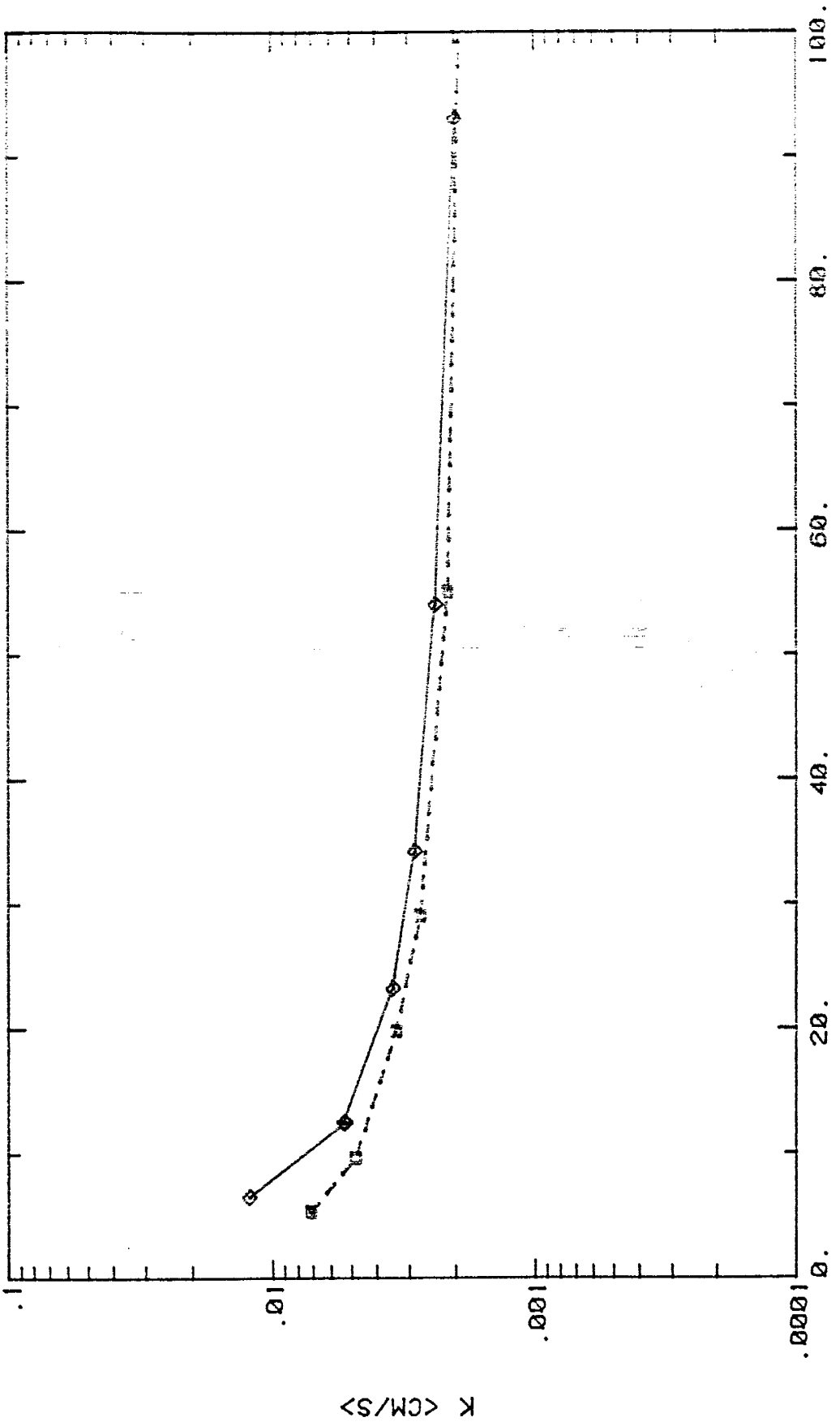

Figure 14. MILLINGTON-QUIRK: K - PSI

Mualem (1976) has developed a model for K_r based on soil-moisture characteristic curves and saturated hydraulic conductivity data. This model lead to the derivation of a closed-form analytical equation for relative hydraulic conductivity[17]. Riel van Genuchten (1978) encoded the Mualem model (two or three parameter fit) and the Burdine (1953) analytical model to estimate the relationship between K_r and Psi from soil moisture characteristic curves and $K_{sat/@}$ data. The numerical code for the van Genuchten model is presented in Appendix 4.

The van Genuchten model was run with the corresponding input data obtained from hanging-column and constant-head-permeameter results. The K_r - Psi data are presented in Figure 15 while the soil- moisture characteristic curve obtained from a curve-fitting procedure was shown in Figure 12. A problem to be considered concerns the changing particle-size distribution during prolonged saturation. Sieve analysis revealed the material to be largely composed of sands and cobbles, with only a minimal amount of clays, whereas the residual water content and the curve-fitting parameters estimated by the model reveal the characteristics associated more commonly with clay-dominated materials.

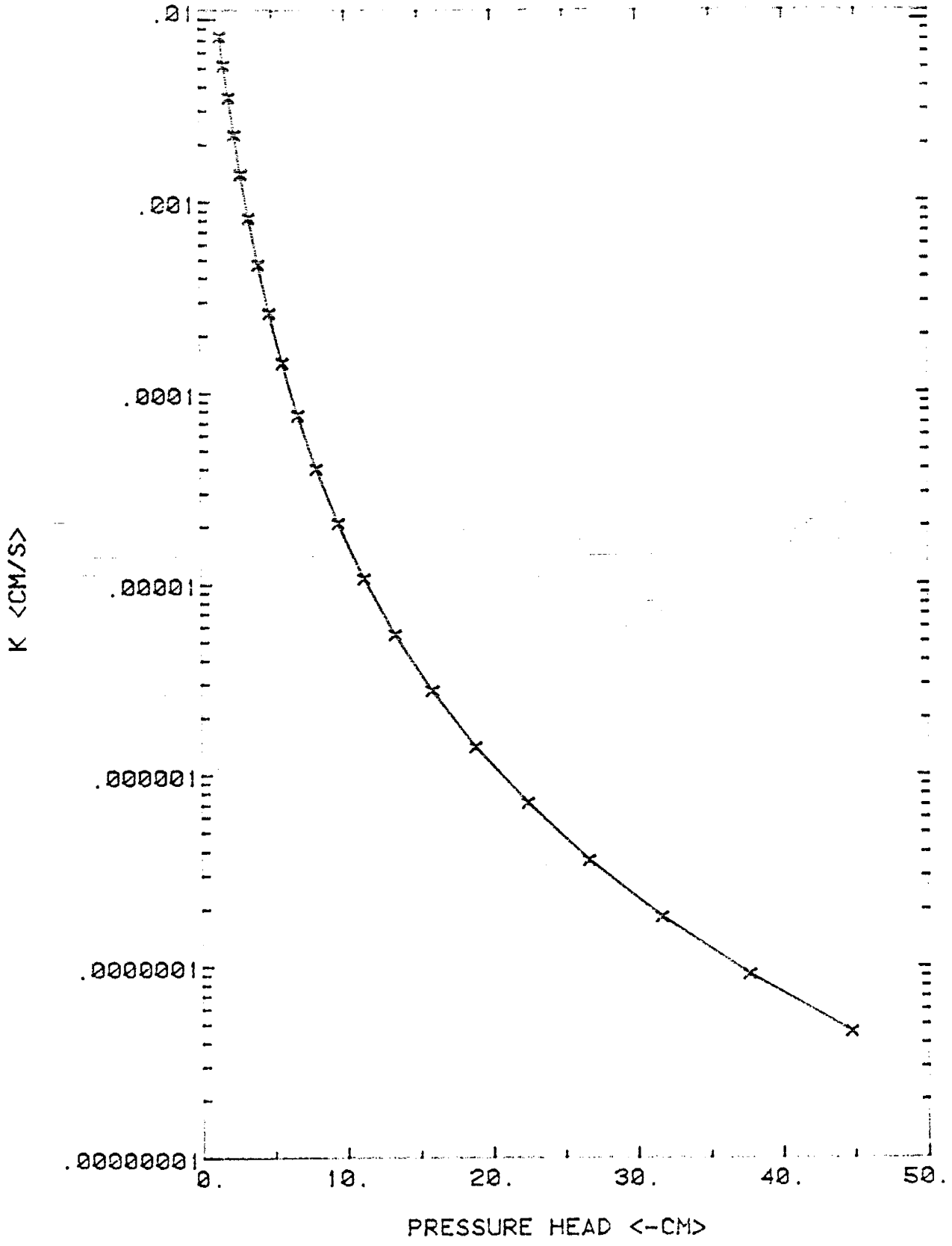

Figure 15. HYDRAULIC CONDUCTIVITY VS. SUCTION

TRACER SELECTION

During the column experiment, tracers were employed to determine the velocity, pore volume, dispersivity, and extent of material contacted by the leachate. In an effort to resolve all of these parameters during a single test multiple tracers are required of a conservative and non-conservative nature. Conservative tracers move with the bulk water and closely follow the path of the water molecules. Non-conservative tracers exhibit some degree of adsorption when in contact with the soil material, and thus, are retarded in their velocity of movement through the system.

The choice of which combination of tracers to use is a difficult one. Two standard tracers in use are chloride (conservative) and Rhodamine-B (non-conservative). Chloride is a good groundwater tracer for systems with small amounts of clay, (which would minimize any anion exclusion effects), since chloride breakthrough coincides with bulk water breakthrough. Rhodamine-B is a fluorescent dye which exhibits a high affinity for adsorption on copper ore and has been extensively documented by hydrometallurgists as a good tracer for determining the extent of solution contact with ore. Since the copper ore had been exposed to Rhodamine-B from prior leaching experiments, it was necessary to conduct a series of batch tests to determine

whether sufficient tracer could be detected following adsorption. Analytical determinations of both of these tracers are quite simple, utilizing a chloride electrode which detects the presence of chloride ion in solution, and the fluorometer, which detects the amount of fluorescent emissions within a sample.

The combination of chloride ion and rhodamine-B will be used as "reference" tracers. In addition to the pair of "reference" tracers, experimental organic acids for potential use as groundwater tracers were provided by Dr. Harold Bentley (Hydrogeochem Inc. Consultants). Their names and structures are shown in Figure 16, while intrinsic physical and chemical properties are listed in Table 4. Of these tracers, para-fluorobenzoic acid (PFB) and meta-trifluorobenzoic acid (m-TFMB) are considered to be conservative in nature, while the rest, classified as amines, are thought to be potentially non-conservative. All of these experimental tracers may be measured using reverse-phase high pressure liquid chromatographic techniques (reverse-phase HPLC).

Fluorometry is an analytical technique used to measure the degree of fluorescence of a tracer after contact with a material of interest. In this case, rhodamine-B is the tracer being used to tag copper ore contacted by the leach solution during a column experiment. Since the copper ore has a history of rhoadmine-B contact, batch tests were

Figure 16.

CHEMICAL STRUCTURE OF ORGANIC TRACERS

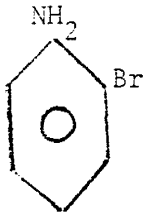

o-Bromoaniline

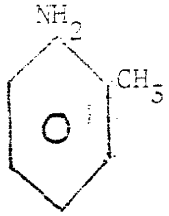

o-Toluidine

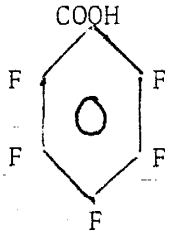

Pentafluoro Benzoic Acid

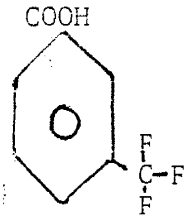

Trifluoro Methyl Benzoic Acid

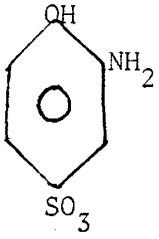

2-amino,1-phenol,4-sulfonic acid

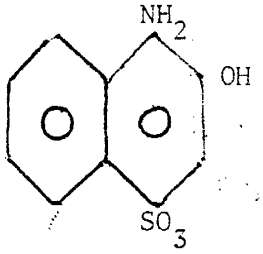

1-amino,2-napthol,4-sulfonic acid

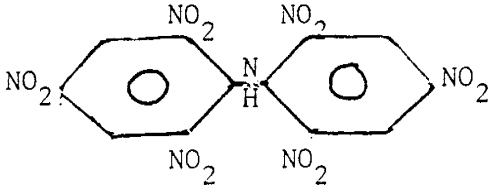

Hexanitro diphenyl amine (2,4,6,2',4',6')

Table 4. PROPERTIES OF EXPERIMENTAL ORGANIC TRACERS

TRACER	FORM	SOL.	$T_{sol.}$	Wt.	pK
2-amino,1-phenol,4-sulfonic acid[a]	xytal	1 pt./1000	14	198.2	10.77
1-amino,2-napthol,4-sulfonic acid[a]	ndles	v.sl. sol.	20	248.26	10.77
Pentafluoro benzoic acid[b]	grn	200g./L (NaOH)	20	216.0	11.3
Trifluoro methyl benzoic acid[b]	grn	200g./L (NaOH)	20	194.0	9.6
o-Bromoaniline[a]	xytal	v.sl. sol.	20	172.03	11.5
o-Toluidine[a]	liq	1.5g./100g.	25	107.16	9.6
Hexanitro diphenyl amine[a] (2,4,6,2',4',6')	pwdr	36mg./L	20	288.0	13.2

REFERENCES: [a] Lange's Handbook of Chemistry 12th Edition, 1979, McGraw Hill

[b] Correspondence - Harold Bentley, Ph.D., University of Arizona

Abbreviations used: xytal = crystalline; pwdr = powder; ndles = needles; liq = liquid; grn = granular; v.sl. sol. = very slightly soluble; Sol. = solubility; Wt. = formula weight in grams

conducted to affirm that sufficient adsorption of tracer would take place.

The measurement of flucrescence requires the use of a fluorometer and two filters. The primary filter selects the wavelength that causes the tracer to fluoresce, while the secondary filter isolates the emitted (fluorescent) light. The procedure, has been described by G.K. Turner (1978)[18]:

1. Set wavelength to 346 mu.
2. Insert appropriate primary and secondary filters.
   1: 110-814 (I-60) and 110-822 (58)
   2: 110-820 (25)
3. Load sample in cuvette
4. Read a sample of distilled water
5. Read a sample with maximum amount of tracer, this will be the sample of known concentration.
6. Read the unknown samples.
7. To estimate the quantity of tracer in the unknown sample:
   a. subtract the H_2O reading from the unknown tracer reading.
   b. divide the concentration of tracer in the blank (a known value) by the water adjusted reading of the blank sample.
   c. multiply the quantity in part b by the reading of the unknown sample to obtain the concentration of tracer in the unknown sample.

The data from the fluorometer analysis for the batch test and the experimental column are presented in Table 5. The batch test was designed to provide maximum contact between the soil and the tracer. Assuming all of the available

Table 5.

BATCH TEST RESULTS - ADSORPTION OF RHODAMINE-B

Sample	I	II	III	IV
Sample wt. (g)	133.95	124.83	137.80	122.55
Time (min)	15	30	60	90
Recovered (ml)	135	122	136	121
Fluorometer	25.5	26.0	27.0	25.0
- H2O	15.5	16.0	17.0	15.0
Conc. (g/L)	0.048	0.050	0.053	0.047

H2O BLANK = 10
STOCK SOLUTION = (42 - 10) = 32

Analytical Conditions: Wavelength: 346 mu
Primary Filters: 110-814 (I-60) and 110-822 (58)
Secondary Filters: 110-820 (25)

PROCEDURE:

1. Weigh samples and place in 250 ml. beaker.
2. Add 150 ml. of 0.1g/L tracer stock solution and let sit for prescribed time period.
3. Filter solution with suction on coarse pre-filter paper.
4. Read fluorescence of samples on fluorometer: obtain readings for original solution and water blanks.
5. Take sample of known concentration, divide by its reading, then multiply by fluorometer reading of unknown sample to obtain concentration of the unknown sample.

surface area is contacted by the tracer, the maximum amount of adsorption is obtained. The results for each of four samples are shown under the heading Conc. (g/L). Since the initial soluton contained 0.1 g/L, and the final results indicated residual concentrations of approximately 0.05 g/L, the distribution coefficient was aproximately 50%.

Reverse-phase HPLC is a technique employed by analytical chemists to measure trace amounts of a substance. Generally, in column chromatography a liquid phase containing the material of interest is passed through a column with the result being the adherence of tracer on this column. (The adherence being due to ionic, polar, hydrophobic or other force.) The column is then saturated with a liquid that has a higher affinity for the column material than the tracer, and elution of the tracer results.

In HPLC the system is under a great deal of internal pressure, with the result being faster elution times with smaller volumes of sample required. The reverse-phase technique implies a partition system where the mobile phase is more polar than the stationary phase (being the chromatographic column material). The mobile phase is generally water-based, with the addition of a water-miscible organic solvent. The organic solvent tends to modify the elution characteristics of the sample, with a noticeable trend towards quicker elution with increased concentration of organic solvent. Retention is based on the hydrophobic

characteristics of the solute. Polar solutes prefer a polar mobile phase, and thus they elute before the non-polar components. In the H_2O - acetonitrile mobile phase, very polar and ionic compounds elute very quickly, with the result being poor peaks and increased tailing. To enhance the resolution, a pH control of the mobile phase is necessary to suppress ionization in order to increase retention. The pH control results in better, more symmetrical peaks. (The pH is maintained via the use of a phosphate buffer.) The stationary phase is generally a hydrocarbon column of specific particle size. Factors affecting the selectivity of the HPLC technique are the chemical composition of the mobile phase, the chemical composition of the stationary phase, and the temperature and nature of the surface support layer. The column capacity is a function of the available surface and the levels of stationary phase on the packing.

Applications and advantages of reverse-phase HPLC include[19]:

1. The separation of non-ionic, ionic, and ionizable compounds on a single column and with a single mobile phase.
2. The bonded-phase columns are stable and fairly reproducible. (They are easily replaced and eliminate the necessity of repacking broken columns, a procedure which may induce local heterogeneities.)
3. The mobile phase, water, is inexpensive and abundant. In addition, aqueous samples may be injected directly into the mobile phase.

4. Acetonitrile modifier offers a good separation of closely related compounds.

5. Elution order is predictable based on the hydrophobic characteristics of the molecule.

Thus the technique seems to be an ideal means of analysis for organic or ionic tracers in groundwater. Trace quantities are easily detected, with the sensitivity of the technique being in the tenths of a part per million in many cases. Since several different tracers can be analyzed in the same run, the use of HPLC can cut down on the time and cost of laboratory anlaysis.

Results of batch tests conducted on the experimental organic tracers are shown in Table 6. The batch test was designed to determine the maximum amount of a tracer that can be adsorbed by exposure to a maximum amount of surface area for a particular material. Note that all of the non-conservative tracers show distribution coefficients in excess of 50%. Thus, use of the non-conservative tracers during the column test should provide a good estimate of surface area contacted during the leaching process.

Table 6

Batch Test Results - Organic Tracers

Tracer	Kd
Rhodamine-B	0.50
Phenyl-sulfonic acid	0.55
Napthyl-sulfonic acid	0.43
Chloride	0.01
Para-fluoro benzoic acid	0.03
meta-Trifluoro methyl benzoic acid	0.05

LONG COLUMN EXPERIMENT

TANK APPARATUS - A QUESTION OF SCALE

Based on results of the grain size distribution analysis, the coarseness of the material raises the question of appropriate scale. Since the laboratory is limited in size and materials are costly, an attempt was made to approximate a representative elementary volume (REV) of the leach dump, whose size would reflect the nature of actual physical flow processes occuring in a field-sized dump. Murr (1980) and Roman (1974) conducted column-leaching tests in an effort to empirically determine the appropriate scale for such a test. The "medium sized" column (3 m. high and 0.57 m. in diameter according to Murr, 1980) seemed to behave similarly to the large column in terms of the channelization observed, copper recovered, and a minimal amount of wall channeling[20]. Since the primary concerns are the hydraulics of the leach process and the feasibility of column construction, a "medium sized" column was chosen. A column height of approximately 3 meters and diameter of 0.5 meters was selected for the laboratory test.

Empty oil barrels were readily available for the construction of such a column. When four of these barrels were welded end to end, the resulting column was 3.0 meters high and 0.57 meters in diameter. The apparatus thus

satisfied the requirements of scale for approximating a representative volume of a leach pile.

SAMPLING INSTRUMENTATION and INFILTRATION APPARATUS

Since liquid samples were required along the vertical length of the column, simple pan lysimeters were constructed from funnels and plastic tubing. As long as near-saturation of a solution channel occurs samples can be collected merely from the interception and gravity drainage of the leachate. The samplers were placed in a downward spiraling arrangement at the north, south, east, and west sectors of the tank. Each lysimeter was separated from the next by a vertical distance of 60 cm. within any sector. Twenty samplers in total were employed for the column study.

In addition to the lysimeters, the column was equipped with a bottom drain to collect the composite effluent representing the total fluid flow through the column. Piezometers were installed along the bottom 25% of the column in order to monitor the free-surface zone. See Figure 17 for a detail of the column instrumentation.

The introduction of leachate to the column was achieved by means of a constant flux apparatus. A sponge, cut to the shape of the tank, was used as a flow spreader for a sprinkler device emitting leach solution at a constant rate. The rate was controlled by means of a constant-head reservoir. Since the sponge was saturated prior to use, it transmited a uniform flow of fluid to the material. When tracers were desired, a duplicate sponge (saturated with

Figure 17.

SCHEMATIC OF LYSIMETER and PIEZOMETER LOCATIONS

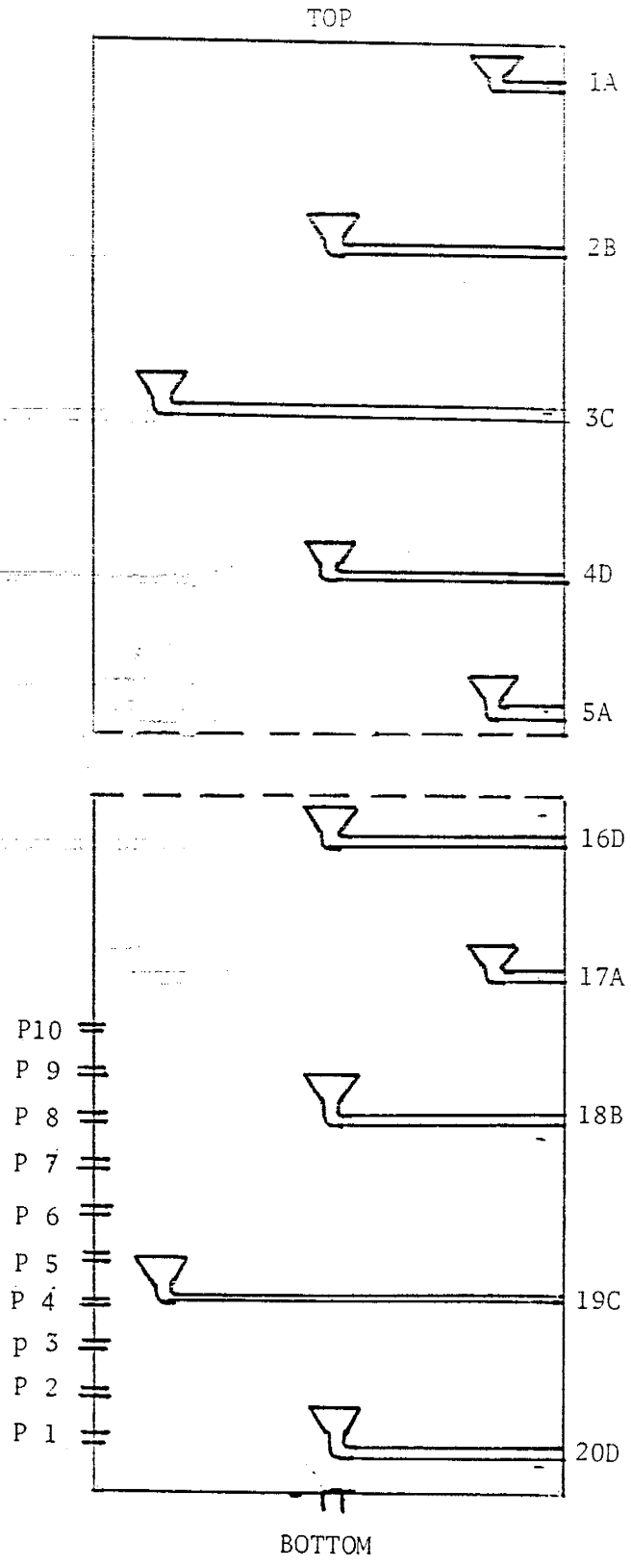

tracer solution) and sprinkler system were attached to the constant-head reservoir allowing for instantaneous pulse input of tracer into the column. Once the fixed volume of tracer was applied, the water-saturated sponge was once again affixed to the column for continued percolation.

The preparation of the column for the leaching experiment involved the loading of the copper ore and the positioning of the lysimeter samplers. Since copper wastes are generally piled randomly into waste heaps, the copper ore was simply top-loaded into the column and allowed to settle naturally. Lysimeters were positioned prior to the actual loading event and held in place by a wire rigging assembly designed to maintain the position of the lysimeter under the stress of falling copper ore. The column was then loaded to a height of 290 cm. The loaded column was allowed to settle for two weeks, during which the column height declined to 275 cm. The column was then filled to a total height of 300 cm.

The complete experimental long-column apparatus is shown in Figure 18. Stopcocks and clamps were positioned as follows: one stopcock was located on the bottom of the constant head reservoir, another one was located at the infiltration sponge as a fine control on the amount of flow, and clamps were located on every lysimeter tubing exit in order to allow quick sampling.

Figure 18.
COLUMN TRACER TEST APPARATUS

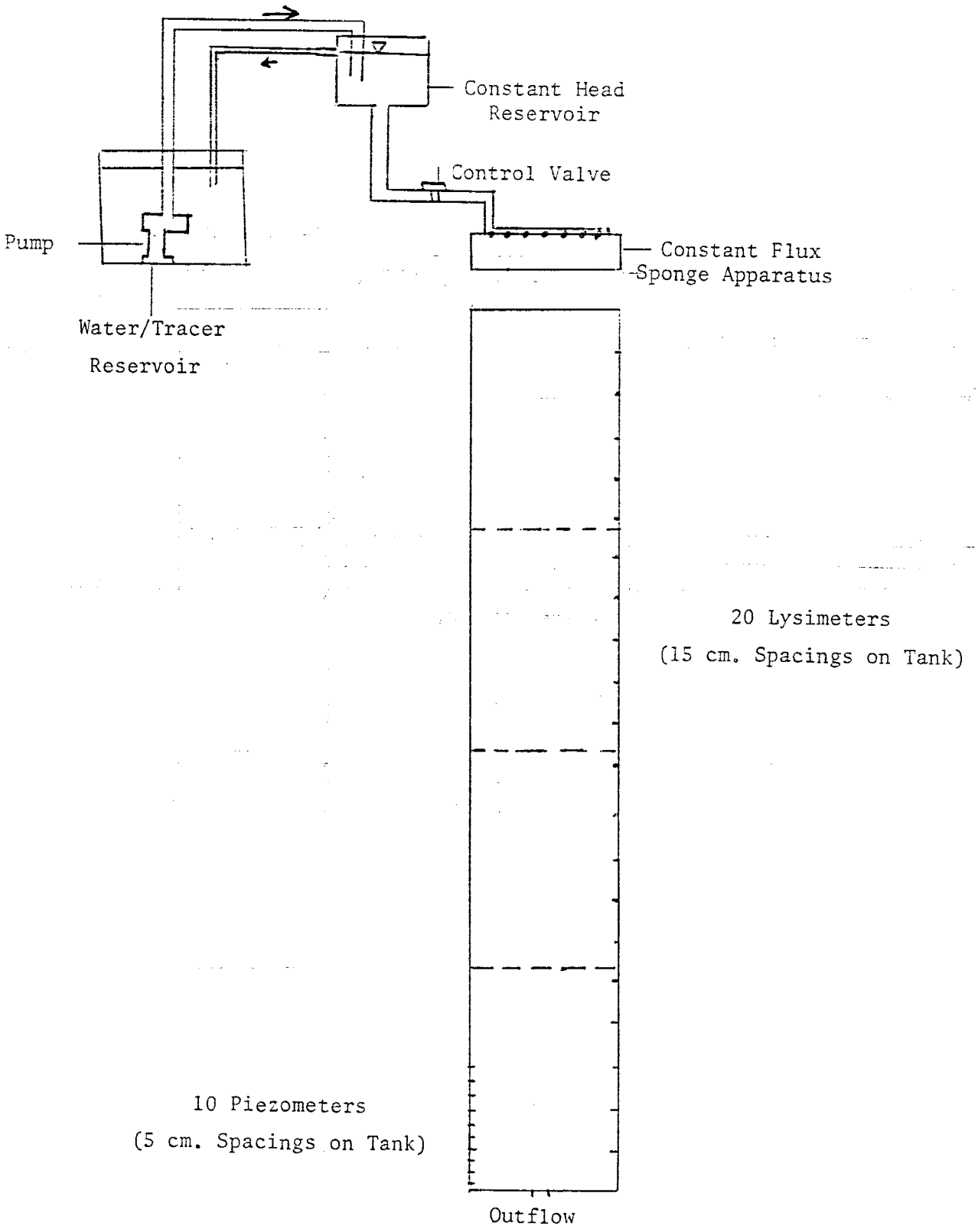

SCALE:
1.5" = 0.75 m.
1" = 0.50 m.

The time and costs involved to prepare distilled water, for flushing the column, were found to be prohibitive, thus tap water was used. The presence of small quantities of salts and other ions found in tap water was not expected to interfere with tracer results. The constant-head reservoir inlet was hooked up to a barrel with a float valve connected to the tap. Thus, an unrestricted water supply was available for continuous application.

The flushing rate was set at 8 cm/hr, comparable to that of a moderately heavy precipitation event, while not exceeding the infiltration capacity (as determined by K_{sat}) of the media. The column was flushed with water for a 40 hr period in order to establish a constant flux and achieve a unit gradient for the column. (This period also produced further consolidation of the ore, as well as the establishment of solution channels and preferential flow paths.)

Once the steady flux was achieved, tracers were added in pulse form. The organic tracers were diluted to a concentration of 1 ppm from stock solutions. (This included both the conservative and non-conservative organic tracers.) Chloride and rhodamine-B were added at 10 ppm. The total volume of tracer-laden water was 25 L. The procedure for this long column experiment was:

I. Primary Flushing

1. Close all stopcocks and clamps on the tank apparatus.

2. Saturate infiltration sponge; hook up pump with the stopcocks closed.

3. Open lysimeter clamps

4. Place sponge on tank; open stopcocks to achieve the desired rate of flux.

5. Open tank valve (start stopwatch) and let the column soak at the specified flux.

6. Time arrival of H_2O to lysimeter collection bottles along the length of the column (include effluent drain).

7. Check sample collection times; analyze for for presence of chloride ion using the chloride electrode.

8. Check development of free surface at tank bottom and adjust to desired level.

9. Let infiltration continue for several hours.

II. Tracer Test

1. Close off tank and bottom valves simultaneously.

2. Close lysimeter clamps; empty sample collection bottles.

3. Replace with clean bottles; open lysimeter clamps.

4. Replace water reservoir with desired volume of tracer-laden water and saturate new infiltration sponge.

5. Adjust flux through the sponge and place the sponge on the tank (start stopwatch).

6. Open tank bottom valve and adjust free surface position so that the saturated zone is minimal.

7. Collect samples at appropriate intervals along the length of the column; note which samplers are producing and which are not.

8. Get the water-infiltration sponge and reservoir prepared for infiltration once the tracer volume is exhausted.

9. Continue flushing the column and collecting samples for several pore volumes (6) from the chloride peak arrival at the bottom drain. (Measure the volume of fluid under the chloride peak.)

Note: The procedure for the tracer test was conducted for a chloride pulse test prior to loading with the suite of organic and reference tracers in an effort to estimate pore volume; elution times; and effective velocities. The chloride ion calibration curve is shown in Figure 19.

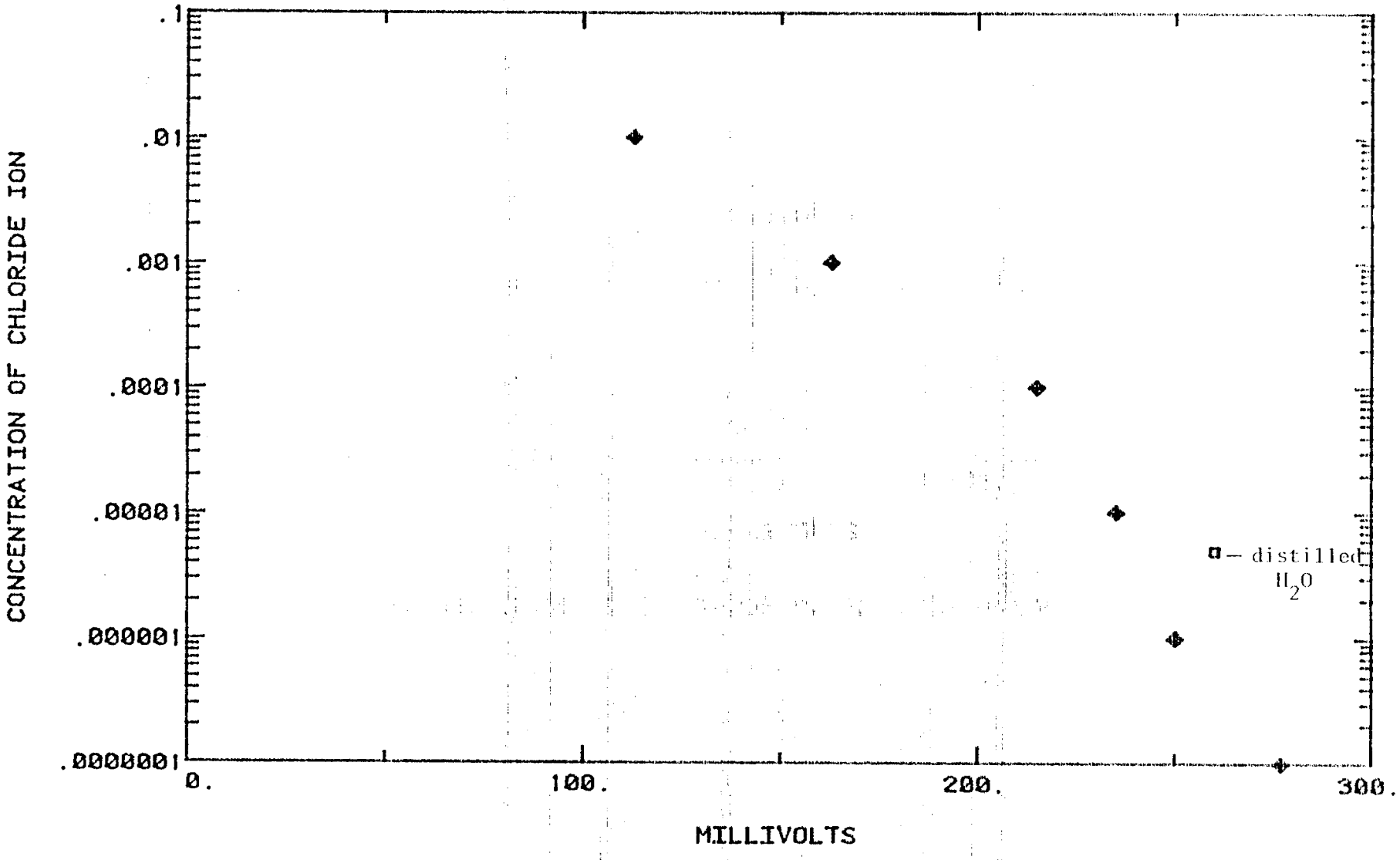

Figure 19. CHLORIDE ELECTRODE CALIBRATION CURVE

Observations

Once the water application was started, it was noted that all lysimeters were not producing sample volumes in measureable quantities. This was attributed to several probable causes. The column packing was a random process; the crushed ore, consisting of 50% cobbles, 48% sand and 2% fines, was deposited in the column from top down. As a result, the boundary effects of the column walls on the medium-sized column were imposed upon the material, causing a unique arrangement of grain sizes at various lengths of the column. As the column was allowed to settle, finer grains filled the interstitial spaces between coarse grains. Thus, the bottom one half of the column was a matrix of cobbles, sands and fines. The next quarter of the column had a mounding of coarse grained particles in the center while sand from the upper portion filled the interstitial spaces as well as the voids between the mound and the walls of the column. Finally, the top quarter of the column was composed entirely of cobbles whose pore spaces were filled with air.

Solution channeling defines the preferential flow of fluid along a certain path through a porous medium. In this case, large parts of the porous medium may be effectively isolated from the major flow paths. Thus they may not be hydrated to the extent of producing samples that are collectable through gravity drainage into a lysimeter as a

result of this packing phenomenon. As an infiltrating fluid travels through the column, it will travel quickly in a cascading motion through the coarse top quarter of the column. Then it will contact a small area of coarse material surrounded by sand. Since water travels the path of least resistance, it will generally enter the gravels and flow downwards quickly; while in the sands, it will adhere to the individual grains until moisure content builds to a significant level, (where the hydration envelopes surrounding the grains overlap to cause a continuum of water), and then flow may occur through the sand. (Samplers in the sand area may show delays in fluid arrival or may never collect enough water to be of significance in the tracer analysis.)

In the bottom half of the column, where the sand and cobble matrix exists, water had to flow through the sands which fill the inter-cobble spaces, thus the hydraulic conductivity of the sand was the dominant factor in this half of the column. In addition to solution channeling, a certain amount of infiltration fluid was lost to wall channeling (cascading flow) on the east side of the column: this was ascertained from distinct audible evidence of flow between the walls of the column and the ore, sounding like a cascade of pebbles. Another factor in lysimeter inefficiency may have been the loss of lysimeter orientation with respect to fluid flow as a result of the top-loading of the column: the force of the falling copper ore may have

disturbed the rigging system and tilted the sampler in such a manner that only a very precise angle of contact between solution channel and sampler would result in a fluid sample. Table 7 illustrates a schematic of the sampler efficiency for the water and the tracer tests. The packing arrangement described above was verified upon destruction of the column. The approximate grain size distributions as a result of packing, consolidation, and leaching are shown in Figure 20.

The effective velocity of the system was very high: the first appearance of leachate at the effluent drain occurred after 13.5 minutes, having travelled a distance of nearly 3 m during this time. The sampling times were spaced very closely, (at least a sample every two minutes for each lysimeter location), in order to obtain good results for tracer distribution profiles. In addition, the arrival time for the chloride slug and monitoring of the pore volumes passing through the system was necessary to determine the length of the sampling time.

The copper-ore flushing parameters that were evaluated as a result of the long column test are shown in Table 8. The results of the chloride slug input during the water flushing of the column are shown in Figure 21. The dispersion coefficient was calculated using the concentration vs. time breakthrough curve for a conservative tracer. Assuming a normal tracer distribution, the dispersion coefficient is given by the following

Table 7.

LYSIMETER SAMPLE RECOVERY DATA

Sampler No.	Water Test Time of sample (min)	Tracer Slug Test Time of sample (min)
1A	:38	:32
2B	:55	:49
3C	1:42	1:36
4D	-	-
5A	1:54	1:24
6B	-	-
7C	2:29	2:01
8D	-	-
9A	3:59	3:32
10B	-	-
11C	4:36	3:59
12D	t	t
13A	4:48	4:18
14B	-	-
15C	6:56	6:13
16D	t	t
17A	t	t
18B	-	-
19C	12:06	11:39
20D	13:32	12:45
EFF	13:30	13:42

Figure 20. Packing Heterogeneities observed while unloading.

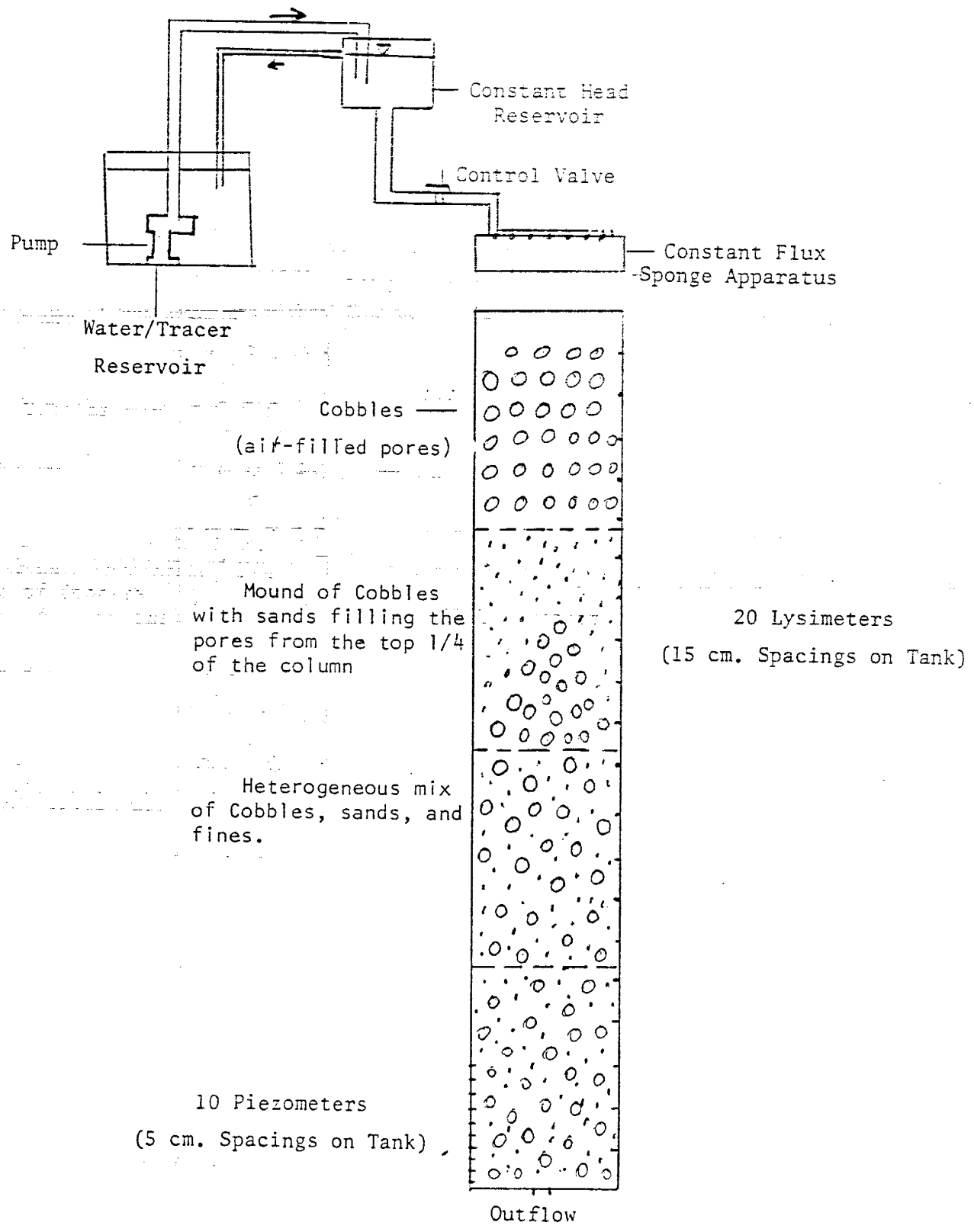

Table X.

COLUMN TEST PARAMETERS

Ore Characteristics

Porosity = 0.366

K_{sat} = 0.57 cm./sec.

SA = 8.177

UC = 24.5

d_{10} = 0.49 mm.

d_{60} = 12.0 mm.

Column Test Parameters

L = 296.8 cm.

r = 28.4 cm.

A = 10135.5 cm.

dz = 15.0 cm.

i_{top} = 0.00222 cm./sec.

Q = 50.68 L/hr.

v_e = 0.37 cm./sec.

Pore Vol. = 44.97 L

t_{pv} = 13.5 min.

D_z = 0.01091 cm.
(from pulse distribution curve)

O_{ave} = 0.24

TRACER RESULTS AND DISCUSSION

Tracers were used in an effort to determine the hydraulics of the flow process. Organic tracers were analyzed using reverse-phase HPLC techniques. The analysis took place at the chemistry laboratory at Hydrogeochem, Inc., in Tucson, Arizona (courtesy of Dr. Harold Bentley). Chloride ion concentrations were obtained from chloride electrode analysis, while the rhodamine-B was analyzed fluorometrically. Tabulated results from these analyses appear in Appendix 3.

It is interesting to note that all of the experimental organic tracers applied were not detected in the effluent using the HPLC. Problems occurred with the stability of several tracers in the experimental environment. A common-ion effect was thought to cause the precipitation of one tracer, hexanitro-diphenyl amine, while high temperatures during sample transport to Tucson may have caused a decrease in the concentrations of bromoaniline and toluidine. Toluidine and bromoaniline were detected in unquantifiably low concentrations, even by the HPLC. (Concentrations of less than 1 ppm were encountered in scattered samples.) Hexanitro-diphenyl amine is stable only at low temperatures, thus, the exposure to warmer conditions during sample transport was thought responsible for the loss of this tracer.

The results of concentration vs. time samples obtained during the course of the long-column experiment are shown in Figures 22 to 31. Essentially, chloride (Cl), para-fluoro benzoic acid (PFB), and meta-trifluoro benzoic acid (m-TFMB) are all conservative tracers i.e., they travel with the bulk water and are generally not adsorbed in significant quantity by the media. These three tracers appeared first, exhibiting strong, narrow peaks. Rhodamine-B (RD), the phenyl sulfonic acid (PSA), and the napthyl sulfonic acid (NSA), are all adsorbed and retained on the copper ore in varying degrees (as predicted by the distribution coefficients obtained from the batch tests). This is reflected in the shorter, (less than 60% of C/C_o), and broader peaks, arriving later than the conservative tracers, due to adsorption. General trends include the decrease in peak height and increase in peak breadth with progressive movement down through the column.

Figures 22 to 25 show the concentration vs. time curves for tracer migration through the western sector (A) of the column. Samplers are vertically separated by 60 cm along any sector. Sampler 1 is located 5 cm from the top of the column, due to the effects of consolidation. In addition, it is also the sampler nearest to the source of leachate application. This boundary effect is reflected in tracer movement with time for the tracer suite. Since only 5 cm of material are encountered (vertical distance) by sampler 1, retardation is not in appreciable evidence in

Figure 22. QUADRANT A BREAKTHROUGH CURVES

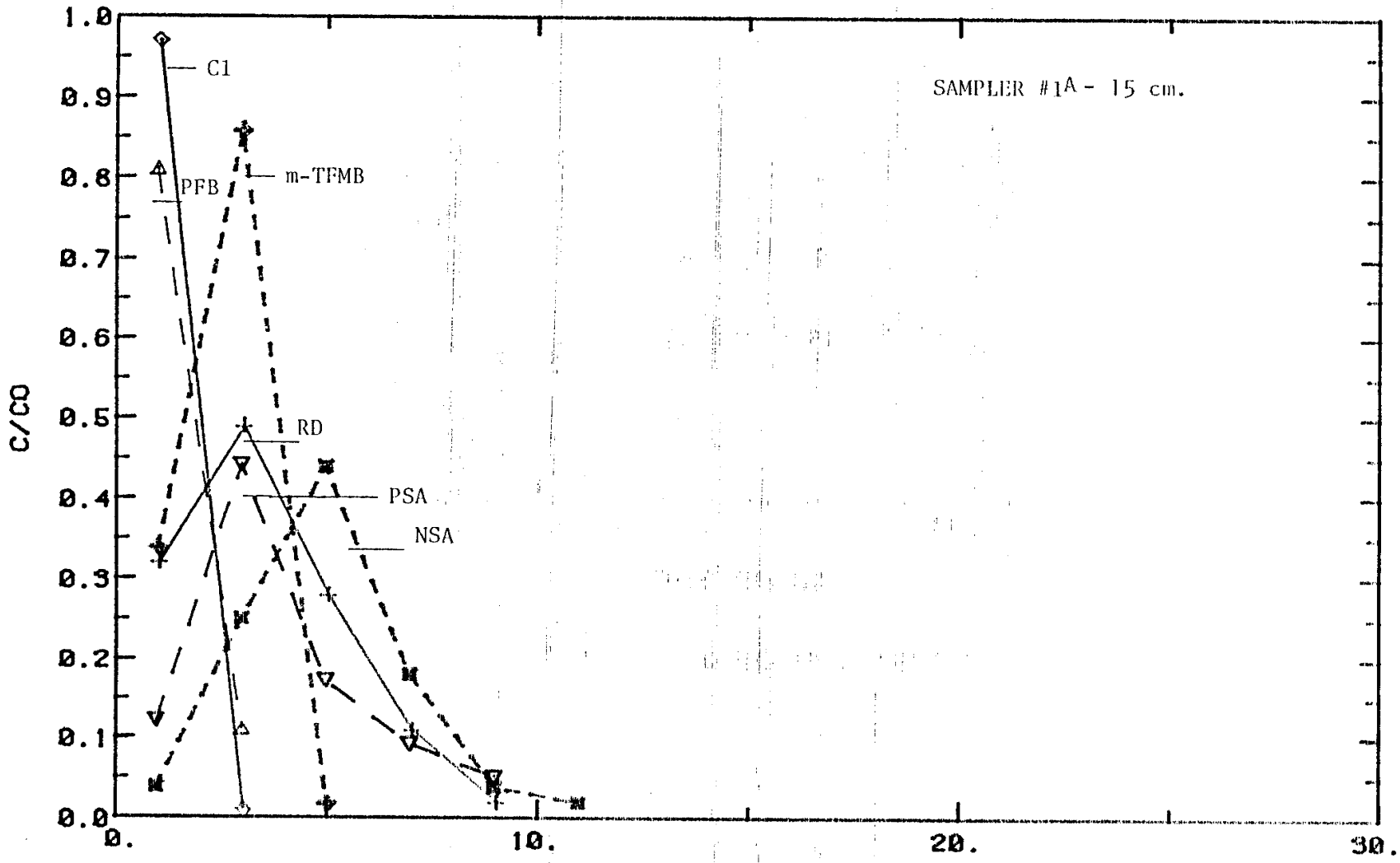

TRACER BREAKTHROUGH CURVES

Figure 23. QUADRANT A BREAKTHROUGH CURVES

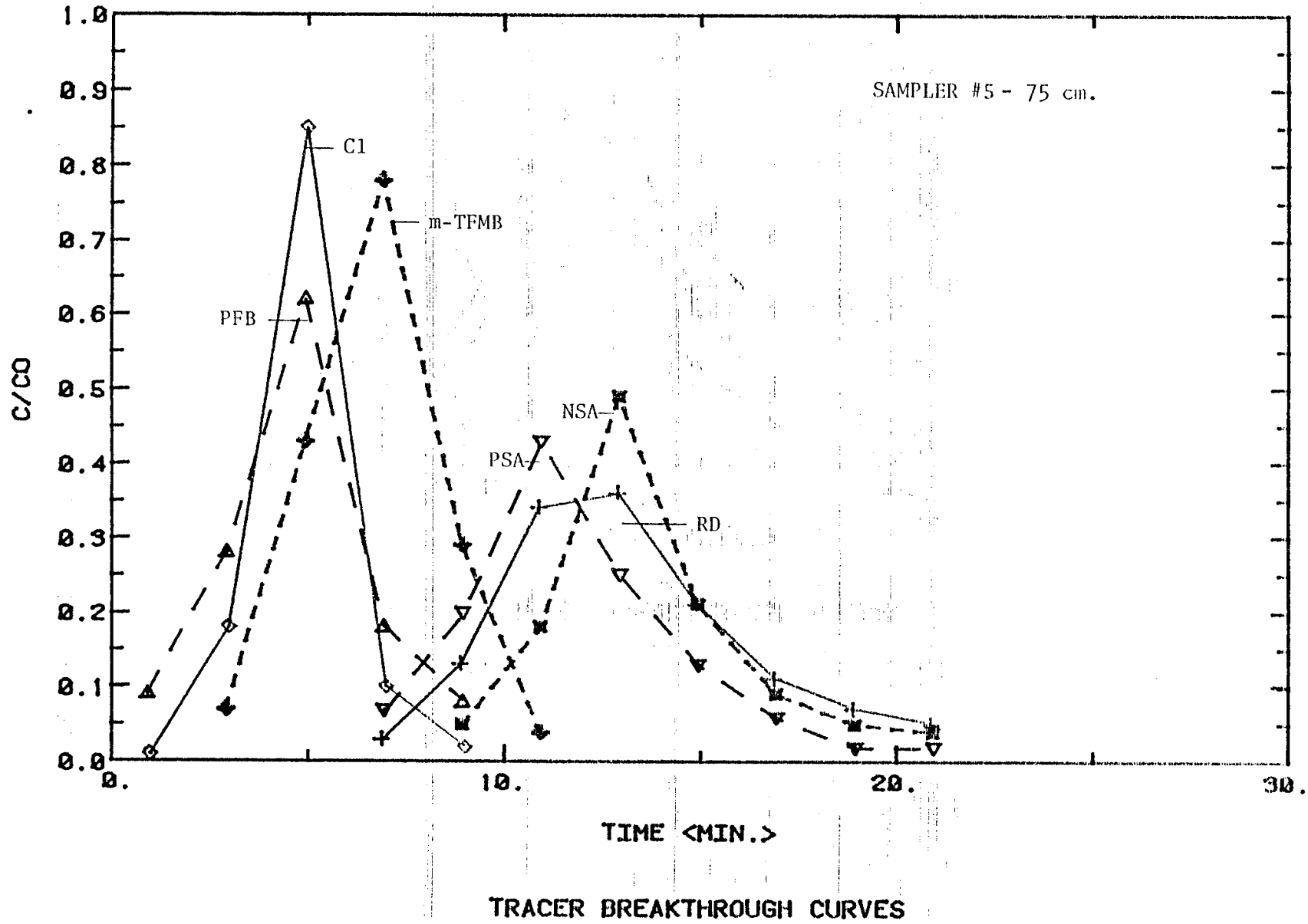

Figure 24. QUADRANT A BREAKTHROUGH CURVES

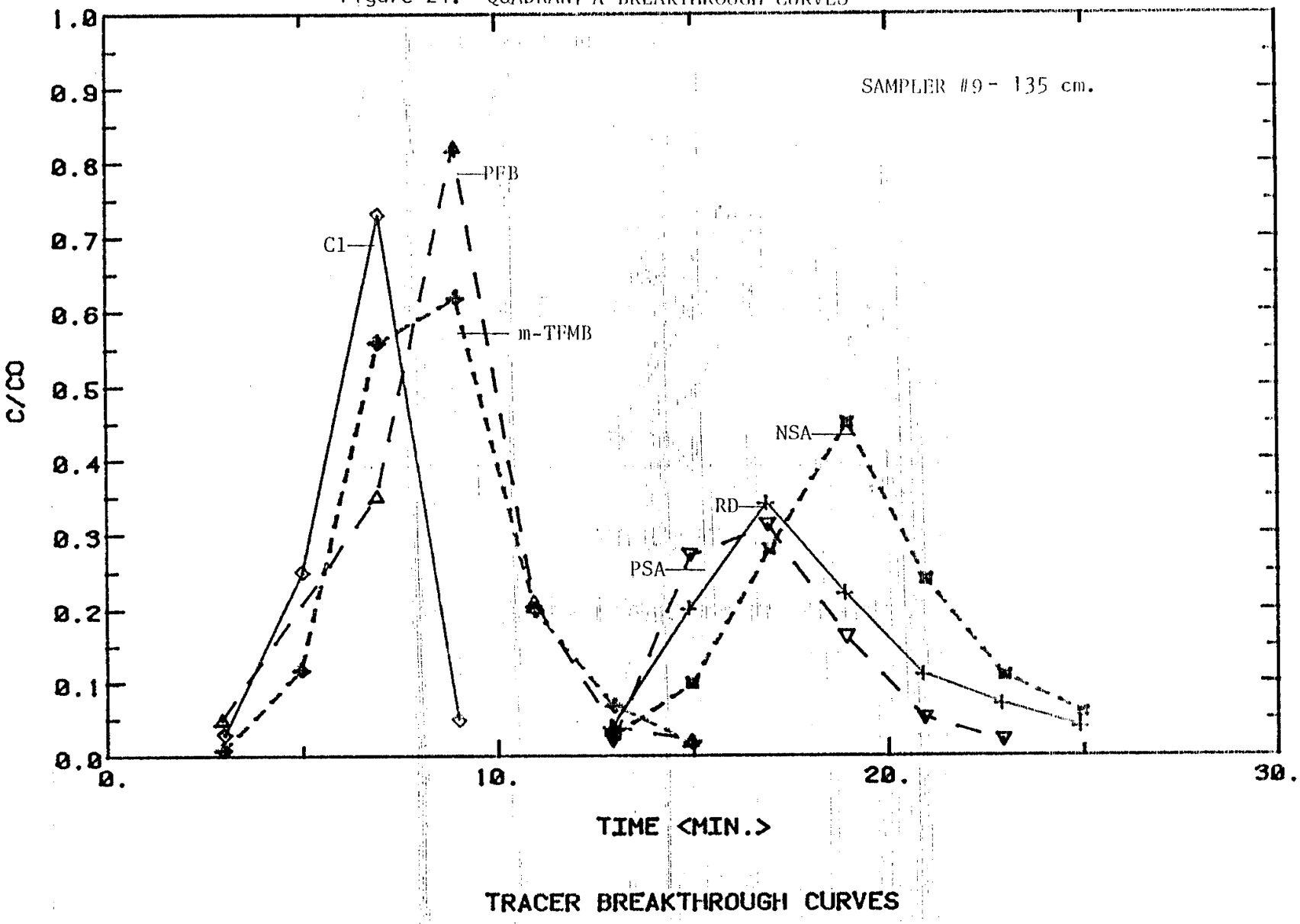

TRACER BREAKTHROUGH CURVES

Figure 25. QUADRANT A BREAKTHROUGH CURVES

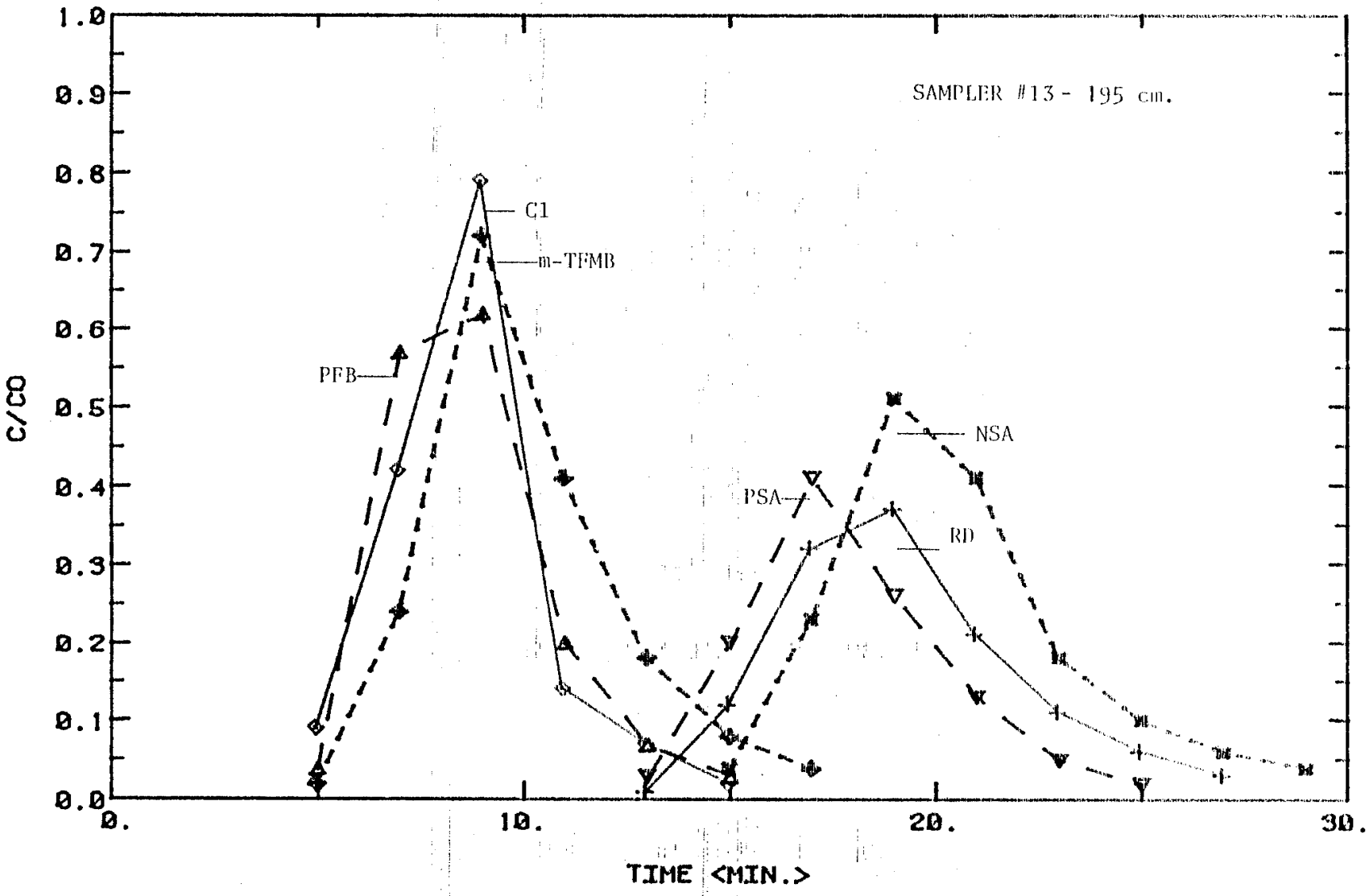

TRACER BREAKTHROUGH CURVES

Figure 22. Retardation is dependent on velocity, which is dependent on time and distance. In this case, the non-conservative and conservtive tracers all arrived within a narrow range of time due to the proximity of the constant flux boundary. The non-conservative tracers (RD, PSA, and NSA) are characterized by their small peak heights. In Figures 23 to 25, the progressive downward move- ment of tracers is shown. Note that peak heights decrease; the arrival of non-conservative tracers shows increasing delays from that of the conservative tracers and the breadth of all peaks show an increase. Chloride, PFB and m-TFMB all break through at roughly the same time, although the m-TFMB peak arrival is consistently behind the chloride and PFB peaks. Retardation of the non-conservative tracers increases with downward movement through the sector, and with distance from the boundary, which is a function of an increase in the amount of material encountered by the tracers. Similar results to those of the western sector (A) are shown for the eastern sector (C) in Figures 26 to 29.

It should be noted that while the relative trends in any sector are essentially the same, comparison of the two sectors by means of overlaying the tracer distribution curves reveals differences between the two sectors in terms of the effective velocities of travel. Solution flows through sector C at a faster rate than it flows through sector A. Overlays of Figures 25 and 29 (corresponding to samplers 13A and 15C) reveal that the peak arrivals occur at

Figure 26. QUADRANT C BREAKTHROUGH CURVES

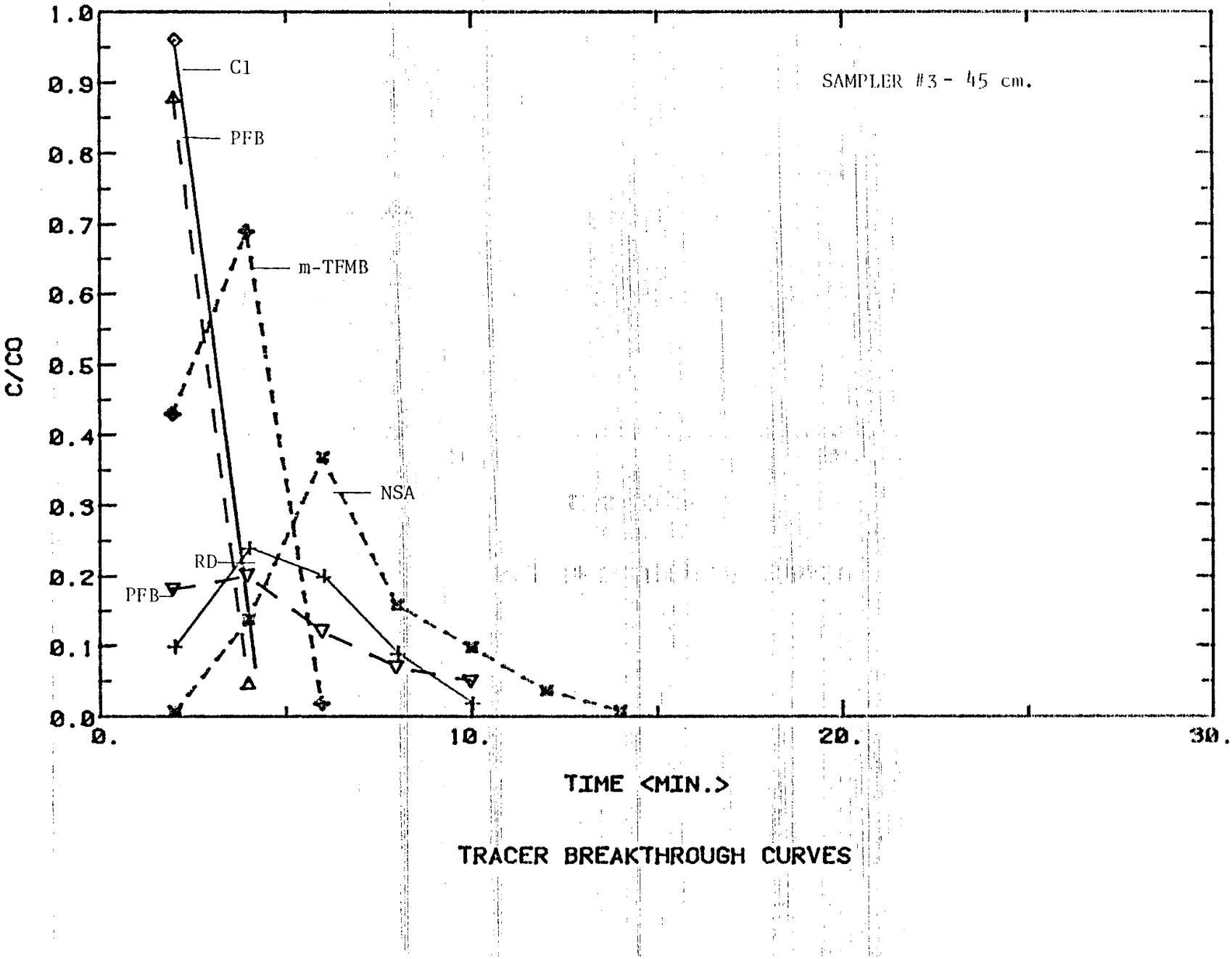

Figure 27. QUADRANT C BREAKTHROUGH CURVES

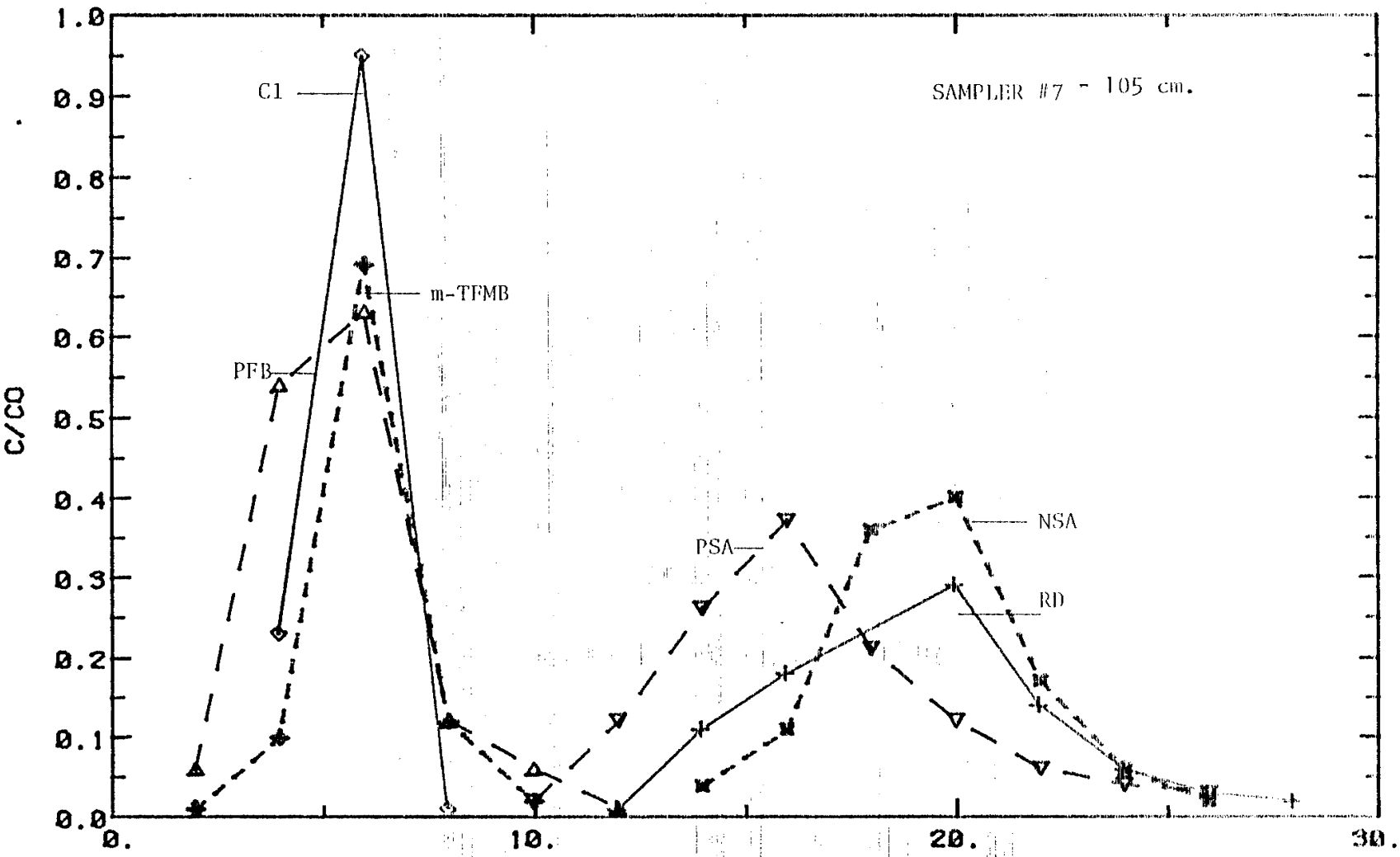

Figure 28. QUADRANT C BREAKTHROUGH CURVES

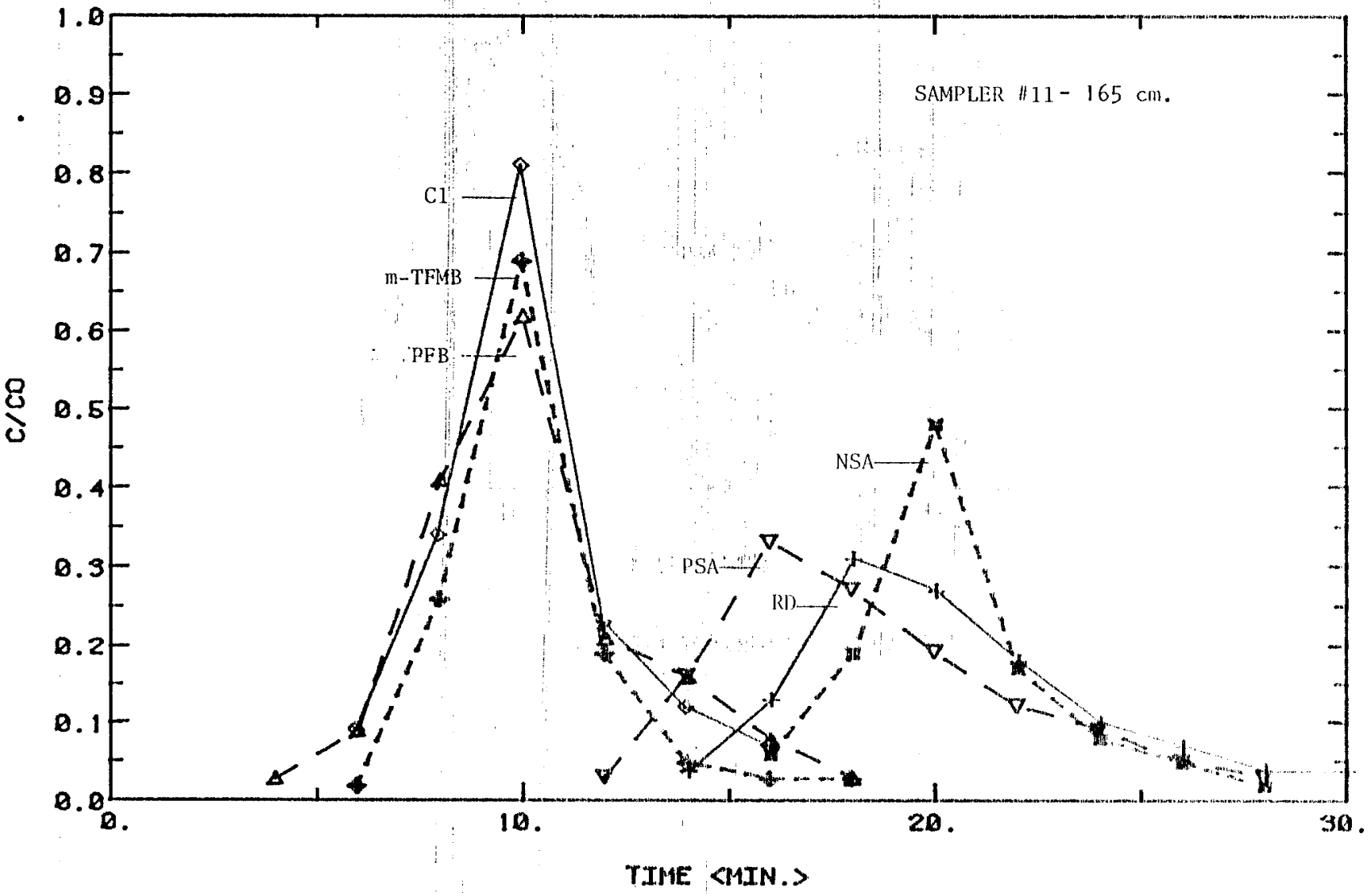

TRACER BREAKTHROUGH CURVES

Figure 29. QUADRANT C BREAKTHROUGH CURVES

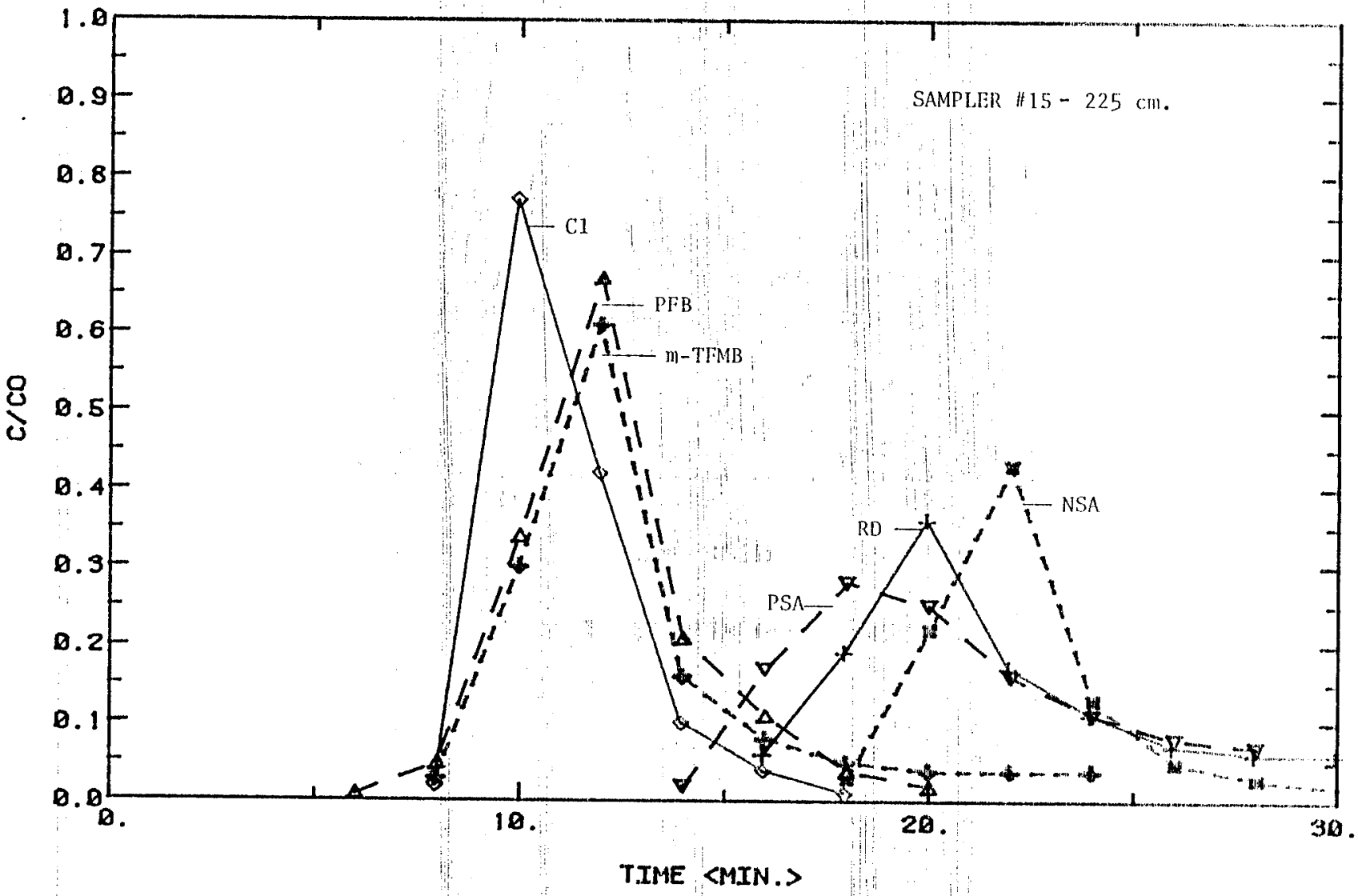

the same times, while the samplers are separated by a vertical distance of 30 cm. Thus flow velocities are slightly higher for sector C than sector A. Heterogeneity of the copper-ore particle-size distributions within the column are considered to be the main factor for the differing flow velocities between sectors.

Figure 30 shows the tracer distribution results for the column effluent. One prominent feature of this tracer distribution is the presence of multiple peaks in several of the conservative and non-conservative tracer profiles. Solution channeling, coupled with varying flow velocities among the solution channels, seems to be the most likely cause of this phenomenon. The disparity in flow velocities between sectors A and C (demonstrated by overlays of tracer distribution profiles) corroborates this hypothesis. The fact that not all lysimeters produced leachate provides additional evidence for solution channeling.

In a large waste heap in the field, the effluent breakthrough curve often resembles that of a homogeneous porous media (i.e., one well-defined peak) [21]. Yet researchers document the occurrence of solution within these waste heaps as the predominant means of leachate travel. If the number of solution channels in a field-scale leach heap is large, and the effluent is collected from one drainage point (generally a topographic low), then the resulting tracer profile will represent a statistical average of the

Figure 30. Column Effluent Tracer Breakthrough Curves

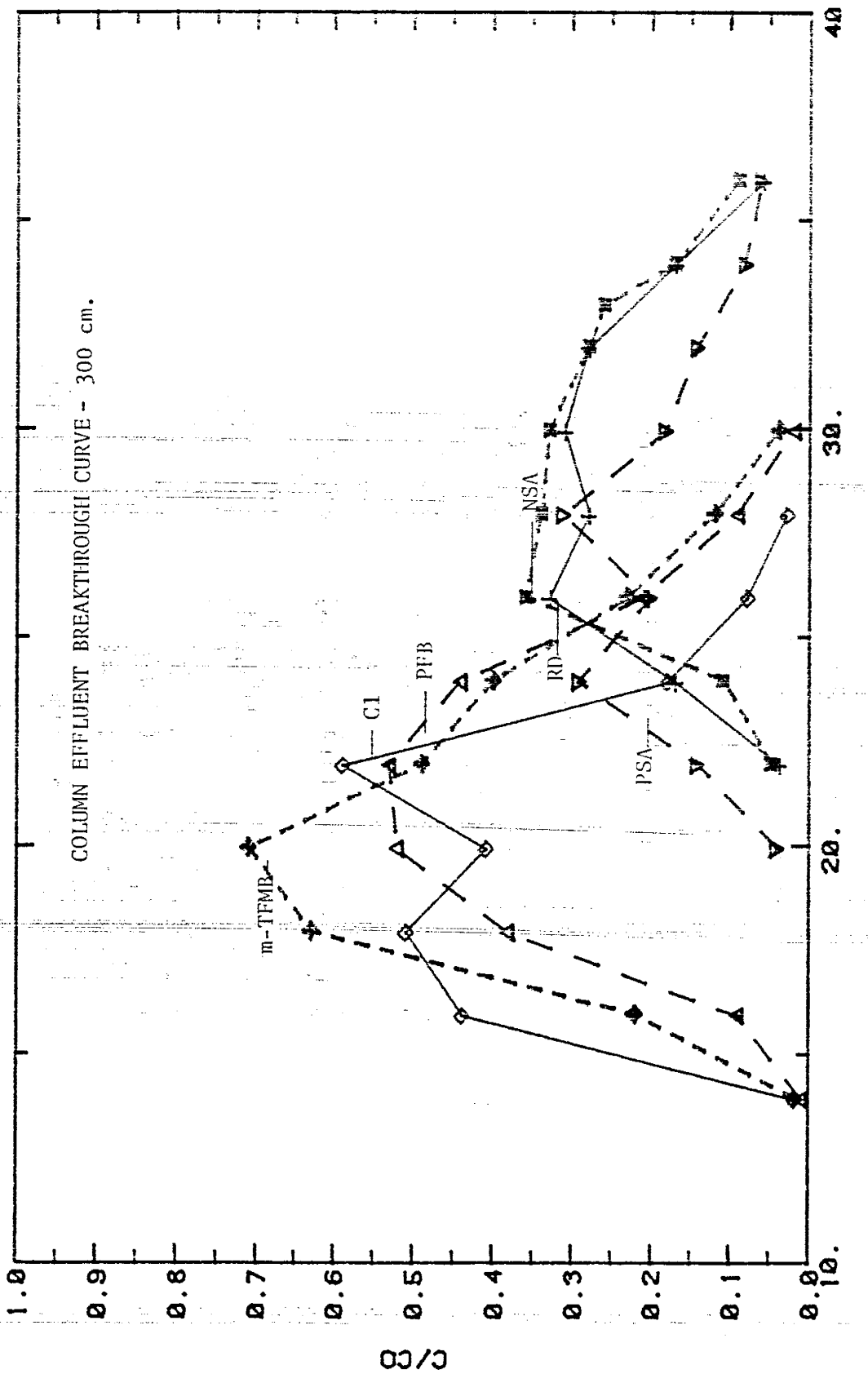

solution channels contributing leachate to the bottom drain. When a large number of solution channels is involved, statistics dictate that a normal curve should result, characterized by a single well-defined peak. Such a peak is thus the result of a large number of individual solution channels whose average contributions form a statistically normal distribution. The experimental column, on the other hand, is representative of a small volume within a field leach heap. Due to its finite size and surface area, the number of solution channels is limited. When only a small number of channels contribute to a large amount of leachate collected, differing travel times through different channels result.

The concept of a representative volume providing differing sampling statistics may be useful to hydrometallurgists attempting to maximize the efficiency of the leach process. When using a conservative and non-conservative tracer pair, one should look at the relative shapes of the effluent peaks. If the peaks are split or very broad, this would indicate the presence of solution channeling. (Compare the peak breadths and shapes in the effluent sample, Figure 30, with those of other samplers, Figures 22 to 29, for illustration of the potential differences in peak geometries induced by channeling.) Thus, someone in the business of field leaching could observe the peak geometry of effluent samples and obtain a quick estimate on the degree of channelization

occurring within the leach heap.

As a result of this column experiment, new and potentially valuable organic tracers have been identified for use in the characterization of fluid hydraulics. From the tracer studies, it seems that the combination of para-fluorobenzoic acid and phenyl sulfonic acid may be the ideal tracer pair for use in a copper heap leaching site for monitoring purposes. PFB is a good conservative organic tracer that closely mimics the transport of chloride. PSA has the least retardation of the non-conservative tracers, and was at least 50% sorbed upon contact with copper ore. Since PSA was retarded, yet not held up as much as the other adsorbed tracers, it should prove ideal in monitoring situations, where the number of samples rquired should be kept to a minimum, in an effort to keep monitoring costs low. The use of PFB and PSA in conjunction may provide an analysis on the extent of chanelization ongoing in a leach heap. In addition, this information may also be helpful in evaluating the efficiency of the leach process itself based on the amount of ore-leachate contact.

NUMERICAL SIMULATION RESULTS AND DISCUSSION

The models UNSAT and TRANS were employed in conjunction, to predict the distribution of a solute moving through the column. The solute transport model TRANS uses input generated by UNSAT in addition to the dispersion and retardation coefficients. The input data for TRANS is summarized in Table 9. The moisture-content profile at steady state was fairly constant (as calculated by UNSAT), thus the moisture content was introduced as a constant for the system. The retardation coefficients were estimated from the non-conservative tracer results.

The following figures compare the simulation results for the analytical step-input solution (the Greene's function approximation), and the numerical upstream-weighted solution. Figure 31 shows the comparison of numerical dispersion effects at an early time in the tracer distribution. At early time, the numerical peak precedes the arrival of the analytical peak, due to numerical smearing. The numerical peak is also slightly broader, also a result of smearing.

Figure 32 shows the tracer peak evolution as the solute moves down the column. Note the uniform decreases in peak heights and the increase in peak breadths. A small amount of smearing is evident in the tails of the peaks. The first two peaks are closer together simply as a result of the time

Table 9.

Numerical Model Input Parameters

UNSAT

Theta-Psi Relationships	Hanging Column Data
Kr - Psi Relationships	van Genuchten model Data
Ksat	0.057 cm/sec (Permeameter results)
Tolerance	0.01

TRANS

Parameter	Test Run	Tracer Simulation
Velocity	0.1411 cm/s	0.363 cm/s
Dispersion Coefficient	0.00294	0.0109
Nodes	49	81
Element Length	1.905	3.75
Elements	48	80
Total Length	91.44	300.
Weighting Coefficient	0.5	0.5
Time step	1 min	60 sec
Total time	100 min.	2400 sec.
Retardation Coefficient	1 - 4	1 - 3
Void Volume	0.32	0.4
Moisture Content	0.2	0.2
Upstream Weigting Factor	0.15	0.15

Figure 31. Comparison of Numerical Dispersion - Early Time

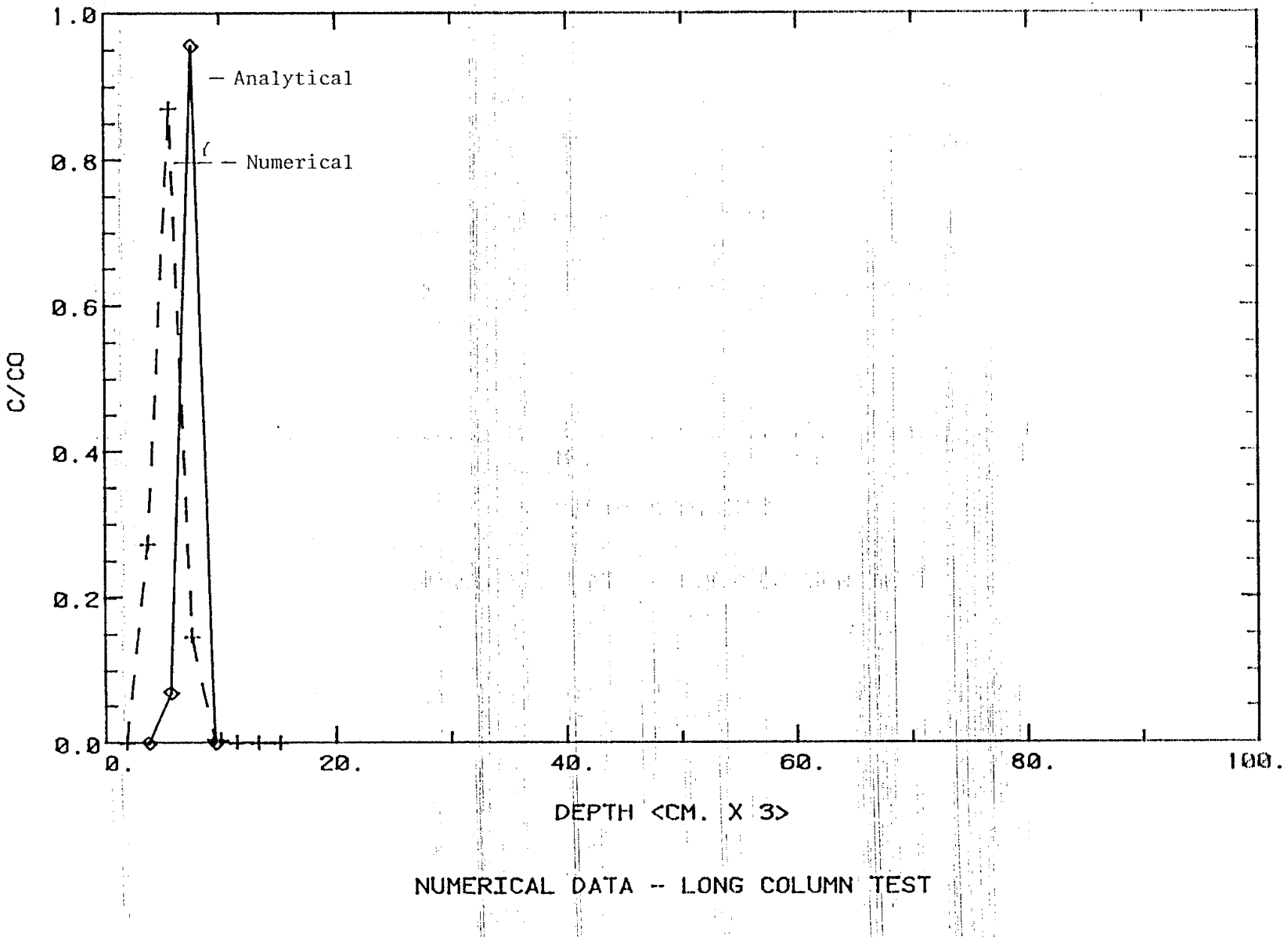

Figure 32. TIME EVOLUTION OF TRACER DISTRIBUTION

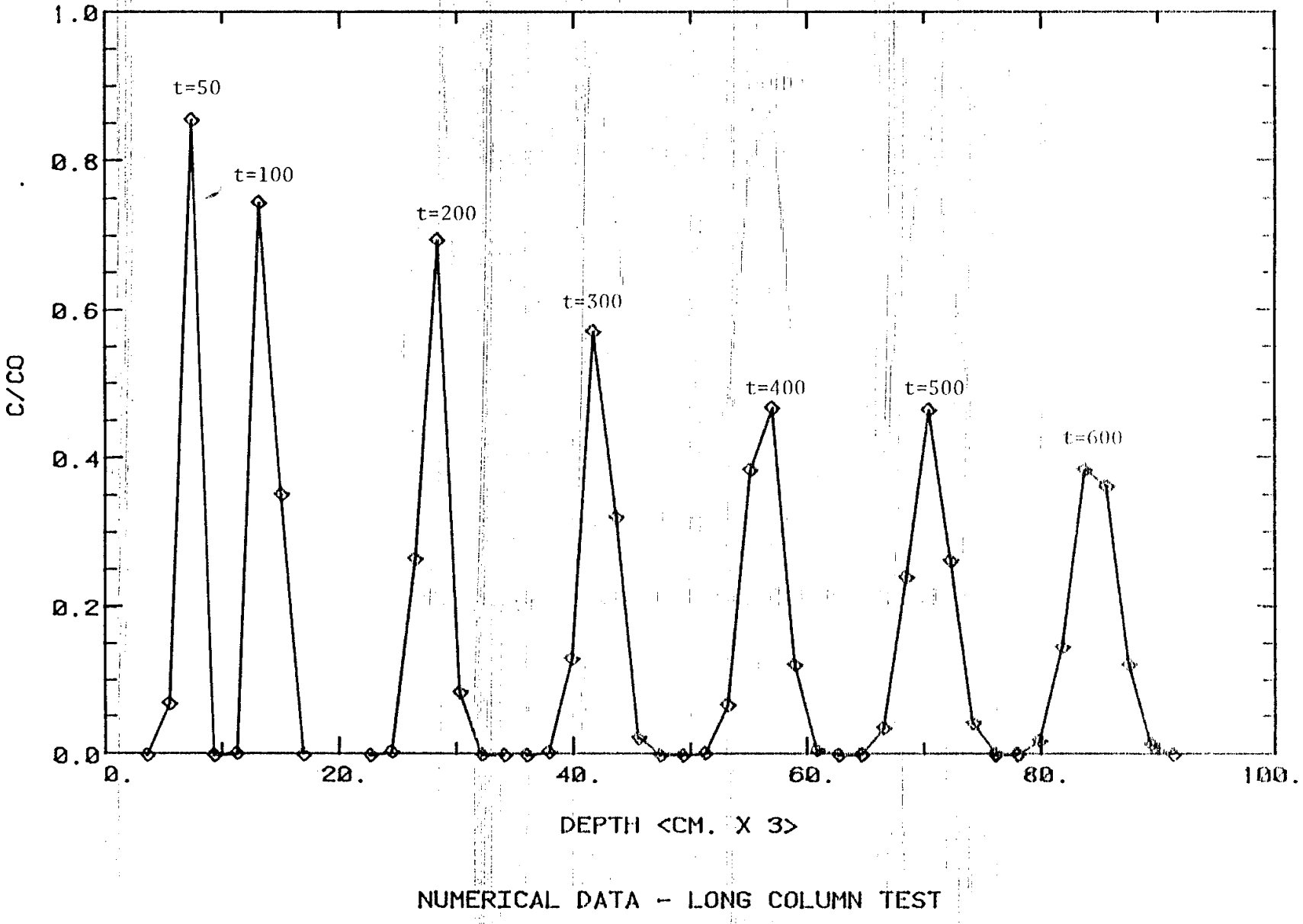

differences being half that of the times separating the other six peaks. It should be noted that the time designations in the figure reflect the numerical simulation time. A time step increment of 40 was utilized, thus the total travel time for the last peak (t = 600.) was fifteen minutes.

Retardation effects are shown in the breakthrough curves (see Figure 33) for the tracers with differing distribution coefficients. There is a larger tailing of the peaks with increased retardation while the peak heights decrease with increased retardation. Calculation of retardation coefficients (from the distribution coefficients obtained from batch tests) for the non-conservative tracers reveals a range from 1.5 - 3.0.

Thus, the model TRANS is effective in generating predicted tracer breakthrough curves for a one-dimensional system. Leach heap height may be varied, along with the degree of saturation, and the degree of retardation expected from the use of a non-conservative tracer.

Surface area contacted may also be calculated from the model. In the case of rhodamine B, which has a retardation coefficient approaching 2.0, the surface area contacted was established to be 43.3%. This quantity is calculated from the equation for R_d described in the section for modifications to TRANS. Calculations of surface area contacted are useful in determining the efficiency of copper

Figure 33. Retardation Effects: Potential Breakthrough Curves for Non-Conservative Tracers.

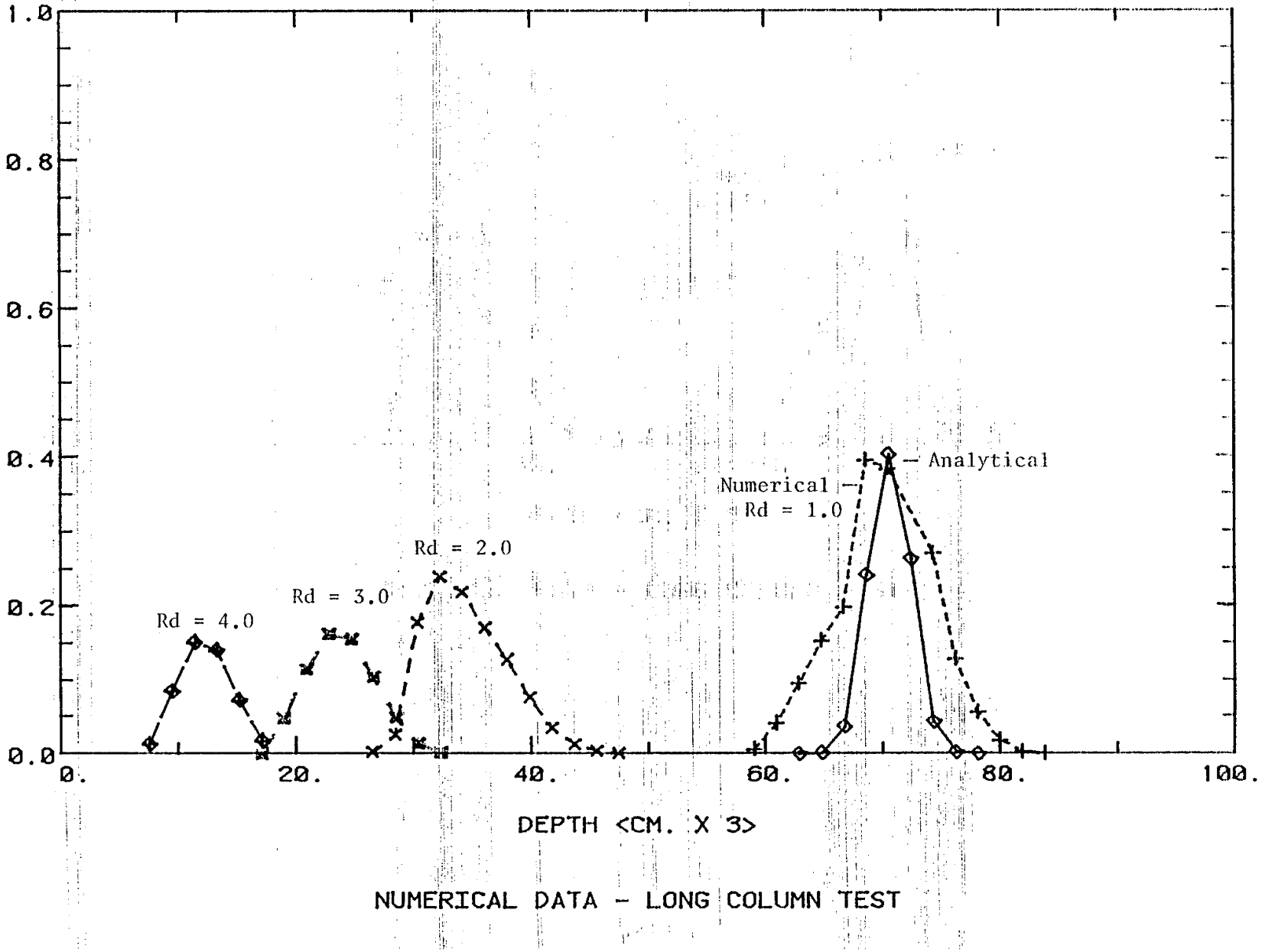

recovery.

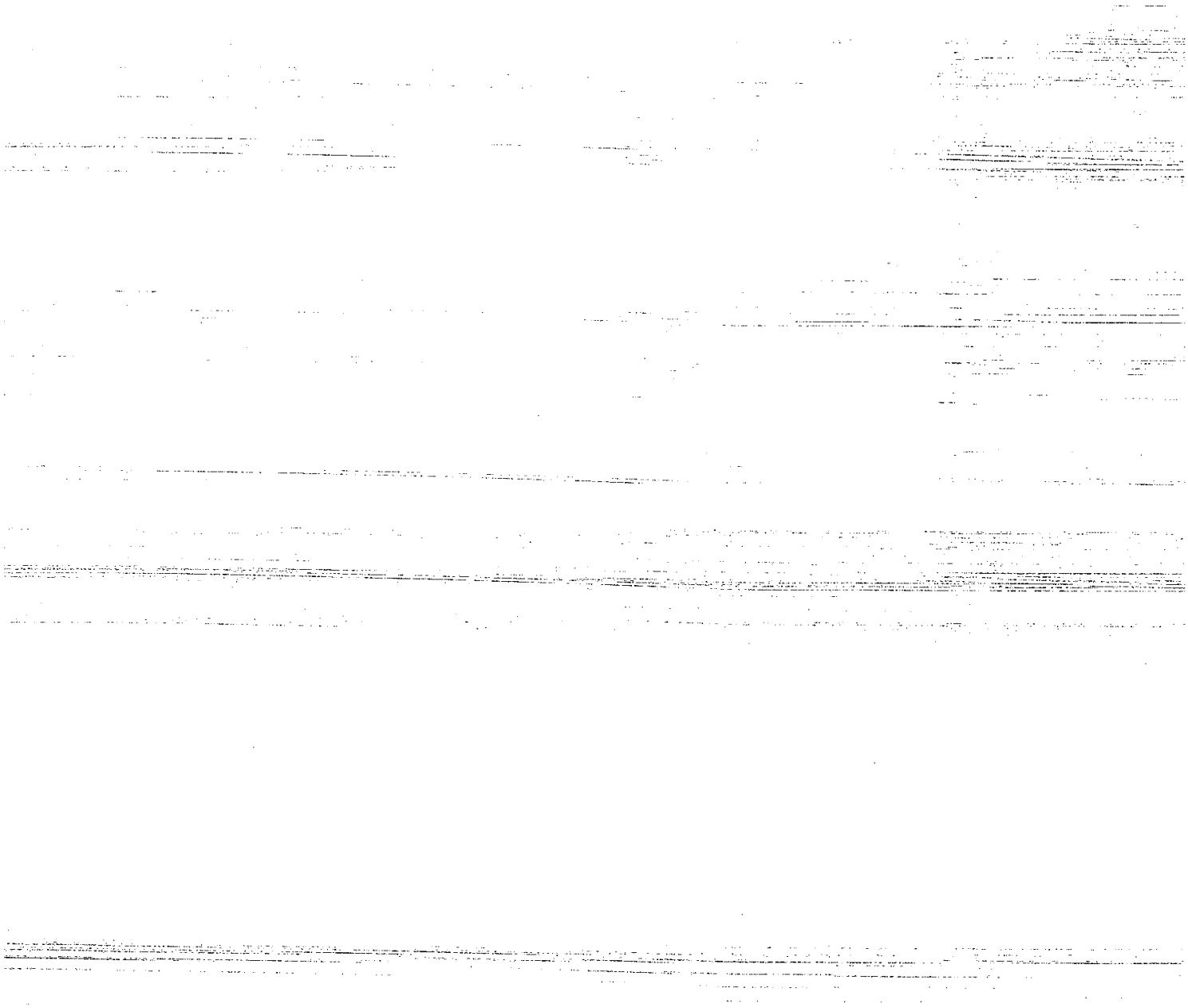

COMPARISON OF SIMULATION AND TRACER RESULTS

The models UNSAT and TRANS were employed to simulate the results obtained from the long-column tracer experiment. The observed effective velocity, the actual column length, the dispersion coefficient calculated from tracer results, and other experimentally determined data were used as the input parameters for the numerical models. Concentration vs. time data were obtained for each element and for tracer retardation coefficients of 1.0 -3.0. Four depths corresponding to experimental column tracer data were selected and the concentration vs. time curves presented in Figures 34 through 37.

Figure 34 represents a depth of 45 cm from the top of the column. When overlain with the analagous tracer breakthrough curve (Figure 26) it is apparent that a good agreement exists between the overall rate of transport for the actual tracer and the numerical simultation results. The chloride, PFB and m-TFMB peak arrivals coincided with the simulation peak with a retardation coefficient 1.0. The non-conservative tracers PSA and Rhodamine B exhibited transport characteristics of a retardation coefficient equal to 2.0, and indicated very short peak heights. NSA had a retardation coefficient of 3.0, and represented the latest peak arrival time for all of the tracers.

Figure 26. QUADRANT C BREAKTHROUGH CURVES

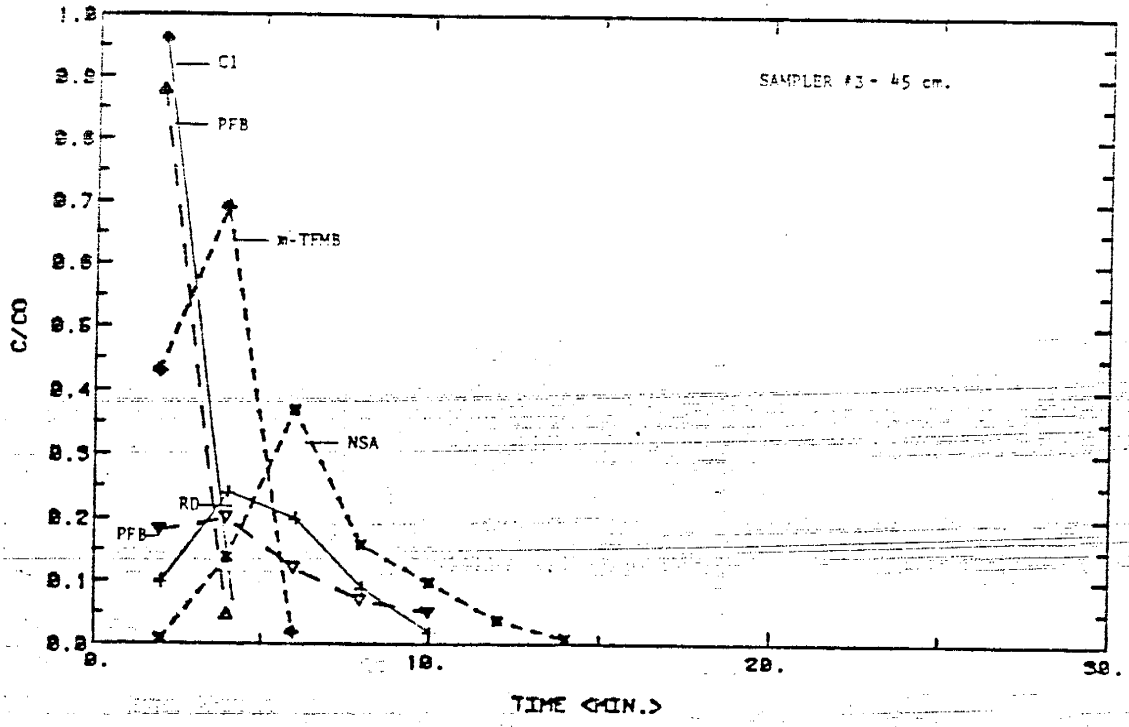

TRACER BREAKTHROUGH CURVES

Figure 34. Numerical simulation breakthrough curves: z = 45 cm.

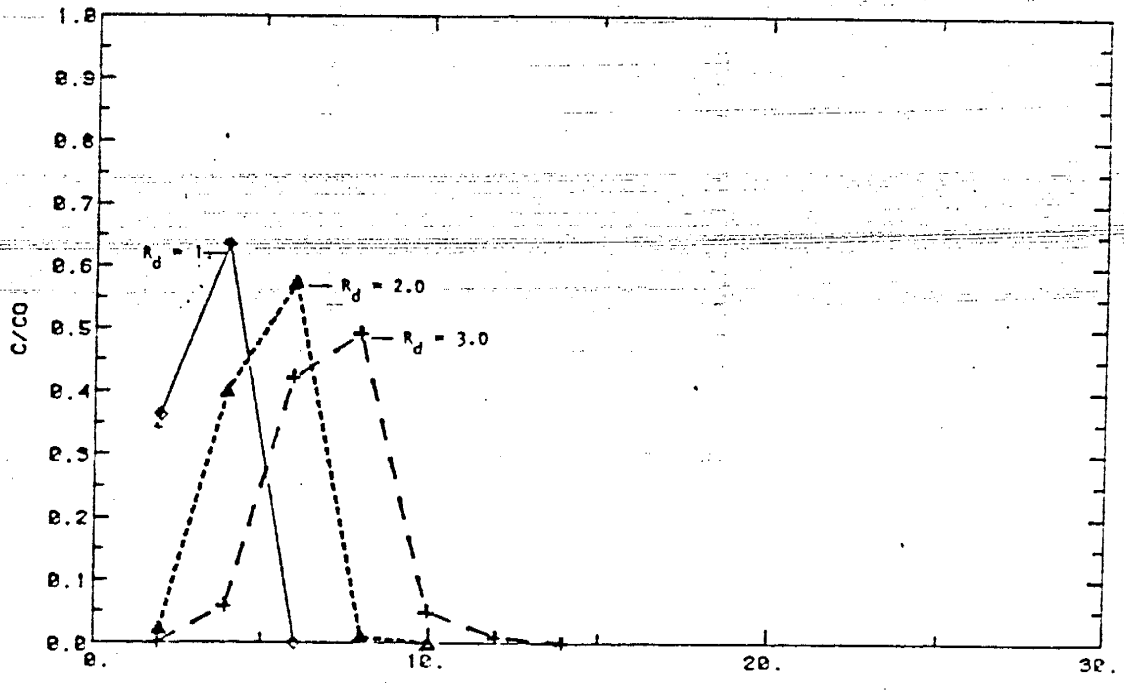

NUMERICAL SIMULATION BREAKTHROUGH CURVES

Figure 35 reflected the breakthrough curve at a depth of 75 cm. corresponding to Figure 23. In the exeprimental tracer curve,the conservative and non-conservative tracer peaks reflected an increased spread with respect to arrival times. Retardation coefficients for the non-conservative tracers were easily identified from comparison of numerical and tracer breakthrough curves. The overlain figures indicated non-conservative tracers exhibited movement corresponding to a retardation coefficient between 2.0 and 3.0. Curiously enough m-TFMB, a supposedly conservative tracer (K_d = 0.05), displayed some retardation (R_d = 1.5) effects. Column heterogeneities may be responsible for this through matrix diffusion effects. The experimental sampling depth was located within the zone of sands with little cobbles, whereas the previous sampler was located within a mostly cobble section. Thus the transition from one soil region to the next may have produced this unusual result.

Figure 36 shows the numerical simulation results for a depth of 175 cm, which corresponds to Figure 28. The chloride, PFB and m-TFMB peaks all coincided with the numerical conservative tracer peak. Thus, the effect of the heterogeneity with depth on the m-TFMB peak seemed to dissipate with continued movement through the column. These breakthrough curves were valuable in terms of the analysis of the retardation coefficients for the non-conservative tracers. Enough time had elapsed to show a clear distinction between tracers rhodamine-B, PSA and NSA. PSA

Figure 23. QUADRANT A BREAKTHROUGH CURVES

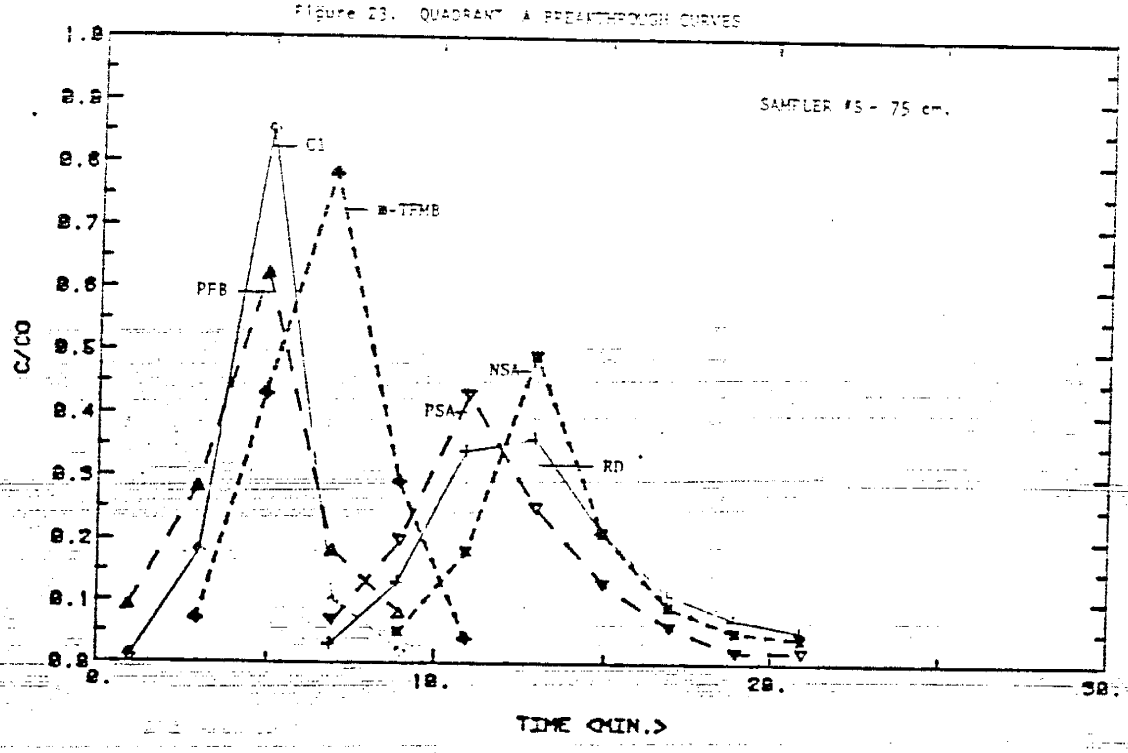

TRACER BREAKTHROUGH CURVES

Figure 35. Numerical Simulation Breakthrough Curves: z = 75 cm.

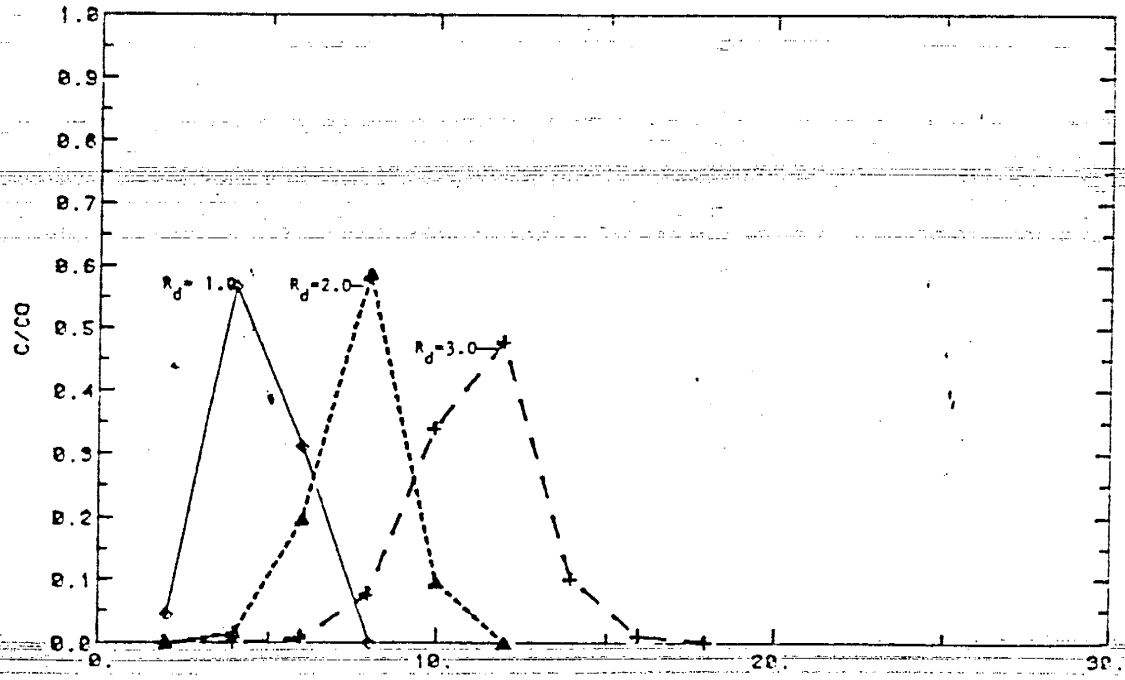

NUMERICAL SIMULATION BREAKTHROUGH CURVES

Figure 28. QUADRANT C BREAKTHROUGH CURVES

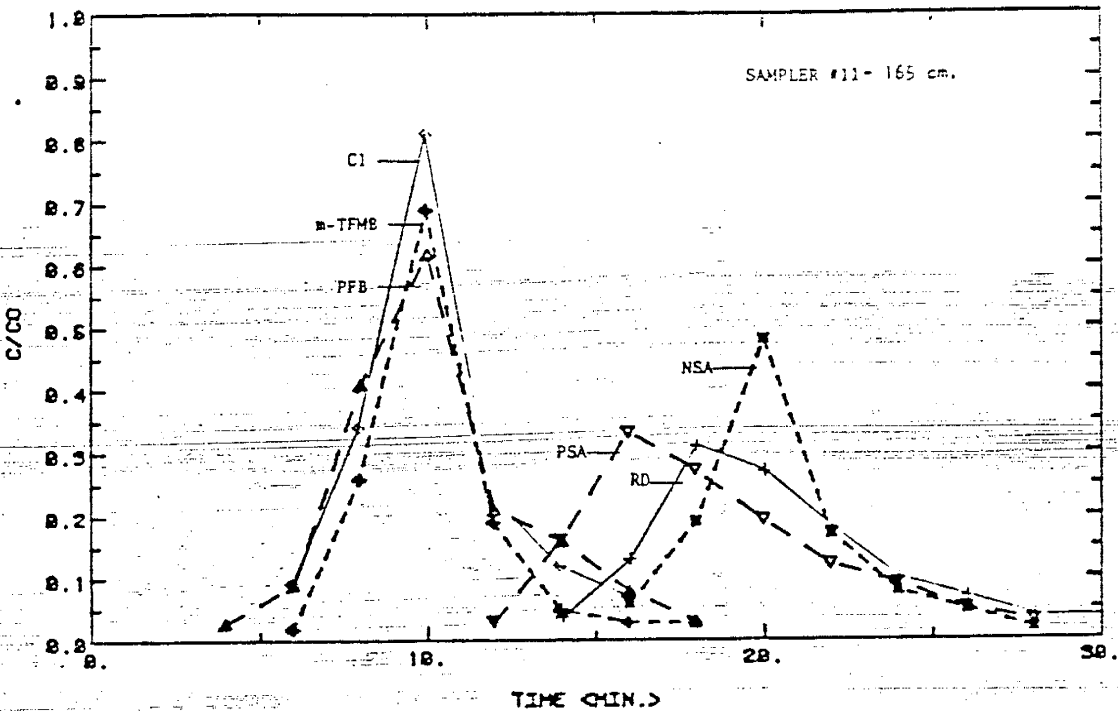

TRACER BREAKTHROUGH CURVES

Figure 36. Numerical Simulation Breakthrough Curves: z = 175 cm.

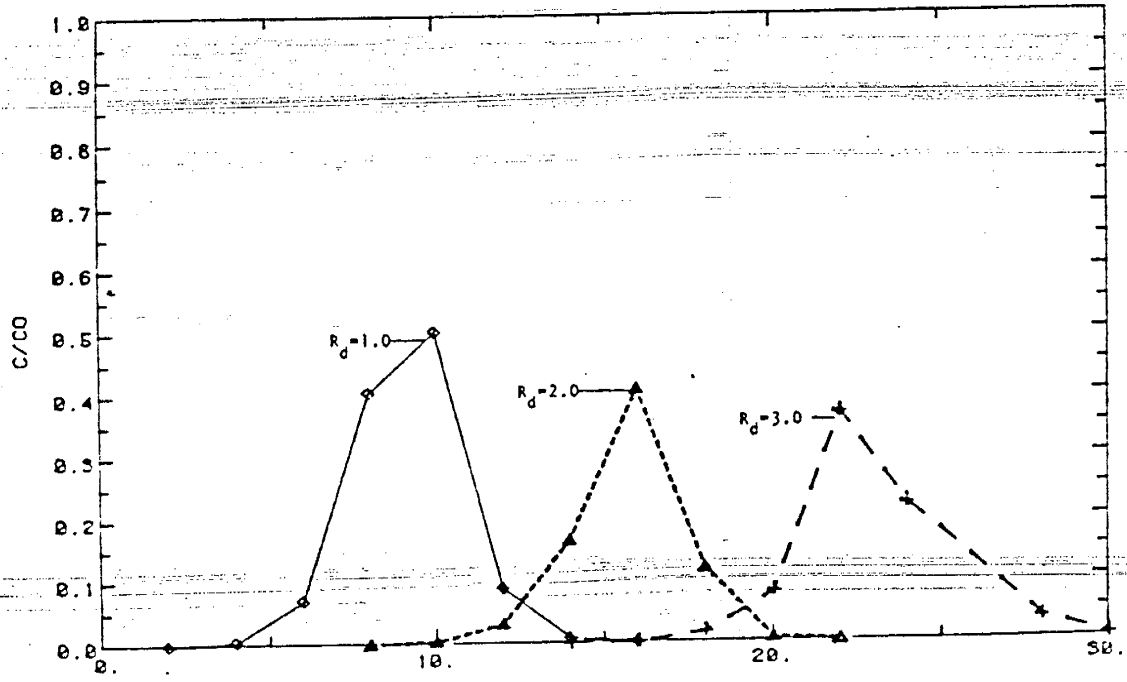

NUMERICAL SIMULATION BREAKTHROUGH CURVES

exhibited a retardation coefficient of approximately 2.0, while rhodamine-B and NSA were clearly lagging with retardation coefficients of 2.5 or greater. This may have been due to a media-effect. Overall the transport of the conservative tracers seems to be in excellent agreement with the degree of solute transport predicted by the model. Thus the model, despite its assumptions of a homogeneous and isotropic media, was able to predict the transport of the conservative and non-conservative tracers through the heterogeneous column of copper ore.

Figures 37 and 29 were compared for the sampling depth of 225 cm. In this case, the conservative tracer peaks were once again consistent with the non-retarded peak shown in the simulation breakthrough curve. Yet, it was interesting to observe that the non-conservative tracers generally had retardation coefficients of approximately 2.0. Also the non-conservative tracer peaks never fluctuated in their elution order. PSA arrived first, followed by rhodamine-B, and finally by NSA.

The comparison of simulation and tracer breakthrough curves yielded valuable insight into the efficiency of the numerical model. In terms of transport through the system, comparison of the conservative tracer peaks with the numerically simulated peak (corresponding to $R_d = 1.0$) showed good agreement. In most cases the conservative tracer peak arrivals coincided exactly with numerically

Figure 29. QUADRANT C BREAKTHROUGH CURVES

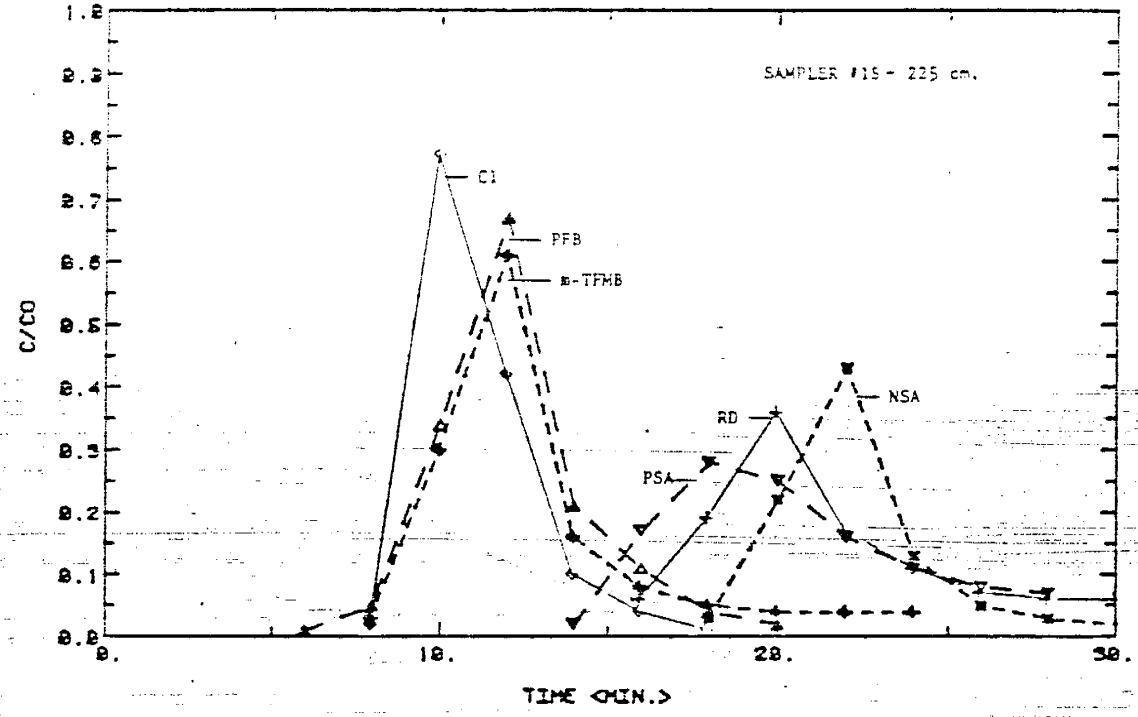

TRACER BREAKTHROUGH CURVES

Figure 37. Numerical Simulation Breakthrough Curves: z = 225 cm.

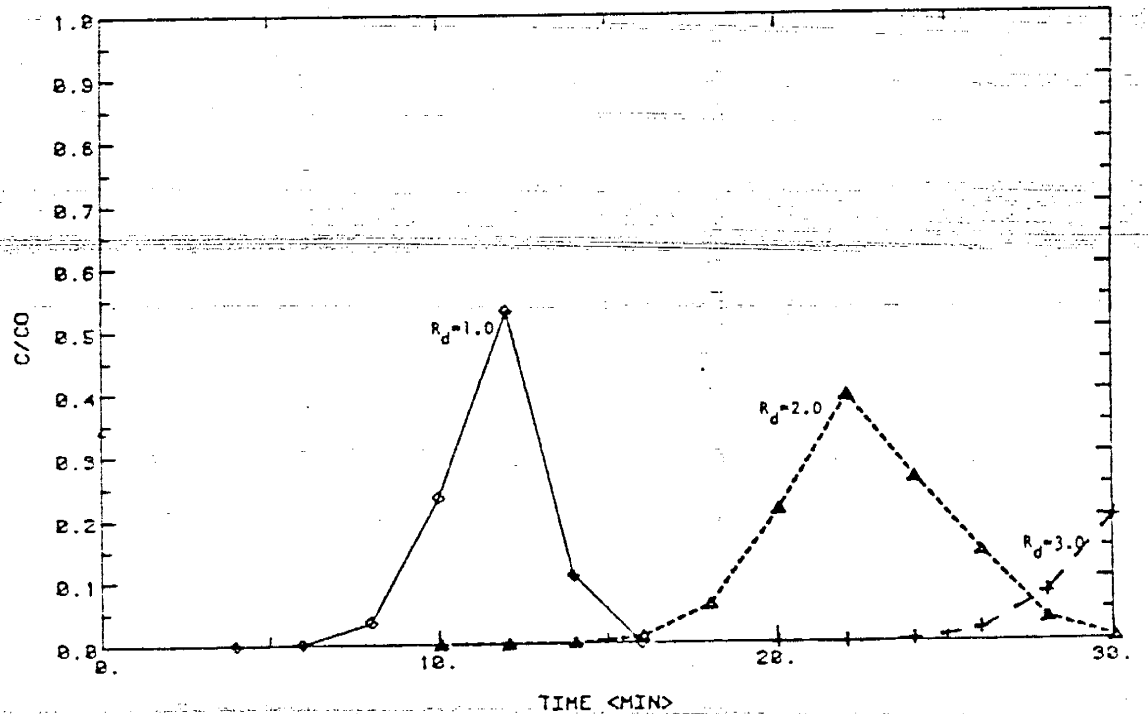

NUMERICAL SIMULATION BREAKTHROUGH CURVES

predicted peak arrivals. Therefore the assumptions made by the model, with regard to an isotropic and homogeneous system, were effective in predicting solute transport behaviour within this known heterogeneous system.

Chloride and PFB seemed to be the most reliable conservative tracers, while m-TFMB exhibited minor retardation effects, probably due to column heterogeneities and slight adsorption. The non-conservative tracers rhodamine-B, PSA and NSA displayed greater variation in transport than that predicted by the numerical model. In this case the retardation coefficients for non-conservative tracers vary from 1.5 - 3.0. Generally, PSA and rhodamine-B exhibited the least variation in adsorption patterns, while the transport of NSA was subject to increased variations in R_d. While the model did not exactly predict non-conservative tracer behaviour, the role of media heterogeneity and its effects on transport should be noted. The range of retardation coefficients was fairly tight, and should not affect estimates of the percentage of surface area contacted to a great degree. The estimates of surface area contacted ranged from 35% to 48%, thus indicating a relatively inefficient copper recovery process. These estimates could be improved by using model input data for a finer average grain size and increasing the moisture content (under saturation the percent of ore contacted should be approximately 100%). Based on comparisons of the simulation and tracer breakthrough curves, the models UNSAT and TRANS

were deemed effective in predicting the transport of tracers through an experimental column of copper ore.

CONCLUSIONS

The results of this experimental - numerical study of flow through a leach heap has produced results which may be considered significant to the improvement of heap leaching in the field. The experimental long-column study, with its suite of experimental tracers, is of potential use to the copper leaching industry in terms of determining how best to monitor the efficiency of a waste-heap leach process. The numerical model offers the potential for predicting the amount of surface area contacted during the leaching process; and can predict the tracer distribution through heaps of varying physical parameters. The combination of an unsaturated flow model and a solute transport model should prove effective for a more accurate prediction of the hyrology of leachate flow.

A summary of the conlusions is provided below:

1. Channeling is the major mechanism of leachate flow in a large waste heap composed of a coarse grained material. The degree of channeling is dependent on the particle size distribution; loading-induced heterogeneities; heap height; and the degree of compaction. For ideal recovery, the solution channel separation distance should be minimal; i.e. the movement of a united leachate front through the porous media.

2. The benefits derived from the use of numerous samplers in the sampling of a leach heap can help determine the degree of solution channeling occurring in a leach heap. Decreasing the amount of ore contributing to each sampler site aids in the identification of separate solution channels

when a tracer is used. (Both the conservative and non-conservative tracers can indicate solution channels due to differing velocities of travel along any channel.) Analysis of effluent breakthrough curves is a quick means of determining the presence of channelization.

3. The use of conservative and non-conservative tracers in conjunction is the preferred means for monitoring a leach heap, since the degree of leachate-ore contact may be estimated from the tracer breakthrough curves if sampling is done along the vertical axis of the heap.

4. Four experimental tracers are effective as monitors of leachate flow, and may have applications for groundwater flow problems. The ease of the HPLC analytical technique is a decided advantage. Para-fluorobenzoic acid and phenyl sulfonic acid are the tracers of choice among the experimental organic acids. PFB is a conservative tracer that exhibits breakthrough characteristics similar to chloride, while PSA is a non-conservative tracer that is strongly sorbed and exhibits a reasonable amount of retardation relative to PFB. Reverse-phase HPLC is rapid and able to detect minute quantities of these tracers.

5. The numerical models UPSTRM and TRANS can predict the hydrology of flow processes during the leach cycle for different types of waste heaps. Varyiable application rates; flow velocities; tracer characteristics; leach heap physical parameters; and grain-size effects are easily handled by these models.

6. Surface area contacted by leachate may be calculated from the model, providing an accurate estimation of the efficiency of the leaching process, and thus, the recovery of copper ore. As long as a non-conservative tracer is used, the retardation coefficient can provide an estimate of surface area contacted.

RECOMMENDATIONS FOR FUTURE RESEARCH

In view of the results obtained from this combined experimental and numerical study, it becomes obvious that more research is required into the hydrologic characteristics of the leach process. In terms of a direct follow-up study, a leach heap in the field could be instrumented for moisture content, pressure head, and the collection of chemical samples. Once data is obtained, the numerical models may be verified for the larger scale processes.

Long-column experiments of a larger scale, with increased capacity for the measurement of physical parameters (especially, moisture content - pressure head relationships during the leach process) should be conducted for purposes of discerning the effects of scale on leach-pile hydraulics. The systematic documentation of column heterogeneity and the effects of anisotropy would be useful. The concept of channel separation distance, in terms of leaching efficieny, could be examined by intensive sampling efforts. (The problem then becomes interference with the leaching process by the presence of the sampling device). The use of a clear material for the column itself may be considered to determine the effects or presence of wall channelization in small scale column studies.

There is much work left to be done in the numerical modeling of the leach process. The models presented here offer a one-dimensional solution for the flow and transport of leachate. If these solutions are expanded to two and/or three dimensions the effects of solution channels, channel separation distances, and transverse disperson may be easily incorporated. Applications of these models to larger- scale leach heaps may also be considered, along with the use of field studies for testing the predictive accuracy of numerical models.

BIBLIOGRAPEY

Aulenbach, D.B.; Bull, J.H. and Middlesworth, B.C. (1978). Use of Tracers to Confirm Ground-Water Flow. Ground Water 16 (3), pp. 149-157.

Bear, J. (1972) Dynamics of Fluids in Porous Media. American Elsevier, New York pp. 162-177.

Beven, K. and Germann, P. (1982) Macropores and Water Flow in Soils. Water Resources Research 18 (5), pp. 1311-1325.

Blake, G.R. (1965) "Bulk Density" Methods of Soil Analysis: Part I., ed. C.A. Black, Amer. Soc. of Agron. Inc., Wisconsin. 257 pp.

Bouma, J. and others (1974) Measurements of Water Movement in Soil Pedons Above the Water Table. University of Wisconsin, Ext. Geol. and Nat. Hist. Survey Info. Circular No. 27.

Bouwer, H. (1966) Rapid Field Measurement of Air Entry Value and Hydraulic Conductivity of Soil as Significant Parameters in Flow System Analysis. Water Resources Research 2 (4), pp. 729-738.

Bouwer, H. and Rice, R.C. (1984) Hydraulic Properties of Stony Vadose Zones. Ground Water 22 (6), pp. 696-705.

Brutsaert, W. (1977) Vertical Infiltration in Dry Soil. Water Resources Research 13 (2), pp. 363-368.

Cathles, L.M. and Murr L.E. (1980) Evaluation of an Experiment Involving Large Column Leaching of Low Grade Copper Sulfide Waste: A Critical Test of a Model of the Waste Leaching Process. Leaching and Recovering Mined Materials. Schlitt, W.J. (ed), New York, AIME, pp. 29-48.

Cathles, L.M. and Schlitt, W.J. (1980) A Model of the Dump Leaching Process that Incorporates Oxygen Balance, Heat Balance, and Two-Dimensional Air Convection. Leaching and Recovering Copper from Mined Materials. Schlitt, W.J. (ed), New York, AIME, pp. 29-48.

Csaba, Horvath (1983) High Pressure Liquid Chromatography: Advances and Perspectives. Volumes 1-3. Academic Press New York.

Davis, S.N.; Thompson, G.M.; Bentley, H.W. and Stiles, G. (1978) GroundWater Tracers - A Short Review. Ground Water 18 (1) pp. 14-23.

Day, P.R. (1965) "Particle Fractionation and Particle-Size Analysis" Methods of Soil Analysis: Part I., ed. C.A. Black, American Society of Agronomy Inc., Wisconsin.

Edwards, W.M.; van der Ploeg, R.R.; and Ehlers, W. (1979) A Numerical Study of the Effects of Noncapillary-Sized Pores Upon Infiltration. Soil Sciences Society of America Journal 45, pp. 851-856.

Elzeftawy, A. and Mansell, R.S. (1975) Hydraulic Conductivity Calculations for Unsaturated Steady-State and Transient-State FLow in Sand. Soil Science Society of America Proceedings 39 (4), pp. 599-603.

Fara,H.D. and Scheidegger, A.E. (1961) Statistical Geometry of Porous Media. Journal of Geophysical Research 66, pp. 3279-3284.

Freeze, R.A. and Cherry, J.A. (1979) Groundwater. Prentice Hall, Inc; New Jersey.

G.K. Turner Associates Inc. (1978) The Determination of Fluoroscein - An Introduction to Fluorimetry.

Grisak, G.E. and Pickens, J.F. (1980) Solute Transport Through Fractured Media, I. The Effect of Matrix Diffusion. Water Resources Research 16 (4), pp. 719-730.

Grisak, G.E.; Pickens, J.F. and Cherry, J.A. (1980) Solute Transport Through Fractured Media: 2. Column Study of Fractured Till. Water Resources Research 16 (4), pp. 719-730.

Harkins, W.D. and Jura, G. (1944) Surfaces of Solids XII. An Absolute Method for the Determination of the Area of a Finely Divided Crystalline Solid. Soil Science Society of America Journal Vol.66 pp. 1362-1366.

Hillel, D. (1980) Fundamentals of Soil Physics. Academic Press, NY, 413 pages.

Huyakorn, P.S. and Nilkuha, K. (1979) Solution of Transient Transport Equation Using an Upstream Finite Element Scheme. Applied Mathematical Modelling 3, pp. 7-17.

Huyakorn, P.S. and Pinder, G.F. (1983) Computational Methods in Subsurface Flow. Academic Press. New York.

Jacobson, R.H., Jr. (1971) A Computer Model Study of Unsaturated Flow in a Leach Dump. New Mexico Institute of Mining and Technology, Socorro, NM, Ph.D. Dissertation.

Jaynes, D.B. and Tyler, E.J. (1980) Comparison of the One-Step Outflow Laboratory Method to an In-Situ Method for Measuring Hydraulic Conductivity. Soil Science Society of America Journal 44, pp.903-907.

Joseph, D.D.; Nield, D.A. and Papanicolau, G. (1982) Nonlinear Equations Governing Flow in a Saturated Porous Medium. Water Resources Research 18 (4), pp. 1049-1052.

Jury, William A. (1982) Simulation of Solute Transport Using a Transfer Function Model. Water Resources Research 18 (2), pp. 363-368.

Khaleel, R. and Payne L.K. (1984) A Comparison of Several Numerical Schemes for Simulating Dispersion in Unsaturated Media. Private Communication

Krstulovic, A.M.; and Brown, P.R. (1982) Reveresed-Phase High Pressure Liquid Chromatography: Theory, Practice and Biomedical Applications. John Wiley and Sons. New York.

Kuhn,M. (1976) Annual Review: Mineral Processing-Hydrometallurgy. Mining Engineering 12/76.

Lyman; Reehl; and Rosenblat (1982) Handbook of Chemical Property Estimation Methods. McGraw Hill. New York.

McWhorter, D.B. and Nelson, J.D. (1979) Unsaturated Flow Beneath Tailings Impoundments. Journal of Geotechnical Division, American Society of Civil Engineering, Vol. 105, GT11, pp. 1317-1334.

Mehuys, G.R.; Stolzy, L.H.; Lehy, J. and Weeks, L.V. (1975) Effect of Stones on the Hydraulic Conductivity of Relatively Dry Desert Soils. Soil Sciences Society of America Proceedings 39, pp. 37-42.

Millington, R.J. and Quirk, J.P. (1959) Permeability of Porous Media. Nature 183, pp. 387-388.

Miniert, J. (1983) An Upstream Finite Element Scheme for the Transient Convection-Dispersion Equation. Term Project - Numerical Simulation Techniques in Hydrology, New Mexico Institute of Mining and Technology, Socorro, New Mexico.

Murr, L.E. (1979) Observations of Solution Transport, Permeability, and Leaching Reactions in Large, Controlled, Copper-bearing Waste Bodies. Hydrometallurgy 5, pp. 67-94.

Murr, L.E. (1980) Theory and Practice of Copper Sulfide Leaching in Dumps and In-Situ. Minerals Science Engineering 12, pp.121-189.

Noorishad, J. and Mehran, M. (1982) An Upstream Finite Element Method for Solution of Transient Transport Equation in Fractured Porous Media. Water Resources Research 18 (3), pp. 588-596.

Omoti, U. and Wild A. (1979) Use of Fluorescent Dyes to Mark the Pathways of Solute Movement Through Soils Under Leaching Conditions: 2. Field Experiments. Soil Science 128. pp. 98-104.

Orchiston, H.D. (1953) Adsorption of Water Vapor: I. Soils at 25 Degrees Centigrade. Soil Science 76, pp. 453-465.

Parizek, R.R. and Lane, B.E. (1970) Soil-Water Sampling Using Pan and Deep Pressure-Vacuum Lysimeters. Journal of Hydrology 11, pp. 1-21.

Parris, N.A. (1976) High Pressure Liquid Chromatography: A Practical Manual. Elsevier Scientific Publishing Company. New York.

Passioura, J.B. (1976) Determination of Soil Water Diffusivities from One-Step Outflow Experiments. Australian Journal of Soil Research 15, pp. 1-8.

Roman, R.J. (1977) Solution Channeling in Leach Dumps. Transactions Society of Mining Engineers. American Institute of Metallurgical Engineering, vol. 262, pp.73-74.

Roman, R.J., Benner, B.R., and Becker, W. (1974) Diffusion Model for Heap Leaching and Its Applications to Scale Up. Transactions Society of Mining Engineers. American Institute of Metallurgical Engineering., vol. 256, pp. 247-252.

Smajstral, A.G.; Redell, D.L. and Barnes, P.L. (1979) Solute Dispersion in Saturated and Unsaturated Soils. Joint Meeting of the ASAE and CSAE. Paper No. 79-2001.

Tang, D.H.; Frind, E.O. and Sudicky, E.A. (1981) Contaminant Transport in Fractured Porous Media: Analytical Solution for a Single Fracture. Water Resources Research 17 (3). pp. 555-564.

Van De Pol, R.M.; Wierenga, P.J. and Nielsen, D.R. (1977) Solute Movement in a Field Soil. Soil Science Society of America Journal 41, pp. 10-13.

Van Genuchten, R. (1978) Calculating the Unsaturated Conductivity with a New Closed-Form Analytical Model. Research Report No.78-WR-08, Princeton University, New Jersey.

Wahler, W.A. and Associates (1974) Evaluation of Mill Tailings Disposal Practices and Potential Dam Stability Problems in the Southwestern United States. U.S. Bureau of Mines OFR-50(1)-75. AppendixB, pp. B1-B111.

Warrick, A.W.; Biggar, J.W. and Nielsen, D.R. (1971) Simultaneous Solute and Water Transfer for an Unsaturated Soil. Water Resources Research 7 (5), pp. 1216-1225.

Wood, W.W. (1973) A Technique for Using Porous Cups for Water Sampling at Any Depth in the Unsaturated Zone. Water Resources Research 9 (2), pp. 486-488.

Yeh, G.T. (1981) On the Computation of Darcian Velocity and Mass Balance in the Finite Element Modelling of Groundwater Flow. Water Resources Research 17 (5), pp. 1529-1534.

Yeh, G.T. and Ward, D.S. (1981) Femwaste: A Finite Element Model of Waste Transport Through Saturated-Unsaturated Porous Media. Oak Ridge National Labs - Environmental Sciences Division No. 1462.

Yeh, J. (1982) Stochastic Analysis of Effects of Spatial Variability on Unsaturated Flow. New Mexico Institute of Mining and Technology, Socorro, NM, Ph.D. Dissertation, 201 pp.

APPENDIX I

Development of Numerical Models UNSAT and TRANS

UNSAT

Governing Differential Equation: $\mathcal{L}(\Psi) = \frac{\partial}{\partial z}\left[K(\Psi)\frac{\partial}{\partial z}(\Psi - z)\right] - C^*(\Psi)\frac{\partial \Psi}{\partial t} = 0$

Initial Condition: $\Psi(z,0) = \Psi_o(z)$

Boundary Conditions: $\Psi(z,t) = \Psi_{s_1}(z,t)$ on s_1 (Dirichlet)

$K(\Psi)\left(\frac{\partial \Psi}{\partial z} - 1\right) n_i + q_{s_2}(z,t) = 0$ on s_2

Trial Function: $\hat{\Psi}(z,t) = \sum_{i=1}^{n} \Psi_i(t)\, N_i(z)$

Shape Functions: $N_1 = 1 - \frac{z}{L_e}$

$N_2 = \frac{z}{L_e}$

Integral Equations for Domain: $\int_R \mathcal{L}(\hat{\Psi})\, N_i\, dz = 0 \qquad i = 1,2,\ldots n$

Finite Element Matrix Equation: $[A]\{\Psi\} + [B]\left\{\frac{\partial \Psi}{\partial t}\right\} = \{F\}$

Element Matrices: $a^e_{ij} = \int_{L_e} \sum_{\ell=1}^{2} N_\ell K_\ell \frac{\partial N_i}{\partial z} \frac{\partial N_j}{\partial z}\, dz, \quad i,j = 1,2$

$b^e_{ij} = \int_{L_e} \sum_{\ell=1}^{2} N_\ell C^*_\ell N_i N_j\, dz$

$f^e_i = \int_{L_e} \sum_{\ell=1}^{2} N_\ell K_\ell \frac{\partial N_i}{\partial z}\, dz - \int_{s_2} N_i q_{s_2}\, ds$

Elements in B Matrix: $b^e_{ii} = \int_{L_e} \sum_{\ell=1}^{2} N_\ell C^*_\ell N\, dz \qquad i = j$

$b^e_{ij} = 0 \qquad i \neq j$

Lumping Matrix for Interior Node:

$$\frac{\varepsilon}{2L_e}\begin{bmatrix}(K_1+K_2) & -(K_1+K_2)\\ -(K_1+K_2) & (K_1+K_2)\end{bmatrix}\begin{Bmatrix}\Psi_1\\ \Psi_2\end{Bmatrix}^{k+1} + \frac{L_e}{\Delta t}\begin{bmatrix}C^*_1/3+C^*_2/6 & 0\\ 0 & C^*_1/6+C^*_2/3\end{bmatrix}\begin{Bmatrix}\Psi_1\\ \Psi_2\end{Bmatrix}^{k+1} =$$

$$\frac{(\varepsilon-1)}{2L_e}\begin{bmatrix}(K_1+K_2) & -(K_1+K_2)\\ -(K_1+K_2) & (K_1+K_2)\end{bmatrix}\begin{Bmatrix}\Psi_1\\ \Psi_2\end{Bmatrix}^{k} + \frac{L_e}{\Delta t}\begin{bmatrix}C^*_1/3+C^*_2/6 & 0\\ 0 & C^*_1/6+C^*_2/3\end{bmatrix}\begin{Bmatrix}\Psi_1\\ \Psi_2\end{Bmatrix}^{k} +$$

$$\begin{Bmatrix}-(K_1+K_2)/2\\ (K_1+K_2)/2\end{Bmatrix}$$

Governing Differential Equation: $\mathcal{L}(c) = \theta R_d^f \frac{\partial C}{\partial t} - \frac{\partial}{\partial z}\left(\theta D \frac{\partial C}{\partial z} - vC\right)$

Initial Condition: $C(z,0) = C_o(z)$

Boundary Condition : $C(z,t) = C_{s_1}(z,t)$ on s_1

$$J_{s_2}(z,t) = \left[q(z,t)C(z,t) - \theta(z,t)D(z,t)\frac{\partial C}{\partial z}\right] n_i \text{ on } s_2$$

where: J_{s_2} = solute flux along Neumann Boundary s_2

Using Shape and Weight Functions : the Differential Equation is

$$\theta R_d^f \int_R \frac{\partial C}{\partial t} N_i \, dR - \int_R \left[v\frac{\partial C}{\partial z} - \theta D \frac{\partial^2 C}{\partial z^2}\right] W_i \, dR = 0$$

Shape Functions: $N_1 = 1 - \frac{x}{L_e}$

$$N_2 = \frac{x}{L_e}$$

Weight Functions: $W_1 = 1 - \frac{x}{L_e} + \alpha\left[\frac{3x(x-L_e)}{(L)_e^2}\right]$

$$W_2 = \frac{x}{L_e} - \alpha\left[\frac{3x(x-L_e)}{(L_e)^2}\right]$$

Using Greene's Identity : $-\theta D \int_L \frac{\partial^2 C}{\partial z^2} dz = \theta D \int_L \frac{\partial W_i}{\partial z} \frac{\partial C}{\partial z} dz$

If Surface Integral = 0.0 : $\int_L \left[\theta D \frac{\partial W_i}{\partial z}\frac{\partial C}{\partial z} + v\frac{\partial C}{\partial z} W_i\right] dz + \int_L \frac{\partial C}{\partial t} N_i \, dz = 0$

Assume Trial Function : $C = \sum_{j=1}^{n} N_j(z) \, C_j(t)$

Matrix Equation : $[A_{IJ}]\{C\} + [M_{IJ}]\{\dot{C}\} = 0$

where :

$$A_{IJ}^{fe} = 2b\theta D_s \int_{Se} \frac{\partial W_i}{\partial z}\frac{\partial N_j}{\partial z} dz - 2bv \int_{Se} \frac{\partial W_i}{\partial z} N_j \, dz$$

$$+ \delta(J-2)2bv + 2b\theta R_d^f \int_{Se} W_I \, N_J \, dz$$

$$M_{IJ}^{fe} = 2b\theta R_d^f \int_{Se} W_I N_J \, dz$$

$$G_I^{fe} = \delta(x-x_i)\,\delta(z-z_i)\, v_{si}\, C$$

Element Matrices: $a_{ij} = \int_L \left[D \frac{\partial W_i}{\partial z} \frac{\partial N_j}{\partial z} + v W_i \frac{\partial N_j}{\partial z} \right] dz$

$$b_{ij} = \int_L N_i N_j \, dz$$

Substitute for Shape Functions & Integrals:

$$[A]^e = \int_{Le} D \begin{bmatrix} (-\frac{1}{Le}+3\alpha(2x/Le^2-1/Le)) & (-1/Le) & -\frac{1}{Le}+3\alpha(2x/Le^2-1/Le)) & (1/Le) \\ (\frac{1}{Le}-3\alpha(2x/Le^2-1/Le)) & (-1/Le) & \frac{1}{Le}-3\alpha(2x/Le^2-1/Le)) & (1/Le) \end{bmatrix} dz$$

$$+ v \; Le \begin{bmatrix} (1-\frac{x}{Le}+\alpha(\frac{3x(x-Le)}{Le^2})) & (-1/Le) & 1-\frac{x}{Le}+\alpha(\frac{3x(x-Le)}{Le^2})) & (1/Le) \\ (\frac{x}{Le}-\alpha(\frac{3x(x-Le)}{Le^2})) & (-1/Le) & \frac{x}{Le}-\alpha(\frac{3x(x-Le)}{Le^2})) & (1/Le) \end{bmatrix}$$

$$A^e = \frac{D}{Le}\begin{bmatrix} 1 & -1 \\ -1 & 1 \end{bmatrix} + \frac{v}{2E}\begin{bmatrix} -1+\alpha & 1-\alpha \\ -1-\alpha & 1+\alpha \end{bmatrix}$$

$$B^e = Le\begin{bmatrix} 1/3 & 1/6 \\ 1/6 & 1/3 \end{bmatrix}$$

The Weighted Average Approximation is :

$$[A]\left(E\{C\}_{t+\Delta t} + (1-E)\{C\}_t\right) + \frac{1}{\Delta t}[B]\left(\{C\}_{t+\Delta t} - \{C\}_t\right) = 0, \quad \text{where } 0 \le E \le 1$$

Assembling the Global Matrices:

$$\frac{DE}{Le}\begin{bmatrix} 1 & -1 & \cdots & & & \\ -1 & 2 & \cdots & & & \\ \cdots & -1 & 2 & & & \\ & & \vdots & & & \\ & & -1 & 2 & -1 & \\ & & & -1 & 1 & \end{bmatrix}\begin{Bmatrix} & \\ C & \\ & \end{Bmatrix}_{t+\Delta t} + \frac{VE}{2}\begin{bmatrix} -1+\alpha & 1-\alpha & & & & \\ -1-\alpha & 1+\alpha-1+\alpha & 1-\alpha & & & \\ & -1-\alpha & 1+\alpha-1+\alpha & 1-\alpha & & \\ & & \vdots & & & \\ & & & -1-\alpha & 2\alpha & 1-\alpha \\ & & & & -1-\alpha & 1+\alpha \end{bmatrix}\begin{Bmatrix} & \\ C & \\ & \end{Bmatrix}_{t+\Delta t}$$

$$+ \frac{Le}{t}\begin{bmatrix} 1/3 & 1/6 & & & & \\ 1/6 & 2/3 & 1/6 & & & \\ & 1/6 & 2/3 & 1/6 & & \\ & & \vdots & & & \\ & & 1/6 & 2/3 & 1/6 & \\ & & & 1/6 & 1/3 & \end{bmatrix}\begin{Bmatrix} & \\ C & \\ & \end{Bmatrix}_{t+\Delta t} = \text{the same matrices multiplied by } C \text{ and the weight function } (1-E).$$

```
C
C-----UNSAT.FOR-----WRITTEN BY R. KHALEEL  AND  T.C. YEH-----N.M.I.M.T.-----
C
C       THIS IS A FINITE ELEMENT PROGRAM TO SIMULATE
C       ONE-DIMENSIONAL UNSATURATED FLOW.
C
C
C       INPUT INFORMATION:
C
C       BEFORE EXECUTING THIS PROGRAM, YOU SHOULD CREATE AN INPUT
C       FILE WHICH CONSISTS OF THE FOLLOWING:
C
C       (1)     SOIL TYPE NAME (NOT TO EXCEED 10 CHARACTERS)
C
C       (2)     FUNCTIONAL RELATIONS OR TABULAR INPUT
C
C                       INT--- 0 FUNCTIONAL RELATIONSHIPS USED FOR
C                                MOISTURE CHARACTERISTIC CURVES
C                              1 TABULAR INPUT DATA
C
C       (3)     HYDRAULIC CONDUCTIVITY AND SUCTION RELATIONSHIP
C               (NP AND KSAT)
C                       NP----NO. OF PSI-K PAIR
C                       KSAT--SATURATED HYDRAULIC CONDUCTIVITY
C
C       (4)     XP AND XK PAIR
C                       XP--PSI
C                       XK--RELATIVE HYDRAULIC CONDUCTIVITY
C       NOTE!!  XP SHOULD BE IN A DESCENDING ORDER
C
C       (5)     SOIL MOISTURE RETENTION DATA (XPP AND XTHE)
C                       XPP--PSI
C                       XTHE--MOISTURE CONTENT
C       NOTE!!  XPP SOULD BE IN A DESCENDING ORDER
C
C       (6)     NODES, DELZ, DELT, TMAX, TOL, MAXIT, TPRIN
C                       NODES--NO. OF NODAL POINTS
C                       DELZ--INTERVAL BETWEEN NODAL POINTS
C                       DELT--TIME INTERVAL
C                       TMAX--MAXIMUM SIMULATION TIME
C                       TOL---TOLERANCE
C                       EPS---TIME WEIGHTING FACTOR
C                       MAXIT-MAXIMUM NO. OF ITERATIONS
C
C       (7)     TOP BOUNDARY CONDITION (NBC(1), BC(1), Q(1))
C                       NBC(1)--0 FOR CONSTANT HEAD BOUNDARY
C                               1 FOR FLUX BOUNDARY
C                       BC(1)---HEAD VALUE FOR THE CONSTANT HEAD BOUNDARY
C                       Q(1)----FLUX FOR FLUX BOUNDARY
C
C       (8)     BOTTOM BOUNDARY CONDITION (NBC(2), BC(2), Q(2))
C       (9)     INITIAL CONDITION
C
C       ALL THE INPUT DATA SHOULD BE IN A FREE FORMAT
C       UNITS OF PARAMETERS SHOULD BE CONSISTENT WITH KSAT
C
C
C
      DOUBLE PRECISION NAME, FILN
      REAL KSAT, L
```

```
      DIMENSION XP(51),XK(51),XC(51),YP(51),XTHE(51),XPP(51),
     *  PPSI(51),PSIH(51),NBC(2),BC(2),Q(2),PP(51),SF(2,2,51),
     *  RHS(2,2,51),R(2,51),TPSI(51),RH(2,2,51)
      COMMON A(51),B(51),C(51),D(51),PSI(51)
      COMMON DELT,DELZ,EPS,NODES,TWIN,TWOUT,TWEN,TWUT,WS,WS1,WIS,
     *  DWIN,DWOUT,DELMAX,POR,TMAX,TIME
      DATA TWIN,TWOUT,TWEN,TWUT,WS,WIS/0.,0.,0.,0.,0.,0./
C
      WRITE(5,1)
1     FORMAT(' ',' INPUT FILE NAME IN A10')
      READ(5,2) FILN
2     FORMAT(A10)
      WRITE(5,999)
999   FORMAT(' DO YOU WANT TO HAVE A HARD COPY?  YES=3, NO=5')
      READ(5,*)NPRT
      OPEN(UNIT=6,FILE='WARRICK.DAT',ACCESS='SEQIN',DEVICE='DSK')
      READ(6,3)NAME
3     FORMAT(A10)
      WRITE(NPRT,1001)NAME
1001  FORMAT(' ',10X,5('-'),A10,'SOIL PROPERTIES ',10('-')//)
      READ(6,*) INT
C
C     READ SOIL PROPERTIES
C
      READ(6,*)NP,KSAT
      IF (INT. EQ. 0) GO TO 770
      WRITE(NPRT,1002)
1002  FORMAT(' ',10X,10('-'),'PSI',13('-'),'KR',10('-'),//)
      DO 10 I=1,NP
      READ(6,*)XP(I),XK(I)
      XP(I)=-XP(I)
      WRITE(NPRT,1003)XP(I),XK(I)
1003  FORMAT(' ',10X,2E16.5)
10    CONTINUE
770   CONTINUE
C
C     READ PSI AND THETA RELATION
C
      READ(6,*)NPT,POR
      IF (INT .EQ. 0) GO TO 772
      WRITE(NPRT,1004)
1004  FORMAT(' ',/,10X,10('-'),'PSI',13('-'),'THETA',13('-'),/)
      DO 20 I=1,NPT
      READ(6,*)XPP(I),XTHE(I)
      XPP(I)=-XPP(I)
      WRITE(NPRT,1005)XPP(I),XTHE(I)
1005  FORMAT(' ',10X,2F16.5)
20    CONTINUE
C
C     DETERMINE PSI AND MOISTURE CAPACITY RELATIONSHIP
C
      WRITE(NPRT,1015)
1015  FORMAT(' ',/,10X,10('-'),'PSI',10('-'),'  C ',10('-'),/)
      NPC=NPT-1
      DO 30 I=1,NPC
      XC(I)=(XTHE(I)-XTHE(I+1))/(XPP(I)-XPP(I+1))
      YP(I)=0.5*(XPP(I)+XPP(I+1))
      WRITE(NPRT,1006)XP(I),XC(I)
1006  FORMAT(' ',10X,2F16.5)
30    CONTINUE
```

```
772     CONTINUE
C
C       READ PARAMETERS
C
        READ(6,*)NODES,DELZ,DELT,TMAX,TOL,EPS,MAXIT,DELMAX
        WRITE(NPRT,1007)NODES,DELZ,DELT,TMAX,TOL,EPS,MAXIT,DELMAX
1007    FORMAT(' ',//,10X,'  TOTAL NO. OF NODES= ',I4,/,
     *  ' ',10X,'    DELZ= ',F16.5,/,11X,'    DELT= ',F16.5,/,
     *  11X,'   TMAX= ',F16.5,/,11X,'TOLERANCE= ',F16.5,/,
     *  11X,'  TIME WEIGHTING FACTOR, EPS = ',F16.5,/,
     *  11X,'  MAXIT= ',I4,/,11X,'  MAXIMUM DELT=',F16.5,/,
     *  //11X,'  BOUNDARY CONDITIONS -------',
     *  13X,'  MODE',' TYPE','    PSI   ','     Q     ')
        NODE1=NODES-1
        NELEM=NODE1
        L=DELZ
        NELEM1=NELEM-1
C
C       INITIAL CONDITION AND BOUNDARY CONDITION
C
C
        DO 35 I=1,2
        N=1
        IF (I.EQ.2)N=NODES
        READ(6,*)NBC(I),BC(I),Q(I)
        WRITE(NPRT,11) N,NBC(I),BC(I),Q(I)
11      FORMAT(' ',10X,2I5,2F10.2)
        PSI(N)=BC(I)
        PPSI(N)=PSI(N)
        TPSI(N)=PPSI(N)
35      CONTINUE
        WRITE(NPRT,1008)
1008    FORMAT(' ',/,10X,10('-'),' INITIAL CONDITION',10('-'),/)
        Z=0.
        IF (INT .EQ. 1) GO TO 96
        DO 402 I=2,NODE1
        Z=Z+DELZ
        CALL FNCZT (Z,THETA)
        CALL FNCTP (THETA,PSI(I))
402     CONTINUE
        GO TO 404
96      READ(6,*) (PSI(I),I=2,NODE1)
404     CONTINUE
        DO 40 I=2,NODE1
        PPSI(I)=PSI(I)
        TPSI(I)=PPSI(I)
40      CONTINUE
        WRITE(NPRT,1009) (I,PSI(I),I=1,NODES)
1009    FORMAT(5(I4,F10.3))
C
C       SIMULATION STARTS HERE
C
        TIME=0.0
        LA=0
C
C       TIME LOOP
C
1000    CONTINUE
        LA=LA+1
        TIME=TIME+DELT
```

```
      WRITE(NPRT,1030)TIME
1030  FORMAT(' ',/,10('-'),'SIMULATION TIME = ',E13.5,10('-'),
     *  //)
C
C     PREDICT PSI AT T-1/2 TIME STEP BY LINEAR EXTRAPOLATION
C
      TWEN=TWIN
      TWOUT=TWOUT
      WS1=WS
      DWIN=0.
      DWOUT=0.
      IF(LA.GT.1) DTT=0.5*DELT/DT1
      DO 100 I=1,NODES
      IF(LA.GT.1)PSIH(I)=PPSI(I)+DTT*(PPSI(I)-TPSI(I))
      IF(LA.LE.1) PSIH(I)=PPSI(I)
100   CONTINUE
      ITER=0
C
C     ITERATION LOOP
C
900   CONTINUE
      ITER=ITER+1
C
C     SET UP ELEMENT STIFFNESS MATRIX
C
      DO 200 K=1,NELEM
      XK1=1.0
      XK2=1.0
      C1=0.0
      C2=0.0
      IF (INT .EQ. 0) GO TO 780
      IF(PSIH(K).LT.0.0)CALL INTERP(XP,XK,PSIH(K),XK1,NP)
      IF(PSIH(K+1).LT.0.0)CALL INTERP(XP,XK,PSIH(K+1),XK2,NP)
      IF(PSIH(K).LT.0.0)CALL INTERP(YP,XC,PSIH(K),C1,NPC)
      IF(PSIH(K+1).LT.0.0)CALL INTERP(YP,XC,PSIH(K+1),C2,NPC)
      GO TO 785
780   CONTINUE
      IF (PSIH(K).LT.0.0)CALL FNCPK(PSIH(K),XK1)
      IF (PSIH(K+1).LT.0.0)CALL FNCPK(PSIH(K+1),XK2)
      IF (PSIH(K).LT.0.0)CALL FNCPC(PSIH(K),C1)
      IF (PSIH(K+1).LT.0.0)CALL FNCPC(PSIH(K+1),C2)
785   CONTINUE
      XK1=XK1*KSAT

      XK2=XK2*KSAT
C
C     DETERMINE INDIVIDUAL ELEMENTS IN EACH ELEMENT MATRIX
C
      A11=(XK1+XK2)*0.5/L
      A12=-A11
      A21=A12
      A22=A11
      B11=L*(C1/3.0+C2/6.0)/DELT
      B12=0.0
      B21=B12
      B22=L*(C1/6.0+C2/3.0)/DELT
      SF(1,1,K)=EPS*A11+B11
      SF(1,2,K)=EPS*A12+B12
      SF(2,1,K)=EPS*A21+B21
      SF(2,2,K)=EPS*A22+B22
```

```
      RHS(1,1,K)=(EPS-1.)*A11+B11
      RHS(1,2,K)=(EPS-1.)*A12+B12
      RHS(2,1,K)=(EPS-1.)*A21+B21
      RHS(2,2,K)=(EPS-1.)*A22+B22
      RH(1,1,K)=B11
      RH(1,2,K)=B12
      RH(2,1,K)=B21
      RH(2,2,K)=B22
      R(1,K)=-0.5*(XK1+XK2)
      R(2,K)= 0.5*(XK1+XK2)
200   CONTINUE
C
C     ASSEMBLE THE ELEMENT STIFFNESS MATRICES INTO A GLOBAL MATRIX
C
C     TOP BOUNDARY CONDITION
C
      IF(NBC(1).EQ.0)GOTO 210
C
C     CONSTANT FLUX BOUNDARY CONDITION
C
      A(1)=SF(1,1,1)
      B(1)=SF(1,2,1)
      D(1)=RHS(1,1,1)*PPSI(1)+RHS(1,2,1)*PPSI(2)+R(1,1)+Q(1)
      GOTO 220
C
C     CONSTANT HEAD BOUNDARY CONDITION
C
210   A(1)=0.0
      B(1)=1.0
      C(1)=0.0
      D(1)=BC(1)
220   CONTINUE
C
C     INTERIOR NODES
C
      DO 250 K=1,NELEM1
      K1=K+1
      A(K1)=SF(2,1,K)
      B(K1)=SF(2,2,K)+SF(1,1,K1)
      C(K1)=SF(1,2,K1)
      AA=RHS(2,1,K)
      BB=RHS(2,2,K)+RHS(1,1,K1)
      CC=RHS(1,2,K1)
      D(K1)=AA*PPSI(K)+BB*PPSI(K+1)+CC*PPSI(K+2)+R(2,K)+R(1,K1)
250   CONTINUE
C
C     LOWER BOUNDARY
C
      IF(NBC(2).EQ.0)  GOTO 260
C
C     CONSTANT FLUX BOUNDARY CONDITION
C
      A(NODES)=SF(2,1,NELEM)
      B(NODES)=SF(2,2,NELEM)
      D(NODES)=RHS(2,1,NELEM)*PPSI(NODES)+RHS(2,2,NELEM)
     *  *PPSI(NODES)+R(2,NELEM)-Q(2)
      GOTO 270
C
C     CONSTANT HEAD BOUNDARY CONDITION
C
```

```
260       A(NODES)=0.0
          B(NODES)=1.0
          C(NODES)=0.0
          D(NODES)=BC(2)
270       CONTINUE
C
C         CALL TRIDIA
C
          CALL TRIDIA(NODES,PSI)
C
C         TEST OF CONVERGENCE
C
          EPSLON=0.0
          DO 300 I=2,NODE1
          CHG=ABS((PSI(I)-PP(I))/PSI(I))
          IF (CHG.LT.EPSLON)GOTO 300
          EPSLON=CHG
          NMAX=I
300       CONTINUE
          WRITE(NPRT,1110)ITER,EPSLON,NMAX
1110      FORMAT(1X,' MAX. RELATIVE CHANGE IN PRESSURE HEAD DURING '
     *    ,' ITERATION'
     *    ,I3,' WAS ',E13.5,' AT NODE ',I4)
          IF (EPSLON.LE.TOL.AND.ITER.NE.1) GOTO 500
C
C         IMPROVE THE PSIH VALUE FOR NEXT ITERATION
C
          DO 350 I=1,NODES
          PSIH(I)=0.5*(PPSI(I)+PSI(I))
          PP(I)=PSI(I)
350       CONTINUE
          IF(ITER.LT.MAXIT)GOTO 900
          WRITE(NPRT,1010)ITER
1010      FORMAT(' ',/,'******* MAX. NO. OF ITERATION EXCEEDED AT ',
     *    I4/)
500       CONTINUE
          WRITE(NPRT,1120)
1120      FORMAT(' ',/,13X,'Z',13X,'PSI',6X,'THETA',/)
          Z=0.0
          IF (INT.EQ.1) GOTO 610
          DO 605 I=1,NODES
          CALL FNCPT (PSI(I),THETA)
          IF (PSI(I).GE.0.0) THETA=POR
          WRITE (NPRT,1011) Z,PSI(I),THETA
          Z=Z+DELZ
605       CONTINUE
          GOTO 620
610       DO 600 I=1,NODES
          CALL INTERP(XPP,XTHE,PSI(I),THETA,NPT)
          psi(I)=-psi(I)
          IF(PSI(I).GE.0.0)THETA=POR
          WRITE(NPRT,1011)Z,PSI(I),THETA
1011      FORMAT(' ',10X,F6.2,F16.4,2X,F7.4)
          Z=Z+DELZ
600       CONTINUE
620       CONTINUE
C
          CALL MATBAL (NPRT,PPSI,R,RH,Q,NBC)
C         DETERMINE A TIME STEP SIZE FOR NEXT TIME STEP
C
```

```
      DT1=DELT
      IF (NBC(1) .EQ. 1) GO TO 47
      Q(1)=(PSI(1)-PSI(2)-DELZ)*EPS*R(2,1)/DELZ +
     &  (PPSI(1)-PPSI(2)-DELZ)*(1.-EPS)*R(2,1)/DELZ
47    DELT=AMIN1(DELT/EPSLON*TOL,0.1*DELZ/Q(1))
      IF (ITER .GT. 5) DELT=0.5*DELT
      IF (DELT .GT. DELMAX) DELT=DELMAX
      IF (TIME+DELT .GE. TMAX) DELT=TMAX-TIME
C
C     STORE THE PSI VALUES FOR NEXT TIME STEP
C
      DO 700 I=1,NODES
      TPSI(I)=PPSI(I)
      PPSI(I)=PSI(I)
700   CONTINUE
C
      IF(TIME.GE.TMAX) STOP
      GOTO 1000
      END
C
C-----------------------------------------------------------------------
C
      SUBROUTINE INTERP(X,Y,XX,YY,N)
      DIMENSION X(N),Y(N)
C
C     LINEAR INTERPOLATION
C
      DO 10 I=2,N
      IF(XX.GT.X(I).AND.I.LT.N)GOTO 10
      AA=Y(I-1)+(XX-X(I-1))*(Y(I)-Y(I-1))/(X(I)-X(I-1))
      YY=AA
      GOTO 20
10    CONTINUE
20    RETURN
      END
C
C-----------------------------------------------------------------------
C
      SUBROUTINE TRIDIA(NN,ANS)
      COMMON A(51),B(51),C(51),D(51),PSI(51)
      DIMENSION BB(51),GG(51),ANS(51)
C
C     SET UP BB AND GG ARRAYS
C
      BB(1)=B(1)
      GG(1)=D(1)/B(1)
      DO 10 I=2,NN
      I1=I-1
      BB(I)=B(I)-A(I)*C(I1)/BB(I1)
      GG(I)=(D(I)-A(I)*GG(I1))/BB(I)
10    CONTINUE
C
C     PERFORM BACK SUBSTITUTION
C
      ANS(NN)=GG(NN)
      N1=NN-1
      DO 15 J=1,N1
      I=NN-J
      ANS(I)=GG(I)-C(I)*ANS(I+1)/BB(I)
15    CONTINUE
```

```
      RETURN
      END
;-----------------------------------------------------------------------
;
;--- NOTE! THE FOLLOWING FIVE FUNCTIONAL SUBROUTINES SPECIFICALLY APPLY TO
;         PANOCHE CLAY LOAM (WARRICK ET AL., 1971) ONLY.  USE ANOTHER
;         FUNCTIONAL RELATION FOR A DIFFERENT SOIL -----
;-----------------------------------------------------------------------
;
      SUBROUTINE FNCTP(XX,YY)
      IF (XX.LE.0.36062234) YY=-1300.*EXP(-10.5*XX)
      IF (XX.GT.0.36062234) YY=-1.59E07*EXP(-36.6*XX)
      RETURN
      END
;-----------------------------------------------------------------------
;
      SUBROUTINE FNCPT(XX,YY)
      IF (XX.LE.-29.484) YY=0.6829-0.09524*ALOG(ABS(XX))
      IF (XX.GT.-29.484.AND.XX.LE.-14.495) YY=0.4531-
     & 0.02732*ALOG(ABS(XX))
      RETURN
      END
;-----------------------------------------------------------------------
;
      SUBROUTINE FNCZT(XX,YY)
      IF (XX.GT.60.0) YY=0.20
      IF (XX.LE.60.0) YY=0.15+0.0008333*XX
      RETURN
      END
C-----------------------------------------------------------------------
C
      SUBROUTINE FNCPK(XX,YY)
      IF (XX.LE.-29.484) YY=19.34E05/37.8*(ABS(XX))**(-3.4095)
      IF (XX.GT.-29.484.AND.XX.LE.-14.495)YY=516.8/
     & 37.8*(ABS(XX))**(-0.97814)
      RETURN
      END
C-----------------------------------------------------------------------
C
      SUBROUTINE FNCPC(XX,YY)
      IF (XX.LE.-29.484) YY=0.09524/ABS(XX)
      IF (XX.GT.-29.484.AND.XX.LE.-14.495) YY=
     & 0.02732/(ABS(XX))
      RETURN
      END
C-----------------------------------------------------------------------
C
      SUBROUTINE MATBAL (NPRT,PPSI,R,RH,Q,NBC)
      DIMENSION PPSI(51),R(2,51),RH(2,2,51),Q(2),NBC(2)
      COMMON A(51),B(51),C(51),D(51),PSI(51)
      COMMON DELT,DELZ,EPS,NODES,TWIN,TWOUT,TWEN,TWUT,WS,WS1,WIS,
     & DWIN,DWOUT,DELMAX,POR,TMAX,TIME
      TWIN=TWEN
      TWOUT=TWUT
C
C     COMPUTES WATER INFLOW OR OUTFLOW THROUGH THE UPPER BOUNDARY
C
      IF (NBC(1) .EQ. 1) GO TO 1
      Q(1)=(PSI(1)-PSI(2)+DELZ)*EPS*R(2,1)/DELZ*DELT
     & + (PPSI(1)-PPSI(2)+DELZ)*(1.-EPS)*R(2,1)/DELZ*DELT
```

```
1       CONTINUE
        IF (Q(1) .GT. 0.0) GO TO 11
        DWOUT=DWOUT-Q(1)
        GO TO 12
11      DWIN=DWIN-Q(1)
12      CONTINUE
C
C       COMPUTES WATER INFLOW OR OUTFLOW THROUGH LOWER BOUNDARY
C
        IF (NBC(2) .EQ. 1) GO TO 2
        Q(2)=-(PSI(NODES-1)-PSI(NODES)+DELZ)*EPS*R(2,NODES-1)/DELZ*DELT
     &  - (PPSI(NODES-1)-PPSI(NODES)+DELZ)*(1.-EPS)*R(2,NODES-1)/DELZ
     &  *DELT
2       CONTINUE
        IF (Q(2) .GT. 0.) GO TO 13
        DWOUT=DWOUT-Q(2)
        GO TO 14
13      DWIN=DWIN-Q(2)
14      CONTINUE
C
C       COMPUTES CHANGE IN WATER STORAGE
C
        DWS=0.
        NODE1=NODES-1
        DO 140 K=2,NODE1
        DWS=DWS+(RH(2,2,K-1)+RH(1,1,K))*(PSI(K)-PPSI(K))*DELT
140     CONTINUE
        WS=WS+DWS
        WS2=WS+WIS
        TWIN=TWIN+DWIN
        TWOUT=TWOUT+DWOUT
        DWDIFF=DWIN-DWOUT
        TWDIFF=TWIN-TWOUT
        DERRW=ABS(DWS-DWDIFF)
        RERRW=ABS(WS-TWDIFF)
        WRITE (NPRT,475)
        WRITE (NPRT,471)
        WRITE (NPRT,473) DWIN,DWOUT,DWDIFF,DWS,TWIN,TWOUT,TWDIFF,
     &  WS,WIS,WS2,DERRW,RERRW
471     FORMAT (/31X,'* * * * MATERIAL BALANCE ERROR ANALYSIS * * * * ')
473     FORMAT (/,1X,'INC. WATER IN =',E11.4,T30,'INC. WATER OUT =',
     &  E11.4,T60,'INC. WATER IN & OUT =',E11.4,T95,'INC. WATER STRG.
     &  CHANGE =',E11.4,/1X,'CUM. WATER IN =',E11.4,T30,'CUM. WATER
     &  OUT =',E11.4,T60,'CUM. WATER IN & OUT =',E11.4,T95,'CUM.
     &  WATER STRG. CHANGE =',E11.4,/,' INTL. WATER STRG. =',E11.4,T30,
     &  'CUM. WATER STRG. =',E11.4,T60,'INC. WATER ERROR, % =',E11.4,
     &  T95,'CUM. WATER ERROR, % =',E11.4)
475     FORMAT (26('====='))
        RETURN
        END
```

TRANS.FOR

Written by J. Miniert (1983) at NMIMT

Modified by V. Terauds (1985)

Trans.for is a finite element program designed to solve the differential equation for convective-dispersive solute transport. It uses an upstream-weighting technique to minimize oscillations and overshoot. The code prompts the user for input at the terminal.

```
      DIMENSION GLBL(99,99),RHS(99),C(99),AA(99),BB(99)
      DIMENSION CC(99),CA(99)
      DIMENSION Z(200),X(200)
      REAL LE
      INTEGER STEP
C     ***READ IN DATA***
      WRITE(5,*)'ENTER OUTPUT CODE: PRINTER=3,TERMINAL=5'
      READ(5,*)IP
      WRITE(5,*)'ENTER NUMBER OF NODES'
      READ(5,*)NODES
      WRITE(5,*)'ENTER ELEMENT LENGTH IN CM.'
      READ(5,*)DELZ
      WRITE(5,*)'ENTER NUMBER OF ELEMENTS'
      READ(5,*)NE
      WRITE(5,*)'ENTER TOTAL DEPTH OF MODEL IN CM.'
      READ(5,*)TL
      WRITE(5,*)'ENTER WEIGHT FOR WEIGHTED AVERAGE APPROXIMATION'
      READ(5,*)E
      WRITE(5,*)'ENTER RETARDATION COEFFICIENT '
      READ(5,*)RD
      WRITE(5,*)'ENTER VELOCITY IN Z DIRECTION IN CM/SEC.'
      READ(5,*)VZ
      WRITE(5,*)'ENTER MOISTURE CONTENT'
      READ(5,*)TH
      WRITE(5,*)'ENTER DISPERSION COEFFICIENT'
      READ(5,*)DL
      WRITE(5,*)'ENTER BULK DENSITY'
      READ(5,*)BP
      WRITE(5,*)'ENTER VOID VOLUME'
      READ(5,*)VV
      WRITE(5,*)'ENTER TIME STEP SIZE IN SECONDS'
      READ(5,*)DELT
      WRITE(5,*)'ENTER TOTAL SIMULATION TIME IN SECONDS'
      READ(5,*)TMAX
      NNE=2
      WRITE(5,*)'ENTER UPSTREAM WEIGHTING FACTOR ALPHA'
      READ(5,*)ALPHA
      WRITE(IP,24)NODES
24    FORMAT(1X,'NUMBER OF NODES =',I3)
```

```
      WRITE(IP,25)DELZ
25    FORMAT(1X,'ELEMENT LENGTH =',F10.4,'cm.')
      WRITE(IP,26)NE
26    FORMAT(1X,'NUMBER OF ELEMENTS =',I3)
      WRITE(IP,34)TL
34    FORMAT(1X,'TOTAL DEPTH OF MODEL =',F12.2,'cm')
      WRITE(IP,27)E
27    FORMAT(1X,'WEIGHTED AVERAGE WEIGHT =',F3.1)
      WRITE(IP,28)RD
28    FORMAT(1X,'RETARDATION COEFFICIENT =',F7.3)
      WRITE(IP,29)VZ
29    FORMAT(1X,'VELOCITY =',F10.5,'cm/sec')
      WRITE(IP,41)TH
41    FORMAT(1X,'MOISTURE CONTENT =',F5.3)
      WRITE(IP,42)DL
42    FORMAT(1X,'DISPERSION COEFFICIENT =',F5.3)
      WRITE(IP,43)BP
43    FORMAT(1X,'BULK DENSITY =',F5.3)
      WRITE(IP,44)VV
44    FORMAT(1X,'VOID VOLUME =',F5.3)
      WRITE(IP,30)DELT
30    FORMAT(1X,'TIMESTEP =',F5.1,'sec')
      WRITE(IP,31)TMAX
31    FORMAT(1X,'TOTAL SIMULATION TIME =',F6.1,'sec')
      WRITE(IP,32)
      WRITE(IP,133)ALPHA
133   FORMAT(1X,'ALPHA =',F5.2)
32    FORMAT(1X,'*******************************************')
      WRITE(IP,32)
C*************************************************************
C*******INITIALIZE C MATRIX ***********************************
      C(1)=1.
      DO 9 I=2,NODES
      C(I)=0.
9     CONTINUE
C*************************************************************
C*******FORM THE GLOBAL MATRIX*********************************
      A=DELZ/(6.*DELT)-DL*E/(RD*DELZ)+VZ*E*(-1.-ALPHA)/(2.*RD)
      B=2.*DELZ/(3.*DELT)+2.*DL*E/(RD*DELZ)+VZ*E*ALPHA/RD
      C2=DELZ/(6.*DELT)-DL*E/(RD*DELZ)+VZ*E*(1.-ALPHA)/(2.*RD)
      BB(1)=DELZ/(3.*DELT)+DL*E/(RD*DELZ)-VZ*E*(1.+ALPHA)/(2.*RD)
      CC(1)=C2
      DO 1 I=2,NODES-1
      AA(I)=A
      BB(I)=B
      CC(I)=C2
1     CONTINUE
      BB(NODES)=DELZ/(3.*DELT)+DL*E/(RD*DELZ)+VZ*E*(1.+ALPHA)/(2.*RD)
      AA(NODES)=A
C*************************************************************
C****** TIME STEP LOOP ***************************************
      NTSTEP=IFIX(TMAX/DELT)
      TSTEP=0
      T=0.
      DO 14 NT=1,NTSTEP
```

```
      TSTEP=TSTEP+1
      T=T+DELT
C*** FORM RIGHT HAND SIDE MATRIX ***************************
      DO 2 I=2,NODES-1
      RHS(I)=(DELZ/(6.*DELT)+DL*(1-E)/(RD*DELZ)-VZ*(1-E)*(-1.-
     _ALPHA)/(2.*RD))*C(I-1)+(2.*DELZ/(3.*DELT)-2.*DL*(1-E)/(RD*
     _DELZ)-VZ*(1-E)*ALPHA/RD)*C(I)+(DELZ/(6.*DELT)+DL*(1-E)/(RD*
     _DELZ)-VZ*(1-E)*(1.-ALPHA)/(2.*RD))*C(I+1)
2     CONTINUE
      RHS(NODES)=(DELZ/(6.*DELT)+DL*(1-E)/(RD*DELZ)-VZ*(1-E)*
     _(-1.-ALPHA)/(2.*RD))*C(NODES-1)+(DELZ/(3.*DELT)-DL*(1-E)/(RD*
     _DELZ)-VZ*(1-E)*(1.+ALPHA)/(2.*RD))*C(NODES)
C*****************************************************************
C**** INCORPORATE THE BOUNDARY CONDITIONS ************************
      BB(1)=BB(1)*(10.**15.)
      IF(T.LT.60)RHS(1)=0.
      IF(T.EQ.60)RHS(1)=BB(1)
      IF (T.GT.60)RHS(1)=0.
C*****************************************************************
C**** SOLVE FOR UNKNOWNS USING TRIDAG ****************************
      IF=1
      CALL TRIDAG(IF,NODES,AA,BB,CC,RHS,C)
C*****************************************************************
C**** PULSE INPUT ANALYTICAL SOLUTION ****************************
      DO 17 I=1,NODES
      J=I-1
      Z(I)=FLOAT(J)*DELZ
      X(I)=Z(I)-VZ*T
      S1=6./(SQRT(12.566*DL*T))
      S2=4.*DL*T
      S3=-((X(I))**2)
      CA(I)=S1*EXP(S3/S2)
17    CONTINUE
C*****************************************************************
      SA=VV*(RD-1)
C**** PRINT RESULTS
*****************************************************
      IF(T.EQ.1)GO TO 33
      IF(T.EQ.3) GO TO 33
      IF(T.EQ.5)GO TO 33
      IF(T.EQ.7)GO TO 33
      IF(T.EQ.10)GO TO 33
      IF(T.EQ.12)GO TO 33
      IF(T.EQ.15) GO TO 33
      IF(T.EQ.50) GO TO 33
      IF(T.EQ.120)GO TO 33
      IF(T.EQ.240) GO TO 33
      IF(T.EQ.360) GO TO 33
      IF(T.EQ.480) GO TO 33
      IF(T.EQ.600) GO TO 33
      IF(T.EQ.720) GO TO 33
      IF(T.EQ.840) GO TO 33
      IF(T.EQ.960) GO TO 33
      IF(T.EQ.1080) GO TO 33
      IF(T.EQ.1200) GO TO 33
```

```
      IF(T.EQ.1320) GO TO 33
      IF(T.EQ.1440) GO TO 33
      IF(T.EQ.1560) GO TO 33
      IF(T.EQ.1680) GO TO 33
      IF(T.EQ.1800) GO TO 33
      IF(T.EQ.1920) GO TO 33
      IF(T.EQ.2040) GO TO 33
      IF(T.EQ.2160) GO TO 33
      IF(T.EQ.2280) GO TO 33
      IF(T.EQ.2400) GO TO 33
      GO TO 14
33    CONTINUE
      WRITE(IP,*)'************************************'
      WRITE(IP,49)RD
49    FORMAT(1X,'RETARDATION COEFFICIENT =',F5.3)
      WRITE(IP,48)SA
48    FORMAT(1X,'SURFACE AREA CONTACTED =',F5.3)
      WRITE(IP,11)TSTEP,T
11    FORMAT(1X,'TIMESTEP ',F5.1,3X,'TIME =',F7.1)
      WRITE(IP,18)
18    FORMAT(1X,'    I     Z      NUMERICAL     ANALYTICAL     ERROR')
      DO 12 I=1,NODES
      ERROR=CA(I)-C(I)
      WRITE(IP,13)I,Z(I),C(I),CA(I),ERROR
13    FORMAT(1X,3X,I3,3X,F8.4,3X,F12.4,3X,F12.4,3X,F8.4)
12    CONTINUE
14    CONTINUE
      STOP
      END
C*****************************************************************
C**** SUBROUTINE TRIDAG ***************************************
      SUBROUTINE TRIDAG(if,NODES,Aa,Bb,Cc,RHS,C)
      dimension Aa(99),Bb(99),Cc(99),RHS(99),C(99),beta(99),gamma(99)
c
c     compute the intermediate arrays beta and gamma
c
      beta(if)=Bb(if)
      gamma(if)=RHS(if)/beta(if)
      ifpl=if+1
      do 1 i=ifpl,NODES
      beta(i)=Bb(i)-Aa(i)*Cc(i-1)/beta(i-1)
1     gamma(i)=(RHS(i)-Aa(i)*gamma(i-1))/beta(i)
c
c     compute the final solution vector v
c
      C(NODES)=gamma(NODES)
      last=NODES-if
      do 2 k=1,last
      i=NODES-k
2     C(i)=gamma(i)-Cc(i)*C(i+1)/beta(i)
      return
      end
```

APPENDIX II.

SATURATED HYDRAULIC CONDUCTIVITY DATA

CONSTANT HEAD PERMEAMETER TESTS

Hr 9 = 3.40	Hr 12 = 3.30	Hr 15 = 3.25
Hs 9 = 3.95	Hs 12 = 3.70	Hs 15 = 4.10

T (C)	9 (sec)	12 (sec)	15 (sec)
22	12.3	25.0	63.2
22	10.4	16.4	51.0
23	9.0	15.0	54.6
23	9.8	31.5	38.0
23	27.4	45.9	55.0
24	13.5	43.6	75.2
24	13.2	46.0	80.2

Hr 9 = 3.30	Hr 12 = 3.25	Hr 15 = 3.20
Hs 9 = 4.05	Hs 12 = 3.80	Hs 15 = 4.05

24	13.7	47.1	79.3
24	13.6	44.8	83.1
24	13.1	46.7	78.4

Area = 19.63 cm2
Length = 3.9 cm
Vol. = 10 cm3 collected

Sampler No. 9

T	Q	Kt	Ko
22	0.7813	0.2822	0.2689
22	0.9615	0.4245	0.4045
23	1.1110	0.4905	0.4565
23	0.3650	0.1611	0.1499
24	0.7407	0.3270	0.2973
24	0.7576	0.3345	0.3041
24	0.7299	0.1934	0.1759
24	0.7353	0.1948	0.1771
24	0.7634	0.2022	0.1839

Sampler No. 12

T	Q	Kt	Ko
22	0.4000	0.1987	0.1893
22	0.6098	0.3029	0.2886
23	0.6667	0.3311	0.3081
23	0.3175	0.1577	0.1468
23	0.1517	0.0753	0.0701
24	0.2123	0.0767	0.0697
24	0.2294	0.1139	0.1036
24	0.2174	0.1080	0.0982
24	0.2232	0.0806	0.0733
24	0.2141	0.0773	0.0703

Sampler No. 15

22	0.1582	0.03698	0.03524
22	0.1961	0.04584	0.04368
23	0.1832	0.04282	0.03985
23	0.2632	0.06152	0.05725
23	0.1818	0.04249	0.03954
24	0.1330	0.03109	0.02827
24	0.1247	0.02915	0.02651
24	0.1261	0.02947	0.02680
24	0.1203	0.02812	0.02557
24	0.1275	0.02980	0.02709

HANGING COLUMN RESULTS

THETA - PSI CALCULATIONS

Sample 1 (wetting)		Sample 2 (both)	
Volume =	66.6 cc.	Volume =	82.32 cc.
Ws =	104.0 g.	Ws =	101.1 g.
Wwet =	236.4 g.	Wdry =	138.1
Porosity =	0.357	Porosity =	0.366

Date	Water Level	Water Vol.	dO	θ	Psi
		Sample 1			
9/8	35.4	6.9	.104	.181	-93.0
9/10	35.9	6.4	.096	.189	-54.0
9/11	36.5	5.8	.087	.198	-34.2
9/12	37.2	5.1	.077	.208	-23.2
9/13	38.7	3.6	.054	.231	-12.4
9/14	38.8	3.5	.053	.232	- 6.5
9/15	42.3	0.0	.000	.285	-
		Sample 2			
8/22	39.5	-6.5	-.079	.335	0.0
8/22	38.0	-5.0	-.061	.317	- 3.3
8/23	35.0	-2.0	-.024	.280	-12.3
8/26	33.7	-0.7	-.009	.265	-19.7
8/29	32.0	1.0	.012	.244	-32.5
9/2	30.4	2.6	.032	.224	-54.5
9/3	28.1	4.9	.060	.196	-92.4
9/5	26.6	6.4	.078	.178	-170.
9/7	27.0	6.0	.073	.183	-110.
9/8	27.5	5.5	.067	.189	- 55.
9/10	28.5	4.5	.055	.201	- 29.
9/11	29.4	3.6	.044	.212	-19.7
9/12	31.0	2.0	.024	.232	- 9.6
9/13	33.0	0.0	.000	.256	- 5.3

APPENDIX III.

HIGH PRESSURE LIQUID CHROMATOGRAPHY PROCEDURES

Reverse-phase with Ion Pairing

I. ANALYSIS OF PFB AND m-TFMB:

Parafluoro benzoic acid
Mol. Wt. = 212.07
pK = 11.3

meta-Trifluoro methyl benzoic acid
Mol. Wt. = 190.12
pK = 9.6

A. Reagents and Standards:

1. Phosphoric acid (Reagent or better grade)
2. pH 4.0 buffer
3. H2O - HPLC grade (Omnisolve)
4. CH3CHN - Acetonitrile (HPLC grade)
5. PFB, m-TFMB
6. Blank (ex. pre-injection well water)

B. Equipment:

1. HPLC pump w/ pulse dampening: Altex Model 110A; Valco 6-port, 7000 psi injector (230 ul/loop).
2. Variable wavelength U-V detector, HPLC flow cell detector: Hitachi 100-10 w/ Altex HPLC flow cell adaptor.
3. Integrator/Recorder: Spectra-Physics SP4100
4. 5 ml. glass syringe w/ 0.3 um filter of Nylon-66 affixed. (Rainin 38-101)
5. Graduated cylinders and volumetric flasks.
6. Millipore filters for buffer filtration. (Rainin 38-100)
7. pH meter: Altex Model 71.

C. Analytical Conditions:

Column: Hamilton PRP-1; 25cm x 4.1mm w/10um particles
Mobile: 35% CH3CN / pH 2.0, .005M phosphoric acid (isocratic)
Flow: 1.6 ml/min
Temp: ambient (25 C)
Detector: 200 nm
Inject Vol: 230 ul (large loop and overfill)

D. Standard Preparation:

1. 100ppm stock of each compound in distilled, deionized wate.
2. Store in refrigerator between uses.

E. Mobile Phase:

1. 1000 ml HPLC water in 2000 ml beaker (prerinse with DDH2O and HPLC-H2O).
2. Calibrate pH meter to 4.0.
3. Adjust pH of solution w/ phosphoric acid to 2.0.
4. Recalibrate pH meter to 4.0.
5. Recheck pH of buffer and adjust as necessary.
6. Add 350 ml CH3CN to 1000 ml volumetric; fill to mark with phosphate buffer.
7. Filter thru 0.2 um Nylon-66 filter and transfer to appropriate bottle.

F. Notes:

1. Buffer needs to be pH 2.0 or less for good resolution.
2. Avoic recessive back pressures by pumping with water, then 50% CH3CN.

G. Analytical Procedure:

1. Set desired U-V wavelength (200 nm).
2. Pre-rinse with buffer (35% CH3CN - phosphoric acid).
3. Load column with sample (filtered through the Nylon-66 affixed filter).
4. Let sample run until elution is complete.
5. Repeat for successive samples steps 3 and 4 with rinsing of syringe between trials.

II. ANALYSIS OF SULFONIC ACIDS: (Ionic pairing of zwitterions)

2-Amino,1-Phenol,4-S. A.
Mol.Wt. = 198.2
pK = 10.77

1-Amino,2-Napthol,4-S. A.
Mol.Wt. = 248.3
pK = 10.77

A. Reagents and Standards:

1. Phosphoric Acid (dibasic - Reagent or better grade).
2. pH 10.0 buffer.
3. H2O - HPLC grade (Omnisolve).
4. CH3CN - Acetonitrile (HPLC grade).
5. Octylamine (ion pairing reagent or better grade).
6. PSA, NSA.
7. Blank.

B. Equipment: see section IB

C. Analytical Conditions:

Column: Hamilton PRP-1; 15cm x 4.1mm w/ 10 um particle size.
Mobile: 22% CH3CN / .005M, pH 8 phosphate w/ .02M octylamine
Flow: 2.2 ml/min
Temp: ambient (25 C)
Detector: 250 nm
Inject Vol: 230 ul (large loop and overfill)

D. Standard Preparation: see section ID

E. Mobile Phase:

1. Dissolve .005M phosphte (dibasic) in 1000 ml HPLC-H2O in a 2000 ml beaker (pre-rinsed with DDH2O and HPLC-H2O).
2. Calibrate pH meter to 10.0.
3. Adjust pH of buffer with NaOH to 8.0.
4. Recalibrate pH meter and check buffer pH - adjust if necessary.
5. Add 220 ml. CH3CN to 1000 ml volumetric; fill to mark with buffer.
6. Filter through 0.2 um Nylon-66 filter.
7. Add n-Octylamine (.02M) to buffer and check pH.

F. Notes:

1. Avoid excessive back pressures by pumping with water first, then 50% CH3CN.

G. Analytical Procedures:

1. Set desired U-V wavelength (250 nm).
2. Pre-rinse with buffer (22% CH3CN-Phosphate with Octylamine).
3. Load column with sample.
4. Let sample run until elution is complete.
5. Repeat for successive samples rinsing syringe before executing steps 3 and 4.

III. ANALYSIS OF BROMOANILINE AND TOLUIDINE:

o-Bromoaniline	o-Toluidine
Mol. Wt. = 172.03	Mol. Wt. = 107.16
pK = 11.5	pK = 9.6

A. Reagents and Standrads:

1. Phosphate - monobasic (Reagent or better grade).
2. pH 7.0 buffer.
3. H2O - HPLC grade (Omnisolve).
4. CH3CN - Acetonitrile (HPLC grade).
5. o-Bromoaniline, o-Toluidine.
6. Blank.

B. Equipment: see section IB

C. Analytical Conditions:

Column: Hamilton PRP-1; 15cm x 4.1mm w/ 10 um particle size.
Mobile: 40% CH3CN / .005M, pH 7.5 phosphate buffer.
Flow: 2.2 ml/min
Temp: ambient (25 C)
Detector: 254 nm
Inject Vol: 230 ul (large loop and overfill)

D. Standard Prep: see section ID

E. Mobile Phase:

1. Dissolve .005M phosphate in 1000 ml HPLC-H2O in a 2000 ml beaker (pre-rinsed with DD-H2O and HPLC-H2O).
2. Calibrate pH meter to 7.0.
3. Adjust pH of buffer to 7.5.
4. Recalibrate pH meter and check pH of buffer solution.
5. Add 400 ml CH3CN to 1000 ml volumetric; fill to mark with buffer.
6. Filter through 0.2 um Nylon-66 filter.

F. Notes: see Section IIF

G. Analytical Procedure:

1. Set desired U-V wavelength (254 nm).
2. Pre-rinse with buffer (40% CH3CN / .005M, pH 7.5 phosphate).
3. Load column with sample.
4. Let sample run until elution is complete.
5. Repeat for successive samples rinsing syringe before executing steps 3 and 4.

HPLC - PFB and m-TFMB : Column A - conc. vs. time

	PFB				m-TFMB		
SAMPLE	Att.	R.T.	Area	( )	R.T.	Area	( )
STD	1024	5.00	23,692,812	50.01	7.10	63,403,843	54.6
STD 1:5	512	3.55	3,188,086	10.02	4.56	17,948,183	10.92
STD 1:10	512	3.57	2,079,792	5.01	4.58	6,491,489	5.46
1A1 1:10	512	3.58	1,941,279	4.05	7.13	1,991,833	1.72
1A2 "	"	4.02	263,643	0.11	7.10	5,014,330	4.33
1A3 "	"	3.59	----------	----	7.09	127,385	0.11
1A4 "	"	----	----------	----	7.11	----------	----
5A1 1:10	512	4.04	215,692	0.45	7.08	----------	----
5A2 "	"	4.00	671,133	1.41	7.10	393,731	0.34
5A3 "	"	3.59	1,485,879	3.10	7.13	2,489,799	2.15
5A4 "	"	3.59	431,393	0.89	7.12	4,551,117	3.93
5A5 "	"	4.01	191,702	0.40	7.12	1,667,580	1.44
5A6 "	"	4.02	----------	----	7.09	220,032	0.19
5A7 "	"	----	----------	----	7.10	----------	----
9A1 1:10	512	4.01	119,833	0.25	7.03	----------	

9A2 "	"	4.02	838,807	1.74	7.06	69,483	0.06
9A3 "	"	4.02	1,965,244	4.11	7.06	701,121	0.61
9A4 "	"	4.02	503,288	1.06	7.04	3,254,112	2.81
9A5 "	"	4.04	95,864	0.21	7.05	3,636,255	3.14
9A6 "	"	4.03	47,799	0.09	7.07	1,192,777	1.03
9A7 "	"	4.02	----------	----	7.10	358,987	0.31
9A8 "	"	----	----------	----	7.11	130,037	0.11
9A9 "	"	----	----------	----	7.09	----------	----
13A1 1:10	512	4.05	----------	----	7.01	----------	----
13A2 "	"	4.01	----------	----	7.03	----------	----
13A3 "	"	4.03	95,903	0.21	7.10	149,579	0.13
13A4 "	"	4.03	1,366,091	2.85	7.09	1,412,817	1.22
13A5 "	"	4.07	1,485,903	3.09	7.08	4,203,663	3.63
13A6 "	"	4.05	484,123	1.01	7.10	2,373,892	2.05
13A7 "	"	4.05	167,769	0.35	7.11	416,899	0.36
13A8 "	"	4.06	73,817	0.15	7.11	106,540	0.09
13A9 "	"	4.07	----------	----	7.07	----------	----
3C1 1:10	512	5.05	2,113,270	4.40	7.19	2,716,774	2.35
3C2 "	"	5.04	119,833	0.25	7.13	4,362,819	3.76
3C3 "	"	5.03	----------	----	7.17	162,458	0.11
3C4 "	"	----	----------	----	7.14	----------	----

			PFB			m-TFMB		
SAMPLE	Att.	R.T.	Area	( )	R.T.	Area	( )
7C1	1:10	512	4.98	144,087	0.30	5.92	63,229	0.06
7C2	"	"	5.02	1,296,779	2.71	5.97	632,497	0.55
7C3	"	"	5.03	1,512,909	3.16	6.04	4,635,830	3.77
7C4	"	"	5.03	288,173	0.60	6.06	758,751	0.66
7C5	"	"	5.01	143,798	0.30	6.08	127,385	0.11
7C6	"	"	5.01	24,014	0.05	6.05	----------	----
7C7	"	"	5.00	----------	----	----	----------	----
11C1	1:10	512	5.00	72,043	0.15	6.09	----------	----
11C2	"	"	5.02	216,130	0.45	6.10	----------	----
11C3	"	"	5.02	984,592	2.05	6.11	379,376	0.33
11C4	"	"	5.01	1,488,895	3.11	6.13	1,643,961	1.42
11C5	"	"	5.02	504,303	1.05	6.09	3,920,214	3.38
11C6	"	"	5.01	384,231	0.81	6.11	1,201,356	1.04
11C7	"	"	5.01	192,115	0.40	6.12	316,146	0.27
11C8	"	"	5.03	71,899	0.15	6.11	189,688	0.16
11C9	"	"	5.04	----------	----	6.11	181,813	0.16
11C10	"	"	----	----------	----	6.10	----------	----
15C1	1:10	512	5.03	----------	----	6.11	----------	----
15C2	"	"	5.05	----------	----	6.13	----------	----
15C3	"	"	5.04	23,991	0.05	6.14	----------	----
15C4	"	"	5.04	120,072	0.25	6.14	196,882	0.17
15C5	"	"	5.03	816,491	1.70	6.12	1,889,929	1.63
15C6	"	"	5.05	1,608,967	3.36	6.15	3,856,985	3.33
15C7	"	"	5.03	504,317	1.05	6.11	1,011,668	0.87
15C8	"	"	5.04	264,159	0.55	6.11	505,844	0.44
15C9	"	"	5.04	96,058	0.21	6.13	316,133	0.27
15C10	"	"	5.04	48,029	0.09	6.12	254,454	0.22
15C11	"	"	5.06	----------	----	6.11	252,454	0.22
15C12	"	"	----	----------	----	6.10	251,875	0.22
15C13	"	"	----	----------	----	6.12	----------	----

Note:
PFB Area/ppm = 479,330/1 ppm m-TFMB Area/ppm = 1,158,045/1 ppm

HPLC - PSA and NSA : Conc. vs. time

		PSA			NSA		
SAMPLE	Att.	R.T.	Area	( )	R.T.	Area	( )
STD	32	1.36	48,392,331	100	7.47	3,958,866	100
STD 1:10	32	1.70	4,650,641	10	7.32	288,162	10
STD 1:20	32	1.68	2,788,343	5	7.30	197,289	5
1A1 1:10	32	1.72	293,768	0.61	7.33	7,728	0.20
1A2 "	"	1.69	1,062,813	2.21	7.35	47,727	1.23
1A3 "	"	1.69	408,468	0.85	7.30	87,830	2.27
1A4 "	"	1.71	215,539	0.45	7.37	35,339	0.91
1A5 "	"	1.68	119,914	0.24	7.31	8,157	0.21
1A6 "	"	1.68	----------	----	7.34	3,771	0.09
1A7 "	"	----	----------	----	7.32	----------	----
5A1 1:10	32	1.69	----------	----	7.33	----------	----
5A2 "	"	----	----------	----	----	----------	----
5A3 "	"	1.74	----------	----	7.30	----------	----
5A4 "	"	1.71	170,895	0.35	7.29	----------	----
5A5 "	"	1.72	537,455	1.11	7.34	9,262	0.23
5A6 "	"	1.74	1,029,210	2.14	7.31	34,141	0.88
5A7 "	"	1.74	600,197	1.25	7.31	94,542	2.44
5A8 "	"	1.68	315,244	0.66	7.32	41,386	1.07
5A9 "	"	1.71	143,917	0.30	7.34	16,847	0.43
5A10 "	"	1.71	51,989	0.11	7.33	9,567	0.24
5A11 "	"	1.73	46,891	0.10	7.30	7,726	0.20
9A1 1:10	32	1.74	----------	----	7.31	----------	----
9A2 "	"	----	----------	----	----	----------	----
9A3 "	"	1.73	----------	----	7.35	----------	----
9A4 "	"	----	----------	----	----	----------	----
9A5 "	"	1.71	----------	----	7.32	----------	----
9A6 "	"	1.69	----------	----	----	----------	----
9A7 "	"	1.69	57,509	0.12	7.31	----------	----
9A8 "	"	1.70	655,641	1.36	7.33	5,637	0.14
9A9 "	"	1.69	744,069	1.55	7.34	19,308	0.50
9A10 "	"	1.71	390,418	0.81	7.34	55,339	1.43
9A11 "	"	1.71	119,866	0.24	7.32	86,424	2.23
9A12 "	"	1.72	63,031	0.13	7.32	46,353	1.20
9A13 "	"	1.74	----------	----	7.33	21,653	0.56
9A14 "	"	----	----------	----	7.31	11,116	0.29
9A15 "	"	----	----------	----	7.33	6.312	0.16

SAMPLE	Att.	R.T.	Area	( )	R.T.	Area	( )
13A1 1:10	32	1.73	----------	----	7.37	----------	----
13A2 "	"	----	----------	----	----	----------	----
13A3 "	"	1.74	----------	----	7.34	----------	----
13A4 "	"	----	----------	----	----	----------	----
13A5 "	"	1.74	----------	----	7.36	----------	----
13A6 "	"	1.74	----------	----	----	----------	----
13A7 "	"	1.71	77,431	0.16	7.37	----------	----
13A8 "	"	1.73	520,366	1.08	7.39	7.791	0.20
13A9 "	"	1.72	990,327	2.06	7.41	44,485	1.15
13A10 "	"	1.72	623,863	1.29	7.36	98,402	2.54
13A11 "	"	1.76	323,164	0.67	7.36	79,982	2.07
13A12 "	"	1.74	121,019	0.25	7.38	34,373	0.88
13A13 "	"	1.71	63,557	0.13	7.39	20,173	0.52
13A14 "	"	1.69	----------	----	7.38	11,541	0.30
13A15 "	"	----	----------	----	7.38	9,123	0.23
3C1 1:10	32	1.47	864,076	1.81	7.46	4,675	0.12
3C2 "	"	1.47	993,686	2.02	7.47	57,372	1.49
3C3 "	"	1.39	583,731	1.22	7.39	143,743	3.72
3C4 "	"	1.43	357,151	0.07	7.42	63,574	1.65
3C5 "	"	1.44	250,102	0.05	7.46	41,344	1.07
3C6 "	"	1.48	----------	----	7.41	16,615	0.43
3C7 "	"	----	----------	----	7.40	4,253	0.11
7C1 1:10	32	1.52	----------	----	7.42	----------	----
7C2 "	"	----	----------	----	----	----------	----
7C3 "	"	1.49	----------	----	7.39	----------	----
7C4 "	"	----	----------	----	----	----------	----
7C5 "	"	1.48	105,609	0.22	7.44	----------	----
7C6 "	"	1.50	580,851	1.21	----	----------	----
7C7 "	"	1.47	1,272,111	2.65	7.46	16,633	0.43
7C8 "	"	1.49	1,790,557	3.73	7.41	45,401	1.17
7C9 "	"	1.49	1,051,292	2.19	7.39	142,278	3.68
7C10 "	"	1.51	595,263	1.24	7.38	156,102	4.04
7C11 "	"	1.53	321,643	0.67	7.42	66,629	1.72
7C12 "	"	1.53	220,809	0.46	7.45	26,684	0.69
7C13 "	"	1.50	144,012	0.30	7.43	9,712	0.25
11C1 1:10	32	1.55	----------	----	7.47	----------	----
11C2 "	"	----	----------	----	----	----------	----
11C3 "	"	1.57	----------	----	7.43	----------	----
11C4 "	"	----	----------	----	----	----------	----
11C5 "	"	1.53	----------	----	7.42	----------	----
11C6 "	"	----	----------	----	----	----------	----
11C7 "	"	1.52	110,429	0.23	7.39	----------	----
11C8 "	"	1.54	849,697	1.77	7.40	----------	----
11C9 "	"	1.53	1,387,321	2.89	7.44	12,075	0.31
11C10 "	"	1.53	1,204,915	2.51	7.43	86,265	2.23
11C11 "	"	1.57	782,469	1.63	7.47	169,703	4.39
11C12 "	"	1.57	547,253	1.14	7.41	53,032	1.37
11C13 "	"	1.51	417,666	0.87	7.42	22,519	0.58
11C14 "	"	1.54	359,632	0.77	7.45	12,021	0.31
11C15 "	"	1.59	----------	----	7.47	10,498	0.27

SAMPLE	Att.	R.T.	Area	( )	R.T.	Area	( )
15C1 1:10	32	2.03	----------	----	7.49	----------	----
15C2 "	"	----	----------	----	----	----------	----
15C3 "	"	2.05	----------	----	7.42	----------	----
15C4 "	"	----	----------	----	----	----------	----
15C5 "	"	2.01	----------	----	7.45	----------	----
15C6 "	"	----	----------	----	----	----------	----
15C7 "	"	1.59	110,429	0.23	7.46	----------	----
15C8 "	"	2.00	849,679	1.77	7.47	----------	----
15C8 "	"	1.56	1,387,321	2.89	7.47	12,075	0.31
15C9 "	"	1.57	1,204,915	2.51	7.43	86,265	2.23
15C10 "	"	2.03	782,469	1.63	7.43	169,703	4.39
15C11 "	"	2.02	547,253	1.14	7.44	53,032	1.37
15C12 "	"	2.05	417,666	0.87	7.47	22,519	0.58
15C13 "	"	2.01	359,632	0.77	7.46	12,021	0.31
15C14 "	"	1.56	----------	----	7.46	10,498	0.27
15C15 "	"	1.59	----------	----	7.47	----------	----

Note:
PSA Area/ppm = 480,042/1ppm NSA Area/ppm = 38,639/1ppm

RESULTS OF RHODAMINE-B ANALYSIS

Column A			Column C		
	Rcorr	S	t	R	Rcorr
).2	10.24	3C	2	13.2	3.20
;.7	15.68		4	17.7	7.68
).0	8.96		6	16.4	6.40
;.5	3.52		8	13.0	2.88
'.6	0.64		10	10.6	0.64
.0	5.96	7C	12	10.3	0.32
.2	4.16		14	13.5	3.52
.9	10.88		16	15.8	5.76
.5	11.52		18	19.3	9.28
.7	6.72		20	14.5	4.48
.5	3.52		22	11.9	1.92
.2	2.24		24	10.9	0.96
.6	1.60		26	10.6	0.64
3	1.28	11C	14	11.3	1.28
4	6.40		16	14.2	4.16
9	10.88		18	19.9	9.92
0	7.04		20	18.6	8.64
5	3.52		22	15.8	5.76
2	2.24		24	13.2	3.20
3	1.28		26	12.2	2.24
			28	11.3	1.28
			30	11.2	1.28
3	0.32	15C	16	11.2	1.92
3	3.84		18	16.1	6.08
)	10.88		20	21.5	11.52
3	11.84		22	15.4	5.44
	6.72		24	13.5	3.52
	3.52		26	12.2	2.24
	1.92		28	12.0	1.92
	0.96		30	11.9	1.92

APPENDIX IV.

MISCELLAENOUS COMPUTER MODELS

MILLINGTON-QUIRK METHOD FOR DETERMINING Kr vs. Psi

```
      REAL K,KSAT
      DIMENSION K(25),T(25),P(25)
      OPEN(UNIT=22,FILE='QUIRK.DAT')
      M=20
      KSAT=5.903E-03
      TSAT=0.21
      DO 50 I=1,M
      READ(22,*)T(I),P(I)
50    CONTINUE
      DO 100 I=1,M
              A=0.
              DO 200 J=1,M
              A=A+(2.*FLOAT(J)+1-2.*FLOAT(I))*P(J)**-2.
200           CONTINUE
      B=0.
      DO 300 J=1,M
              B=B+(2.*FLOAT(J)-1.)*P(J)**-2.
300   CONTINUE
      K(I)=KSAT*((T(I)/TSAT)**4./3.)*A/B
      WRITE (5,400)I,T(I),P(I),K(I)
400   FORMAT(1X,'I=',I3,3X,'THE=',F5.3,3X,'PSI=',F7.2,3X,'K=',E15.8)
100   CONTINUE
      END
```

```
*****************************************************************
*                                                               *
*       SOIL HYDRAULIC PROPERTIES:                              *
*       NON-LINEAR LEAST-SQUARES ANALYSIS                       *
*                                                               *
*       --------------- INPUT INFORMATION ---------------       *
*       CARDS 1,2,3: THREE INFORMATION CARDS                    *
*       CARD 4: MODEL NUMBER (MODE), NUMBER OF COEFFICIENTS (NP),*
*               MAXIMUM NUMBER OF ITERATIONS (MIT), RATIO OF    *
*               COEFFICIENTS CRITERION (STOPCR), RESIDUAL MOISTU-*
*               RE CONTENT (IF MODE=2) (WCR), SATURATED MOISTURE *
*               CONTENT (WCS), CONDUCTIVITY AT SATURATION (SATK) *
*               (3I10,4F10.0)                                   *
*       CARD 5: INITIAL ESTIMATES OF THE COEFFICIENTS (3F10.0)  *
*       CARD 6: NAMES OF THE COEFFICIENTS; 3(A4,A2,4X)          *
*       CARD 7, ETC: EXPERIMENTAL DATA: MOISTURE CONTENT AND    *
*               PRESSURE HEAD, RESPECTIVELY; (2F10.0)           *
*       LAST CARD IS BLANK                                      *
*                                                               *
*       THIS SLIGHTLY MODIFIED VERSION WILL PROMPT THE USER     *
*       FOR NAMES OF THE "REL. K VS PRESSURE" AND               *
*       "ABS. K VS PRESSURE" AND "REL. K VS THETA" AND          *
*       "PRESSURE VS THETA" FILES THAT THIS PROGRAM GENERATES   *
*       FOR EASY PLOTTING.  RICH R.                             *
*****************************************************************
C
C
      DOUBLE PRECISION FLNI, FLNO, FLNM, flnf, FLNZ
      DIMENSION X(300),Y(300),R(300),F(300),DELZ(300,4),LSORT(300),
     1B(3),BI(6),E(3),P(3),PHI(3),Q(3),TB(3),A(3,3),D(3,3),
     1TITLE(20),TH(3)
C
C     ----------
      TYPE 13
   13 FORMAT(1X,'INPUT FILE NAME: ',$)
      READ(5,9)flnf
      open (unit=1,access='seqin',file=flnf)
      TYPE 5
    5 FORMAT(1X, 'REL. K VS PRESSURE FILE NAME: ',$)
      READ(5,9)FLNI
    9 FORMAT(A10)
      OPEN (UNIT=21, DEVICE='DSK', FILE=FLNI, ACCESS='SEQOUT')
      TYPE 11
   11 FORMAT(1X, 'ABS. K VS PRESSURE FILE NAME: ',$)
      READ(5,9)FLNM
      OPEN (UNIT=23, DEVICE='DSK', FILE=FLNM, ACCESS='SEQOUT')
      TYPE 3
    3 FORMAT(1X,'REL. K VS THETA FILE NAME: ',$)
      READ(5,9)FLNZ
      OPEN(UNIT=24,DEVICE='DSK',FILE=FLNZ,ACCESS='SEQOUT')
      TYPE 7
    7 FORMAT(1X,'PRESSURE VS THETA FILE NAME: ',$)
      READ(5,9)FLNO
      OPEN (UNIT=22, DEVICE='DSK', FILE=FLNO, ACCESS='SEQOUT')
```

```
      WRITE(3,1000)
      DO 2 I=1,3
      READ(1,1001) TITLE
    2 write(3,1002) TITLE
      write(3,1003)
C
C     ----- READ INPUT PARAMETERS -----
      read(1,*) MODE,NP,MIT,STOPCR,WCR,WCS,SATK
      write(3,1005) MODE,NP,MIT,STOPCR,WCR,WCS,SATK
C
C     ----- READ INITIAL ESTIMATES -----
C      READ(1,1006) (B(I),I=1,NP)
      READ(1,*) (B(I),I=1,NP)
C
C     ----- READ COEFFICIENTS NAMES -----
      NBI=2*NP
      READ(1,1007) (BI(I),I=1,NBI)
C
C     ----- READ AND WRITE EXPERIMENTAL DATA -----
      write(3,1008)
      I=0
    4 I=I+1
      READ(1,*,END=6) Y(I),X(I)
      write(3,1011) I,X(I),Y(I)
      GOTO 4
C      IF(X(I).EQ.0.) GO TO 6
C      GO TO 4
    6 NOB=I-1
C
C     ----------
      DO 8 I=1,NP
    8 TH(I)=B(I)
      IF((NP-2)*(NP-3)) 12,14,12
   12 write(3,1016)
      GO TO 142
   14 GA=0.02
      CALL MODEL(TH,F,NOB,X,WCS,MODE,NP,WCR)
      SSQ=0.
      DO 32 I=1,NOB
      R(I)=Y(I)-F(I)
   32 SSQ=SSQ+R(I)*R(I)
      NIT=0
      write(3,1030)
      IF(MODE.EQ.2) write(3,1026) NIT,WCR,B(1),B(2),SSQ,MODE
      IF(MODE.NE.2) write(3,1026) NIT,B(1),B(2),B(3),SSQ,MODE
C
C     ----- BEGIN OF ITERATION -----
   34 NIT=NIT+1
      GA=0.1*GA
      DO 38 J=1,NP
      TEMP=TH(J)
      TH(J)=1.01*TH(J)
      Q(J)=0
      CALL MODEL(TH,DELZ(1,J),NOB,X,WCS,MODE,NP,WCR)
      DO 36 I=1,NOB
```

```
      DELZ(I,J,)=DELZ(I,J)-F(I)
   36 Q(J)=Q(J)+DELZ(I,J)*R(I)
      Q(J)=100.*Q(J)/TH(J)
C
C     ----- STEEPEST DESCENT -----
   38 TH(J)=TEMP
      DO 44 I=1,NP
      DO 42 J=1,I
      SUM=0
      DO 40 K=1,NOB
   40 SUM=SUM+DELZ(K,I)*DELZ(K,J)
      D(I,J)=10000.*SUM/(TH(I)*TH(J))
   42 D(J,I)=D(I,J)
C
C     ----- D = MOMENT MATRIX -----
   44 E(I)=SQRT(D(I,I))
   50 DO 52 I=1,NP
      DO 52 J=1,NP
   52 A(I,J)=D(I,J)/(E(I)*E(J))
C
C     ----- A IS THE SCALED MOMENT MATRIX -----
      DO 54 I=1,NP
      P(I)=Q(I)/E(I)
      PHI(I)=P(I)
   54 A(I,I)=A(I,I)+GA
      CALL MATINV(A,NP,P)
C
C     ----- P/E IS THE CORRECTION VECTOR -----
      STEP=1.0
   56 DO 58 I=1,NP
   58 TB(I)=P(I)*STEP/E(I)+TH(I)
      DO 62 I=1,NP
      IF(TH(I)*TB(I))66,66,62
   62 CONTINUE
      SUMB=0.0
      CALL MODEL(TB,F,NOB,X,WCS,MODE,NP,WCR)
      DO 64 I=1,NOB
      R(I)=Y(I)-F(I)
   64 SUMB=SUMB+R(I)*R(I)
   66 SUM1=0.0
      SUM2=0.0
      SUM3=0.0
      DO 68 I=1,NP
      SUM1=SUM1+P(I)*PHI(I)
      SUM2=SUM2+P(I)*P(I)
   68 SUM3=SUM3+PHI(I)*PHI(I)
      ANGLE=57.29578*ACOS(SUM1/SQRT(SUM2*SUM3))
C
C     ----------
      DO 72 I=1,NP
      IF(TH(I)*TB(I))74,74,72
   72 CONTINUE
      IF(SUMB/SSQ-1.0)80,80,74
   74 IF(ANGLE-30.0)76,76,78
   76 STEP=STEP/2.0
```

```
      GO TO 56
   78 GA=10.*GA
      GO TO 50
C
C     ----- PRINT COEFFICIENTS AFTER EACH ITERATION -----
   80 CONTINUE
      DO 82 I=1,NP
   82 TH(I)=TB(I)
      IF(MODE.EQ.2) write(3,1026) NIT,WCR,TH(1),TH(2),SUMB,MODE
      IF(MODE.NE.2) write(3,1026) NIT,TH(1),TH(2),TH(3),SUMB,MODE
      DO 92 I=1,NP
      IF(ABS(P(I)*STEP/E(I))/(1.0E-20+ABS(TH(I)))-STOPCR) 92,92,94
   92 CONTINUE
      GO TO 96
   94 SSQ=SUMB
      IF(NIT-MIT)34,34,96
C
C     ----- END OF ITERATION LOOP -----
   96 IDF=NOB-NP
      CALL MATINV(D,NP,P)
C
C     ----- WRITE CORRELATION MATRIX -----
      DO 98 I=1,NP
   98 E(I)=SQRT(D(I,I))
      write(3,1044) (I,I=1,NP)
      DO 102 I=1,NP
      DO 100 J=1,I
  100 A(J,I)=D(J,I)/(E(I)*E(J))
  102 write(3,1048) I,(A(J,I),J=1,I)
C
C     ----- CALCULATE 95% CONFIDENCE INTERVAL -----
      RMS=SUMB/FLOAT(IDF)
      SDEV=SQRT(RMS)
      write(3,1052)
      TVAR=TTEST(IDF)
      DO 108 I=1,NP
      SECOEF= E(I)*SDEV
      TVALUE= TH(I)/SECOEF
      TSEC=TVAR*SECOEF
      TMCOE=TH(I)-TSEC
      TPCOE=TH(I)+TSEC
      K=2*I
      J=K-1
  108 write(3,1058) BI(J),BI(K),TH(I),SECOEF,TVALUE,TMCOE,TPCOE
C
C     ----- PREPARE FINAL OUTPUT -----
      LSORT(1)=1
      DO 116 J=2,NOB
      TEMP=R(J)
      K=J-1
      DO 111 L=1,K
      LL=LSORT(L)
      IF(TEMP-R(LL)) 112,112,111
  111 CONTINUE
      LSORT(J)=J
```

```
      GO TO 116
  112 KK=J
  113 KK=KK-1
      LSORT(KK-1)=LSORT(KK)
      IF(KK-L) 115,115,113
  115 LSORT(L)=J
  116 CONTINUE
      write(3,1066)
      DO 118 I=1,NOB
      J=LSORT(NOB+1-I)
  118 write(3,1068) I,X(I),Y(I),F(I),R(I),J,X(J),Y(J),F(J),R(J)
C
C     ----- WRITE SOIL HYDRAULIC PROPERTIES -----
      write(3,1069)
      PRESS=1.18850
      RN1=0.0
      RKLN=1.0
      write(3,1072) RN1,WCS,RKLN,SATK
      WRITE(21,1073)RN1, RKLN
      WRITE(22,1074)WCS, RN1
      WRITE(23,1073)RN1, SATK
      WRITE(24,1073)WCS, RKLN
      DO 140 I=1,75
      IF(RKLN.LT.(-16.)) GO TO 142
      PRESS=1.18850*PRESS
      IF(MODE-2) 120,122,120
  120 WCR=TH(1)
      ALPHA=TH(2)
      RN=TH(3)
      GO TO 124
  122 ALPHA=TH(1)
      RN=TH(2)
  124 RM=1.-1./RN
      IF(MODE.EQ.3) RM=1.-2./RN
      RN1=RM*RN
      RWC=1./(1.+(ALPHA*PRESS)**RN)**RM
      WC=WCR+(WCS-WCR)*RWC
      TERM=1.-RWC*(ALPHA*PRESS)**RN1
      IF(RWC.LT.0.06) TERM=RM*RWC**(1./RM)
      IF(MODE.EQ.3) RK=RWC*RWC*TERM
      IF(MODE.NE.3) RK=SQRT(RWC)*TERM*TERM
      TERM=ALPHA*RN1*(WCS-WCR)*RWC*RWC**(1./RM)*(ALPHA*PRESS)**(RN-1.)
      AK=SATK*RK
      DIFFUS=AK/TERM
      PRLN=ALOG10(PRESS)
      AKLN=ALOG10(AK)
      RKLN=ALOG10(RK)
      DIFLN=ALOG10(DIFFUS)
      WRITE(21,1073)PRESS, RK
      WRITE(22,1074)WC, PRESS
      WRITE(23,1073)PRESS, AK
      WRITE(24,1073)WC,RK
  140 write(3,1070) PRESS,PRLN,WC,RK,RKLN,AK,AKLN,DIFFUS,DIFLN
  142 CONTINUE
C     END OF PROBLEM
```

```
 1000 FORMAT(1H1,10X,82(1H*)/11X,1H*,80X,1H*/11X,1H*, 9X,'NON-LINEAR
LEA
     1ST SQUARES ANALYSIS',38X,1H*/11X,1H*,80X,1H*)
 1001 FORMAT(20A4)
 1002 FORMAT(11X,1H*,20A4,1H*)
 1003 FORMAT(11X,1H*,80X,1H*/11X,82(1H*))
C1004 FORMAT(3I10,5F10.0)
 1005 FORMAT(//11X,'INPUT PARAMETERS'/11X,16(1H=)/
     211X,'MODEL NUMBER.....',I3/
     311X,'NUMBER OF COEFFICIENTS.....',I3/
     411X,'MAXIMUM NUMBER OF ITERATIONS.....',I3/
     511X,'RATIO OF COEFFICIENTS CRITERION.....',F10.4/
     611X,'RESIDUAL MOISTURE CONTENT (FOR MODEL 2).....',F10.4/
     711X,'SATURATED MOISTURE CONTENT.....',F10.4/
     811X,'SATURATED HYDRAULIC CONDUCTIVITY.....',F10.4)
 1006 FORMAT(4F10.0)
 1007 FORMAT(4(A4,A2,4X))
 1008 FORMAT(//11X,'OBSERVED DATA',/11X,13(1H=)/11X,'OBS.
NO.',4X,'PRESS
     1URE HEAD',2X,'MOISTURE CONTENT')
 1011 FORMAT(11X,I5,5X,F12.2,4X,F12.4)
 1016 FORMAT(//5X,10(1H*),' ERROR: INCORRECT NUMBER OF COEFFICIENTS')
 1026 FORMAT(15X,I2,10X,F8.4,3X,F10.6,2X,F10.4,5X,F12.7,4X,I4)
 1030 FORMAT(1H1,10X,'ITERATION
NO',8X,'WCR',8X,'ALPHA',10X,'N',13X,'SSQ
     1',8X,'MODEL')
 1044 FORMAT(//11X,'CORRELATION MATRIX'/11X,18(1H=)/14X,10(4X,I2,5X))
 1048 FORMAT(11X,I3,10(2X,F7.4,2X))
 1052 FORMAT(//11X,'NON-LINEAR LEAST-SQUARES ANALYSIS: FINAL RESULTS'/
     111X,48(1H=)/64X,'95% CONFIDENCE
LIMITS'/11X,'VARIABLE',8X,'VALUE',
     27X,'S.E.COEFF.',3X,'T-VALUE',6X,'LOWER',10X,'UPPER')
 1058 FORMAT(13X,A4,A2,4X,F10.5,5X,F9.4,5X,F6.2,4X,F9.4,5X,F9.4)
 1066 FORMAT(//10X,8(1H-),'ORDERED BY COMPUTER INPUT', 8(1H-),
7X,10(1H-
     1),'ORDERED BY RESIDUALS',10(1H-)/26X,'MOISTURE
CONTENT',3X,'RESI-'
     1,24X,'MOISTURE
CONTENT',3X,'RESI-'/10X,'NO',3X,'PRESSURE',5X,'OBS'
     2,4X,'FITTED',4X,'DUAL',
9X,'NO',3X,'PRESSURE',5X,'OBS',4X,'FITTED'
     3,4X,'DUAL')
 1068 FORMAT(10X,I2,F10.2,1X,3F9.4,8X,I2,F10.2,1X,3F9.4)
 1069 FORMAT(1H1,10X,'PRESSURE',4X,'LOG P',6X,'WC',7X,'REL K',5X,'LOG
RK
     1',6X,'ABS K',4X,'LOG KA',5X,'DIFFUS',5X,'LOG D')
 1070 FORMAT(10X,E10.3,F8.3,F10.4,3(E13.3,F8.3))
 1072 FORMAT(10X,E10.3,8X,F10.4,E13.3,8X,E13.3)
 1073 FORMAT(1X,E10.3,1X,E10.3)
 1074 FORMAT(1X,F6.4,1X,E10.3)
      STOP
      END
      SUBROUTINE MODEL(B,FY,NOB,X,WCS,MODE,NP,WCR)
      DIMENSION B(3),FY(40),X(40)
```

```
C      MODE=1 : MUALEM THEORY WITH THREE COEFFICIENTS
C      MODE=2 : MUALEM THEORY WITH TWO COEFFICIENTS
C      MODE=3 : BURDINE THEORY WITH THREE COEFFICIENTS
C
       IF(MODE-2) 10,20,30
   10  CONTINUE
       DO 12 J=1,NOB
   12  FY(J)=B(1)+(WCS-B(1))/(1.+(B(2)*X(J))**B(3))**(1.-1./B(3))
       RETURN
   20  CONTINUE
       DO 22 J=1,NOB
   22  FY(J)=WCR+(WCS-WCR)/(1.+(B(1)*X(J))**B(2))**(1.-1./B(2))
       RETURN
   30  CONTINUE
       DO 32 J=1,NOB
   32  FY(J)=B(1)+(WCS-B(1))/(1.+(B(2)*X(J))**B(3))**(1.-2./B(3))
       RETURN
       END
       FUNCTION TTEST(IDF)
       DIMENSION TA(30)
       DATA TA/12.706,4.303,3.182,2.776,2.571,2.447,2.365,2.306,2.262,

12.228,2.201,2.179,2.160,2.145,2.131,2.120,2.110,2.101,2.093,2.086,
     22.080,2.074,2.069,2.064,2.060,2.056,2.052,2.048,2.045,2.042/
       IF(IDF-30)10,10,11
   10  TTEST=TA(IDF)
       RETURN
   11  IF(IDF-120)12,12,13
   13  TTEST=1.96
       RETURN
   12  IF(IDF-40)14,14,15
   14  TTEST=2.042-0.021*FLOAT(IDF-30)/10.0
       RETURN
   15  IF(IDF-60)16,16,17
   16  TTEST=2.021-0.021*FLOAT(IDF-40)/20.0
       RETURN
   17  TTEST=2.000-0.002*FLOAT(IDF-60)/60.0
       RETURN
       END
       SUBROUTINE MATINV(A,NP,B)
       DIMENSION A(3,3),B(3),INDEX(3,2)
       DO 2 J=1,4
    2  INDEX(J,1)=0
       I=0
    4  AMAX=-1.0
       DO 10 J=1,NP
       IF(INDEX(J,1)) 10,6,10
    6  DO 10 K=1,NP
       IF(INDEX(K,1)) 10,8,10
    8  P=ABS(A(J,K))
       IF(P.LE.AMAX) GO TO 10
       IR=J
       IC=K
       AMAX=P
```